Bulletin of Romanian Chemical Engineering Society

1 2022

ISSN 2360-4697
Edited by SICR and Matrix Rom
The journal is included in the international database
EBSCO, PROQUEST & INDEX COPERNICUS

ISSN 2360-4697

Bulletin of Romanian Chemical Engineering Society

Volume 9 2022 Number 1

Contents

EFFICIENCY AND EFFECTIVENESS IN PLANNING AND CONTROL OF ANY ACTIVITY

Alexandru WOINAROSCHY[1*]

Romanian Academy of Technical Sciences, Bucharest, Romania

Abstract

The terms effectiveness and efficiency, often used interchangeably, actually reflect two very different concepts. The effectiveness and efficiency are two concepts that take on considerable importance in the world of the work and, in general, in the planning and control of any activity, so that they are identified as the two main dimensions of the evaluation process. The effectiveness refers to the "achievement of the final aim" while efficiency "measures the quality". It is presented the full content of these terms, how they can be measured with certain calculations, and examples of efficiency and effectiveness calculation. It also exposed the frequency of efficiency and effectiveness in managing project literature.

Key words: effectiveness, efficiency, definitions, calculation.

1. Introduction

According to Merriam-Webster [1], *Effective, effectual, efficient, and efficacious all mean producing or capable of producing a result or results, but they are not freely interchangeable in idiomatic use*. The terms effectiveness and efficiency, often used interchangeably, actually reflect two very different concepts. The effectiveness indicates the ability to achieve the objective set, while the efficiency assesses the ability to do so using the minimum resources needed [2]. Effectiveness indicates the ability to achieve the stated objective, while efficiency assesses the ability to do so using the minimum resources required. In other words, efficiency measures how well an organisation does what it does, but effectiveness raises value questions about what the organisation should be doing in the first place.

The effectiveness and efficiency are two concepts that take on considerable importance in the world of the work and, in general, in the planning and control of any activity, so that they are identified as the two main dimensions of the evaluation process. In relation to evaluation, effectiveness is declined as internal and external. The internal effectiveness indicates the relationship between the products (product) and the expected objectives, while the external one indicates the relationship between the products and the results obtained. On the

[1]* Corresponding author: email address: awligi@yahoo.com

other hand, efficiency in relation to evaluation underlines the relationship between the resources used (inputs) and the products obtained, so its evaluation implies the analysis of the production process and the management of the production factors.

2. Argumentation

Differences between efficiency and effectiveness

The **efficiency** is to make both bits, whether or not it reaches a target. It is a cost-benefit discourse. A solution is efficient if it costs less than the benefits it generates. But it may not reach the goal, and therefore not be **effective**. The differences between efficiency and effectiveness are more clearly presented in table 1 [2].

Table 1

Differences between efficiency and effectiveness

Definition	Efficiency	Effectiveness
Focus	Focuses on goals	Focuses on the process to reach a goal
Nature	Objective Quantifiable	It can be subjective It can be quantitative or quantifiable
Means	Use resources to reach the goal	Seeks the best use of available resources
Results	Measure the expected results vs. the results that are obtained	**Measures the results and resources that have been used vs the proposed goals and the expected costs**

Efficiency: Efficiency assesses the ability to achieve the goal set using the minimum resources needed. It is the ability to achieve it with the minimum possible allocation of resources (one of which, fundamental, is time). The best results must be achieved with the minimum resources (expenses).
Therefore, it must:
• Focus market demand or job opportunities.
• Focus the target population, that is, the potential needs, the profile
• Adapt to the needs of the population
• Optimize administrative, administrative, and financial management

Efficiency can be measured with certain calculations which resulted check the efficiency of subjective values such as the qualities of a product or resources (time it takes for an employee, cost, materials, etc.)

The efficiency calculation is as follows: It is developed from a table where the lowest results indicate lower efficiency while the highest results indicate good efficiency.

Efficiency = (Result achieved / Actual cost) * Time invested

A general definition, given to efficiency, refers to the report between the outputs and the inputs made to achieve them [3].

Efficiency calculation example

If a factory produces 1,100 shirts in 23 hours for a cost of 0.90 USD, targeting 1,000 in 24 hours, for a cost of 1 USD, the operation would be as follows:

1,100 shirts produced / ($ 0.90 cost incurred x 23 actual hours) = 53.14

1000 expected shirts / (1 USD expected cost x 24 hours expected) = 41.6

53.14 / 41.6 = 1.28 approximately.

In this case, the efficiency has an index of 1.28, which means that indeed the work has been efficient.

On the other hand, if in the same example, the factory produces only 900 shirts in 24 hours at a cost of 1 USD per unit, maintaining the same objective, the result would be the following:

900 shirts produced / (1 USD cost incurred x 24 actual hours) = 37.5

1000 expected shirts / (1 USD expected cost x 24 hours expected) = 41.6

37.5 / 41.6 = 0.9 approximately.

The index is less than, so production has not been very efficient.

The index can also be transformed into a percentage, multiplying it by 100, to be used in the calculation of the effectiveness of the production, together with the result of the effectiveness.

Effectiveness: The effectiveness indicates the ability to achieve the goal set.

Therefore, it must:

• Expand or improve employability conditions
• Promote personal and group development
• Promote job placement together with the improvement of job performance

Effectiveness is the achievement of the proposed results where the company measures the percentage and compares whether the percentiles are low or high. Obviously, the closer is 100% the better.

Therefore:

Effectiveness = (Achieved Result · 100)/(Expected Result)

An effective person or company is the person who meets the objectives set or proposed by the company in an objective and quantifiable way. Although a person can be effective without being efficient, and vice versa, he can also be efficient and not be effective.

Effectiveness is expressed by the ratio between the result achieved and the programmed one and shows the success acquired by using the resources to accomplish the proposed objectives [4].

Calculation of effectiveness

One way to calculate effectiveness is to add the percentages of effectiveness and efficiency, dividing their sum by 2.
For example, if the efficiency of the company that produces shirts is 110% (it has met its objectives) and its efficiency is 128%, the calculation of effectiveness would be as follows:

110% effective + 128% effective / 2 = 119% effective.

This means that the company has a production level of shirts with a positive or high effectiveness.
If, instead, the same company has been 50% effective and 90% efficient, its effectiveness would be:

50% efficiency + 90% efficiency / 2 = 70% effectiveness.

In this scenario, the effectiveness is still below 100% and can be improved.

Frequency of efficiency and effectiveness in management projects literature: Zidane and Olsson [5] have investigate the use of the terms *efficiency*, *effectiveness* and *efficacity* with respect to project management, project success and project evaluation using 351 articles from the journal International *Journal of Managing Projects in Business.* The corresponding results are given in Table 2 [5].

Table 2

The use of the term efficiency, effectiveness and efficacity

Number of words and articles	Total	Percentage
Total number of journal articles downloaded	351	100
Articles with at least one of the three words	255	73
Articles with none of the three words	96	27
Total number of uses of the three terms in the journal	1537	100
Frequency of word “efficiency” in the journal	652	42
Frequency of word “effectiveness” in the journal	782	48
Frequency of word “efficacy” in the journal	103	7
Total number of articles using just one of the terms	140	100
Articles using only the word “efficiency”	65	46
Articles using only the word “effectiveness”	68	49
Articles using only the word “efficacy”	7	7
Total number of articles mentioning each term	379	100
Articles referring to “efficiency”	171	45
Articles referring to “effectiveness”	180	48
Articles referring to “efficacy”	28	7

It is remarkable the high value of the percentage of frequency of the word efficiency (42%) and of the word effectiveness (48%).

3. Conclusions

Effectiveness and efficiency, often used interchangeably, actually reflect two very different concepts. With examples calculation respect to effectiveness and efficiency an attempt was made to show the similarity and difference between these methods for characterizing an activity.

REFERENCES

[1] Merriam-Webster, *Merriam-Webster's Dictionary of Synonyms: A Dictionary of Discriminated Synonyms with Antonyms and Analogous and Contrasted, Words*, Merriam-Webster Inc. Springfield, MA, (1984).
[2] Tempest, J., *Efficiency, and effectiveness*, 2021, https://differentexamples.com/category/economy/
[3] Mihaiu, D.M., Opreana A., Cristescu, M.P., *Efficiency, Effectiveness and Performance of the Public Sector*, Romanian Journal of Economic Forecasting, 13, 4, (2010), 132-147.
[4] Popa, P., *Elements on the Efficiency and Effectiveness of the Public Sector*, *Ovidius* University Annals, Economic Sciences Series, XVII, 2, (2017), 313-319.
[5] Zidane, Y.J.T., Olsson, N.O.E., *Defining project efficiency, effectiveness and efficacy*, International Journal of Managing Projects in Business, 10, 3, (2017), 621-641.

THE EFFICIENCY OF INFECTIOUS MEDICAL WASTE TREATMENT FACILITIES: A COMPARATIVE ANALYSIS

Adela D. CIOBANU[1], AlexandruOZUNU[1], Cristina MODOI[1]*

[1] Faculty of Environmental Science and Engineering, University of Babeş-Bolyai, 30 Fantanele Street, RO-400294, Cluj-Napoca, Romania

Abstract

Maximizing the value of resources and producing more waste are strategic decisions, which influence sustainability and competitive advantage in the profile market. The objective of this paper is to draw up a comparative analysis of the current methods of disposal of existing infectious medical waste and the harmful effects on the environment and on public health. The importance of medical waste management, the application of effective management, regarding the significant reduction of costs involved in the disposal of waste resulting from medical activities, determines the choice of alternative facilities for the treatment of infectious medical waste, with low costs compared to incineration. The identification of medical technologies is directly proportional to the ability to produce energy, fuels, and recoverable materials and eliminate the problem of pollution. Medical waste incinerators emit into the atmosphere dioxins, furans, heavy metals (such as lead, mercury, and cadmium), fine dust particles, hydrochloric acid, sulfur dioxide, carbon monoxide, soot, incomplete combustion products and other pollutants. These compounds have a particularly negative impact on the health of incinerator workers, public health and the environment. The price for storing the hazardous residue resulting from incineration is higher than the price required for storing the waste resulting from the inactivation of medical waste through alternative technologies. Alternative practices to burning waste in incineration can be non-combustible installations, which are based on thermal, chemical, methods based on ionizing radiation, and biological methods. Thermal energy is used to destroy pathogens, contained in infectious medical waste of low temperatures (93-177 °C), medium temperatures (177-370 °C), and high temperatures >370 °C. The production of infectious waste is dependent on developments in the economic sector. The adoption of ecological technologies is a basic factor in the process of developing environmental policies, which contributes to the strengthening of prevention policies at the European and national levels.

Key words: medical waste, treatment facilities, incineration, environmental technologies, hazardous-waste management, national management

* Corresponding author: email address: cristina.modoi@ubbcluj.ro

1. Introduction

Starting with the year 2007(the moment of Romania's accession to the EU and the application of the legislation regarding the phased closure of infectious medical waste incinerators), the activity in the field of waste management generated the need for the identification and immediate application of optimal solutions for the elimination of medical waste. The choice of solutions for the final disposal of infectious medical waste in final waste treatment facilities is directly proportional to the increase in economic efficiency, to be able to remain competitive on a market in a continuous dynamic of modeling and adaptation.

Environmental policies are based on principles of progress and competitiveness. Considering the dynamics of small but constant growth of the amounts of medical waste from year to year, the development of alternative technologies to the existing ones is necessary in parallel with the supplementation of the existing ones.

This comparative analysis is based on the two methods of final disposal of infectious medical waste: incineration and the neutralization method (thermal, chemical, based on ionized radiation, biological).

Medical waste neutralization technologies, apart from anatomic-pathological, chemical, medicinal ones, are the used and preferred alternative instead of disposal by incineration, in countries with strong and developed economies. At the national level, the final waste disposal methods are according to *WHO 1226/2012 art.45*: (i) thermal decontamination (sterilization); (ii) incineration for waste that cannot be decontaminated (anatomical-pathological waste); (iii) storage after decontamination (*WHO 1226/2012).* Environmental policies support an integrated waste management through the systematic approach to the productive use and reuse, depending on the life cycle, of the products that become waste. The hierarchy in waste management is to identify measures with the aim of reducing the waste deposited at the final warehouses. The waste hierarchy establishes the legal framework for medical waste management strategies to reduce resource consumption, thus contributing to the evaluation of the benefits associated with each option. At the base of the waste hierarchy is storage, which must be applied only if it cannot be avoided, because storage also generates costs. If the hazardous waste can no longer be used, including the residues from incineration, storage is chosen as the closing of the waste traceability from generation to final disposal. In this context figure 1shows the waste directives accepted in Europe [1].

Fig. 1. Hierarchy of waste source [2]

2. Analysis

The annual waste management plans drawn up by local authorities in accordance with the national waste management strategy identify the existential need for final waste disposal facilities and their constant adaptation to investments in ecological technologies. Romania annually generates significant amounts of waste, which causes problems related to the traceability of hazardous waste until its storage and final disposal in compliant, authorized facilities. The effective management of hazardous waste means a joint action of the local and national authorities by implementing laws and taking measures to combat the effects of defective management of hazardous waste. At the national level, 8 incineration stations and 12 thermal treatment stations are in operation (source: www.anpm.ro,www.insp.gov.ro).

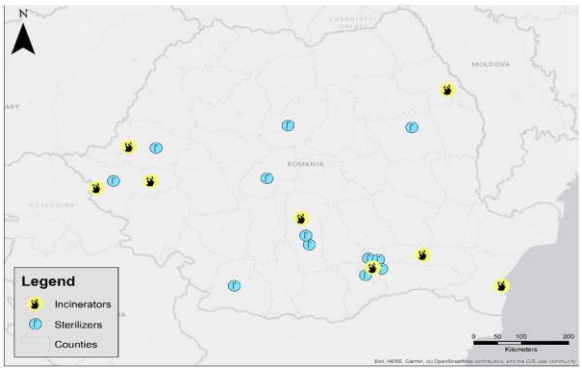

Fig.2. Medical waste disposal facilities-România(own source)

The training and specialization of operators of waste treatment facilities is vital in the compliant operation of technologies on the market. To carry out efficient final waste disposal activities, the operators must give an acute importance to the administered technologies, their life cycle by applying

ecological methods by establishing internal and external plans, procedures that minimize the impact of pollution on the environment based on the relationship: potential-performance-process (competitive advantage). The development of International Standards for the assessment of the life cycle of a product, in this case: Installations for the final disposal of hazardous waste, is an important step for a fair assessment of technologies, of technological profitability with the aim of optimizing the environmental performance of the installation waste disposal - ecological design LCA within a company is an environmental management technique, regarding the evaluation of the environmental aspects of the systems - product - facilities for the final disposal of hazardous waste - and of the potential impacts associated with the field of hazardous waste management. Analyzing the inventory of the relevant elements of input and output of the product system: hazardous waste disposal facilities, the decision-making factors contribute to the adoption and purchase of more efficient technologies, by assessing the risk given by an incineration facility, assessing the environmental performance by excluding gas consumption, adopting a third heat treatment technology based on electricity consumption.

Directive 2001/80/EC regarding the limitation of emissions of certain pollutants in the air from combustion installations aims to reduce the emissions of sulfur dioxide (SO_2) and nitrogen oxides, so that deposits and concentrations are below critical loadings and levels, including reduction of dust emissions. Emissions control plays an important role in the European Union's efforts to combat acidification, eutrophication, and ground-level ozone. The environmental audit and environmental impact assessment, with the identification of the negative aspects of each phase of the life cycle of hazardous waste incineration technologies, gives way to more ecological technologies, which lead to environmental benefits and savings, regarding the costs generated by the operation of the two technologies of hazardous waste disposal, in a comparative analysis: Advantages/Benefits. These LCA studies are important in selecting the best technology for the final disposal of hazardous medical waste, by selecting from several alternative ecological processes, respecting the provided proximity criterion in GEO 98/2021, with the application of "the best available BAT techniques, in achieving a high level of environmental protection.

Table 1

Factors considered in environmental assessment

Comparative analysis	Incineration plants: pyrolytic with two chambers and rotary ovens	• Treatment facilities by • thermal methods • chemical methods • Based on ionized radiation • biology
Technology	• Rotary oven • Furnace with liquid injection • Oven with static hearth • Gas purification by absorption with dry scrubbing or bag filters and/or alkaline wet scrubbing	• Neutralization by thermal sterilization (infectious waste and cutting stings • Autoclaving-chemical and pharmaceutical waste • Neutralization by heat sterilization at low temperatures with steam microwave treatment.
Processing capacity	500kg/h; 700kg/h 18.01.01 sharp objects (with the exception of 18.01.03*) 18.01.03*waste whose collection and disposal are subject to special measures regarding the prevention of infections 18.01.02 human fragments and organs, including blood and blood containers 18.01.08* Waste cytotoxic and cytostatic drugs 18.01.09 medicines, other than those specified in 18 01 08* in HG no. 856/2002 18.01.07. Laboratory chemicals other than those specified on 18.01.08* 18.01.06* Laboratory chemicals	200 kg/h-300 kg/h 18.01.01 sharp objects (with the exception of 18.01.03*) 18.01.03*waste whose collection and disposal are subject to special measures regarding the prevention of infections Surse:http://apmar.anpm.ro/AIM 3/20.10.2015 DEMECO SRL BACAU
Utility	• The water supply • The electricity network • Gas network • Water consumption	• The water supply • Electricity network 37kW • Water consumption 1-208 l water • Condensed water

		after the vaporization process is sterile
Mandatory condition	Oxygen in sufficient quantity to carry out the oxidation of the waste, which transforms the organic components into gaseous oxides: carbon dioxide and water, and the inorganic components are mineralized and transformed into ash	No special conditions are required
Processes preceding the elimination process	• assortment • grind • Maceration (slurries) • shuffle	• assortment • grind • shuffle
Time	The waste burns in a minimum of two seconds at the required temperature. The ratio of the volume of the combustion chamber and the flow of gases must ensure oxidation	The waste is neutralized in min. 10 minutes at the required temperature Source http://apmtm.anpm.ro/ AM 12195/23.02.2016 ECOLMED SRL TIMIS
Temperature	850*C and/or 1100*C (for waste with more than 1% halogen content	Low temperatures (105*C–177*C); Medium temperature (177*C -370*C); High temperature (540*C–830*C). Source: http://apmtm.anpm.ro/ AM 12195/23.02.2016 ECOLMED SRL TIMIS
Turbulence	The mixing continues with the aim of reducing the "cold" areas that can influence the oxidation reactions	Mixing continues
Final product - volume	About 4-6% ash Surse:http://apmct.anpm.ro AIM 3/07.03.2019 ECO FIRE SYSTEMS SRL CONSTANTA	• 20% by shredding • Dimensions max 2 cm, <10-15 mm Source:http://apmtm.anpm.ro/ AM12195/23.02.2016 ECOLMED SRL TIMIS •
Final residues	• Non-hazardous hearth ash according to analysis reports • The fly ash • Gaseous emissions	• Tartar products that require further processing or disposal • 19 02 04* – premixed waste, composed of

	(CO_2, H_2O, traces of organic compounds or acid gases • 19 01 05* – filter cakes from gas treatment; • 19 01 07* – solid waste from gas treatment; • 19 01 10* – spent activated carbon from flue gas treatment; • 19 01 11* – hearth ash and slag containing toxic substances; • 19 01 13* – fly ash containing toxic substances; • 19 01 15* – boiler dust containing toxic substances •	at least one hazardous waste; • 19 02 05* – sludge from physical-chemical purification, containing toxic substances; • 19 02 11* – other waste containing toxic substances; • 19 03 04* – waste marked as hazardous, partially stabilized; • 19 03 06* – waste marked as hazardous, solidified •
The final destination of the final product	Ash storage	Non-hazardous waste is eliminated by storage, being decontaminated waste reaching level IV of microbial inactivation - disintegrated waste
Environment protection	emissions of sulfur dioxide (SO_2), noxes, furans, nitrogen oxides...	• No air emissions • No vapors • Noise < 70 dB
Reuse	Waste gas cooling and self-directed heat recovery http://apmct.anpm.ro AIM 3/07.03.2019 ECO FIRE SYSTEMS SRL CONSTANTA	

3. Results and discussions

From the point of view of environmental protection, the suction system in the thermal treatment plant prevents dust from being thrown from the feed hopper and the exhaust hopper. Treating the air by washing, disinfecting, and filtering through active carbon preserves the quality of the air. The noise is below the minimum level of the standards in force. The efficiency of the technological flow of the thermal treatment installations is between 90-99%. Waste after thermal treatment becomes household waste, the volume reduction being up to 80%-90%. When incinerated, only about 4-6% ash results.

The thermal treatment facility is fully automated, so that the operator does not come into contact with medical waste, being equipped with an integrated control panel with a warning system in case of deficiencies during the process, with the display of operating parameters and alerts. The heat treatment plant is connected to a computer for automatic recording and archiving (on paper and in electronic format) of the heat treatment process.

The heat treatment facility for infectious medical waste works as a closed system so that throughout the heat treatment cycle the waste is not in contact with the atmosphere in the room (premises), starting with the stage of loading it into the equipment and until evacuation. The quality of thermally treated medical waste is constantly checked during the entire treatment process, with temperature recording for continuous monitoring. In order to "earn" the status of "performing" technology, periodic analysis reports are made. The reduction of contamination is determined by evaluating the microbiological degree, regarding the contamination of raw (untreated) and treated waste. During the test, the total flora of the raw waste before treatment varied between 2.2.104 CFU/g and 1.7.104 CFU/g (CFU= colony forming unit). After treatment, the total figures for the treated waste were negative (less than 4 CFU/g). The verification of the quality of the thermal treatment is done with the help of a blank sample that is introduced into the neutralization flow at the entrance to the action area and is recovered at the exit of sterilized waste. The quality of decontamination is checked in real time, and the operating parameters are recorded at the level of every 30 sec. Pungent and infectious waste that has been treated by thermal decontamination, including shredding and shredding, can be stored in a non-hazardous waste repository or incinerated.

Fig. 3. Shredded, sterilized, chopped waste source (own)

Self-monitoring in the case of incineration is the obligation of the economic operator and consists of monitoring emissions and the quality of environmental factors, technological monitoring, monitoring process variables, post-closure monitoring.

The incineration plants are made up of: automatic loading system for solid waste, automatic loading system for liquid waste and sludge, the incineration chamber consisting of 2 combustion zones each equipped with a system for overturning and mixing waste operated by a piston hydraulic for advancing and overturning the waste. Each combustion zone is equipped with a low NOx type burner, a ventilation system to ensure the oxygen required for combustion, an automatic ash cleaning system consisting of the discharge chamber located under the incinerator and which is equipped with an ash extinguishing tank. The tank is equipped with a chain conveyor, the post-combustion chamber for the post-combustion gases at a temperature of 1100˚C, the by-pass gas exhaust system located on the post-combustion chamber in the form of an exhaust chimney with a height of 12.5 m, gas cooling system consisting of a boiler with antifreeze and a system of heat exchangers for cooling gases from 1100˚C to 200 ˚C, system for treating burnt gases with activated carbon and sorbacal, system for creating depression in combustion chamber (exhauster), equipment for continuous monitoring of dust emissions, NOx, SO_2, CO, HCl, CO_2, TOC, O_2, gas pressure and temperature, control panel and electronic adjustment for burner temperature regulation and control automatic of the technological process.

According to the directives issued by the Ministry of Health through the Directorates of Public Health, during the Covid-19 period, all waste resulting from medical activities, including waste resulting from quarantine and vaccination centers, were eliminated only by incineration, which resulted in high sorting costs, their packaging, their temporary storage in compliant spaces, their handling, transport, the safety of exposed personnel and their disposal only by incineration. [15]. This period triggered a considerable pressure on the operators of incineration stations by allocating additional funds, for the compliant operation with the aim of eliminating the entire quantities of collected Covid-19 medical waste, avoiding environmental pollution, through their non-compliant storage, until their incineration.

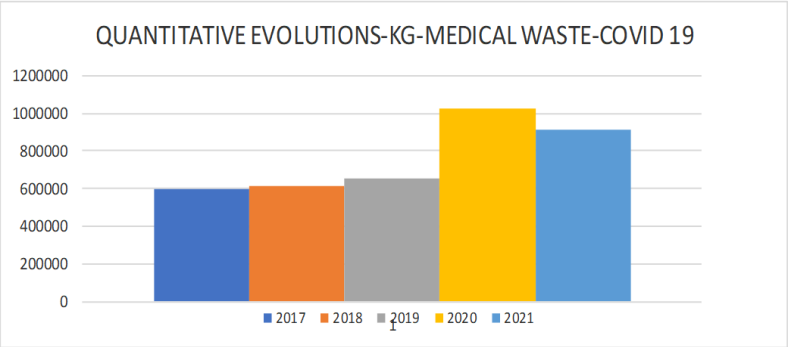

Fig.4. Medical waste (Source: DSP Galati report, APM Galati South-East, Romania)

Economic operators through the technology of waste disposal, which they manage, play an important role in protecting the environment, through the choice of technology, the acquisition of ecological technologies. LCA and LCT represent the concept of "ecological label" at the EU level. These criteria must be met by the installations during their entire life cycle. Public Authorities must support sustainable consumption, to significantly reduce the impact on the environment and the waste of material resources, energy, gas, water. LCA plays an important role in comparing waste disposal facilities. LCA provides an overview of the advantages, disadvantages, impact on the environment, the economic factor subject to amortization, encouraging the promotion of only technologies that register an efficient consumption of energy and raw materials.

4. Conclusions

The management of medical waste involves several factors, namely: the amount of waste generated, temporary storage conditions, heat treatment or incineration, infrastructure, ADR transport, protective equipment, staff specialization, the LCA of the facility for the final disposal of medical waste, the category of waste medical (dangerous/non-dangerous).

Comparing the hazardous waste disposal facilities, it can be observed that the direction is to support ecological facilities, to maximize the ecological, technical and management safety of infectious medical waste in relation to the served area directly proportional to the amounts of waste generated in the territory (demand/offer).

The activity of thermal treatment of infectious medical waste does not eliminate noxious and harmful substances in the atmosphere or in the soil. The waste resulting from heat treatment is microbiologically inert, chopped and compacted. Medical waste thermal treatment facilities work in such a way that following the process infectious medical waste will be harmless and unrecognizable [16].

Economic efficiency consists in reduced operational costs: no high-water consumption, no gas at some treatment stations, chopping technology with very good yield. Reducing the volume of waste implies reducing transport and storage costs. With heat treatment technologies, there are no risks to environmental factors. The technology of shredding infectious medical waste minimizes the risks of ineffective neutralization, on part of the waste introduced in the process. No pressure vessels are used, which eliminates the risk of explosions. It does not require effluents in operation (water, liquid, or steam). There are no odors emitted and there is no atmospheric pollution. The discharge of the resulting household

water will be carried out in the existing network on the site that is served by the treatment plant and then in the existing sewerage network [17].

The risks of the medical waste treatment operation are represented by the possibility of technical malfunctions, malfunctions of the shredder or waste compactors, making the operation of the installation impossible. Depending on the hazardous content of the medical waste, the water from the medical waste treatment facilities may contain contaminated organic and inorganic substances. In this case, analysis reports must be made, to be able to discharge the wastewater into the sewage networks or directly into the treatment plants.

The risks of the incineration operation are associated with the control of emissions, dioxins, furans, hydrocarbons. The content of heavy metals in the resulting ash, before it is finally deposited, represents a danger to the environment [18].

Understanding the situation at the national level regarding the medical waste management system implies the need to access new funds with the creation of a favorable environment to acquire facilities for the final disposal of medical waste, considering the LCA of the currently authorized facilities, the technological capacity of them regarding the processing of medical waste directly proportional to the amount of medical waste generated at the medical level, taking into account special situations such as Covid-19.

Due to the fact that public and private sanitary units generate the entire amount of Class 18.01 medical waste (HG856/2022), it is preferable from the point of view of economic efficiency and environmental protection, for an authorized operator on the market to own both disposal facilities medical waste, of different capacities, being able to eliminate all categories of waste generated in the serviced area. The efficient use of resources refers to the amount of resources consumed, which balances natural resources in relation to economic benefits. Efficiency means the relationship between inputs and material outputs, raw materials [19]. Possibilities for efficiency are realized in improving the benefits obtained per resource unit, which reduces the impact on the environment, namely the life cycle of the product. From the point of view of the economic result given by the good management of the resources necessary for the proper functioning of the facilities for the final disposal of medical waste, it is a challenge for both the public and the private sector. Both sectors must work together to implement successful environmental policies. Efficient management of resources reduces operating costs, increases profit, while reducing non-generable materials. These indicators provide a potential for operators to improve and develop their activity[20]. These streamlining actions open the way to a sustainable and circular economy, which will require the adoption of technologies to change the status of waste following the treatment treatments applied to by-products, for example the recovery of metals from the product resulting from the final disposal of medical

waste. For example: waste class 18.01.01 after the treatment operation, the status of the waste changes and it can be subject to recovery valorization of metals.

REFERENCES

[1] https://environment.ec.europa.eu/topics/waste-and-recycling/waste-framework-directive_en
[2]https://expertdeseuri.ro/wp-content/uploads/2019/02/gestionarea-deseurilor.png,accessed 03.11.2022
[3].Directive 2008/98/EC of the European Parliament and of the Council of November 19, 2008 on waste and the repeal of certain directives.
[4].Regulation 2014/1357/EU replacing Annex III to Directive 2008/98/EC on waste and repealing certain directives
[5].Directive 98/31/EC on waste disposal
[6].Directive 2018/850 of the European Parliament and of the Council of 30 May 2018 amending Directive 1999/31/EC on waste deposits.
[7].Regulation 2017/997/EU amending Annex III to Directive 2008/98/EC regarding the property of hazardous substances HP 14 "Ecotoxic"; Directive 99/31/EC on waste storage;
[8].Directive (EU) 2018/850 of the European Parliament and of the Council of 30 May 2018 amending Directive 1999/31/EC on landfills;
[9].Directive 2010/75/EU on industrial emissions.
[10].Commission Decision 2014/955/EU of December 18, 2014 amending Decision 2000/532/EC establishing a list of waste pursuant to Directive 2008/98/EC of the European Parliament and of the Council.
[11].WHO no. 1226/2012 - *Technical norms regarding the management of waste resulting from medical activities*
[12].WHO no. 1279/2012 - *Criteria for evaluating the operating conditions and monitoring of treatment equipment through thermal decontamination at low temperatures*
[13].WHO no. 119/2014 *Public health hygiene norms regarding the living environment of the population*
[14].Directive 2000/76/EC of the European Parliament and of the Council of December 4, 2000 on waste incineration
[15].CureaO., BratuA.M., ConstantinM., TeodorescuS.E.,*Waste resulting from medical activity - Legal requirements and good practices*, INS Bucharest, 2021.
[16].AlamO.,*A preliminary life cycle assessment on healthcare waste management in Chittagong City, Bangladesh*, (2019).
[17].DeepakA., *Life cycle assessment of biomedical waste management for reduced environmental impacts*, (2022).
[18].GhoushchiS.J.,*Barriers to circular economy implementation in designing of sustainable medical waste management systems using a new extended decision-making and FMEA models*, (2022).
[19].GovindanK.,*Green reverse logistics network design for medical waste management: A circular economy transition through case approach*, (2022).
[20].MacNeillA.J.,*Transforming the Medical Device Industry: Road Map To A Circular Economy*, (2020).

[21].www.nonarm-europe.orgHCWH Europe,*Sustainable healthcare waste management in the EU Circular Economy model*.
[22].November 2020 costs, health, efficient management
[23].MantzarasG.,*An optimization model for collection, haul, transfer, treatment and disposal of infectious medical waste: Application to a Greek region Transportation costs location of treatment stations Waste*, (2017).
[24].GEO no. 68/2016 for the amendment and completion of Law no. 211/2011 on the waste regime.
[25].GEO no. 92/2021 - waste regime.
[26].GD no. 856/2002 regarding waste management record and approval of the list including hazardous waste.
[27].Law no. 278/2013 on industrial emissions.
[28].HG no. 942/20.12.2017 National waste management plan 2018-2025.
[29].GD no. 870/06.11.2013 regarding the approval of the National Waste Management Strategy 2014-2020.
[30].GD no. 942/2017 National waste management plan of December 20, 2017
[31].https://legislatie.just.ro/Public/DetaliiDocumentAfis/198167 accessed 03.11.2022 at 16.51
[32].http://www.mmediu.ro/beta/wp-content/uploads/2013/01/2013-01-11-DGDSP-SNGD.pdf accessed 03.11.2022 16.55.
[33].www.anpm – List of operators authorized at national level for collection, transport and disposal of medical waste.
[34].www.anpmhttp://apmmm.anpm.ro/documents/23445/34579012/SNGD-Strategia+Nationala+Gestionare+Deseuri_2014-2020.pdf/1d8438f4-be58-414f-97d8423095050001, accessed 03.11.2022 at 15.00
[35].http://apmtm.anpm.ro/ AM 12195/23.02.2016 ECOLMED SRL TIMIS.
[36].http://apmar.anpm.ro/ AIM 3/20.10.2015 DEMECO SRL BACAU.
[37].http://apmct.anpm.ro AIM 3/07.03.2019 ECO FIRE SISTEMS SRL CONSTANTA.

IMPACT OF POLAR COMPOUNDS AND ADDITIVES ON DIESEL FUEL LUBRICATION

Mariana A. GRIGORE (GEAMĂN)[1], Anișoara A. NEAGU[1*]

[1] Ovidius University of Constanta, 124 Mamaia Blvd., Constanta, 900527, Romania

Abstract

The study aims to evaluate and improve the lubricity of the hydrotreated gas oil by additivation with any polar compounds, especially designed for this purpose. The primary distillation diesel had a sulphur content of 1093.0 ppm and nitrogen 90.04 ppm, compared to the other four hydrotreated diesel where the sulphur content varied between 3.0 and 13.1 ppm, and the nitrogen content varied between 26.9 and 47.3 ppm. Regarding the lubricity of diesel fractions, before and after hydrofining, a rather large difference is found between the lubricating power of the diesel before the hydrogenation (Wear Scar Diameter WSD=186 μm) and the other four hydrorefined (WSD>186 μm), the former demonstrating a very good lubrication, compared to the other hydrotreated where polar species content decreased. Lubrication testing of two diesel mixtures produced in an oil refinery, which serves as a test in the additivation process, showed that the blend consisting of diesel mixture M1 demonstrated poorer lubrication properties (WSD=625 μm) than diesel mixture M2 (WSD=560 μm). The diesel mixture M1 with reduced lubricating properties is subjected to additivation with four commercial lubricity additives (Additive I, Additive II, Additive III and Additive IV) in concentrations of 50, 100, 150 and 200 ppm, respectively. The results showed an increase in lubricity of diesel mixture M1, for every 50 ppm of additive added, pointing out that Additive IV had the biggest effect on lubrication, becoming the most efficient of all. The diesel fuel with Additive IV presents variable stability of WSD, slightly decreasing in time, almost linearly.

Keywords: diesel fuel, lubricity, wear scar diameter, additivation,

1. Introduction

The continuing worldwide trend to develop engine performances and reduce emissions has caused the development of new generations of fuel injection equipment and diesel fuels, such as low-sulphur diesel fuel.

Due to wide range of compositions, it is significant to understand how the various constituents in diesel fuel contribute to natural lubrication. Components in fuels with polar character (naphthenes, polyaromatics, compounds with sulphur, nitrogen, and oxygen) managed good lubrication of diesel engine [1]. Unfortunately, these components are removed during the hydrotreating process of diesel, leading to the loss of lubricating properties.

*Corresponding author: email address: zanisoara@univ-ovidius.ro

Lubrication is a qualitative term describing the ability of a fluid to reduce friction and wear between two surfaces in relative motion under load.

The injection system in compression combustion engines is based on the lubricating properties of diesel fuel. The short life of engine components such as fuel injection pumps has been attributed to the lack of diesel lubrication [2-3].

Earlier researchers and studies, as well as the current ones, aim to elucidate and solve the problems at the diesel fuel processing level. Solving the shortcomings of lubrication is based on the qualitative evaluation of the lubricating properties, the characterization of the structural composition, considering repercussion and the improvement of deficiencies. The preliminary research of Wei and Spike [1] consistently noted that the presence of sulphur compounds and nitrogen compounds reduced wear scar and is related to further studies [4-16] on characterization and improvement of diesel oil's lubricating properties.

The present experimental work is meant to contribute to improve the lubricity of the hydrotreated gas oil by additivation. Laboratory test methods have been developed to simulate authentic wear mechanisms and consist both in measuring the lubricity of the fuel and finding the active components providing good lubrication to the fuel, but also in characterization of what can be considered *fuel with adequate lubrication*. Wear Scar Diameter (WSD) evaluates lubricity. To meet lubrication standards, the wear scar diameter generated under specified conditions must not exceed 460μm or 560μm, according to European and USA regulations, respectively. One of standard methods is the High-Frequency Reciprocating Rig (HFRR) and was applied in this study.

2. Experimental

The study consists in a series of interdependent analytical experiments, namely:

- ✓ Determination of sulphur and nitrogen concentration in diesel fuel before and after hydrotreating process, knowing that they are present in polar compounds, assumed to be responsible for the natural lubrication of diesel fuel.
- ✓ Evaluation of polar compounds' impact on natural lubrication, by characterizing the wearing behaviour of the fuel before and after the hydrotreating process.
- ✓ Comparative lubricity characterization of two diesel mixtures produced in a refinery, which will serve as a base in the additivation process.

- ✓ Study of four lubricity additives, with the aim of finding the most effective among them [17].
- ✓ Monitoring of the selected additive during eight weeks of storage, by weekly wear spot tests.

Materials

The samples analysed are: one gas oil from crude oil primary distillation (AD), before being processes in the hydrotreating process, and four hydrotreated types of gas oil. The four hydrotreated gas oils samples come from the mild hydrocracking (MHC) process, vacuum distillate hydrofining (VDH) process, diesel hydrofining (DH) process and from kerosene-diesel hydrofining (KDH) process. These four samples of gas oils are the basis of the formulation and qualitative evaluation of two mixtures of diesel (M1 and M2), which served as a test in the additivation process. From the two mixtures, the mixture with the lowest lubrication will be selected to accentuate the effect of the additives on it. The mixture of diesel (M1) is made of three gas oils fractions (60% of DH-MHC and 40% of VOH) and the mixture of diesel (M2) is made of from three gas oils fractions (60% of KDH -MHC and 40% of VDH). These samples were obtained in an oil refinery in the southeast of the country.

Four commercial lubricity additives (Additive I, Additive II, Additive III and Additive IV) were added in the mixture of diesel fractions M1, in various concentrations. Most commercial additives are made-up of long-chain carboxylic acids. Lubricity additives also include a range of surface-active chemicals. They show an affinity for metal surfaces and form barrier films at the metal-to-metal contact, which would otherwise have resulted in wear under light to moderate loads. The lubrication/anti-wear properties of diesel fuel are provided in trace concentration and form a protective layer on the metal surface.

All reagents used in this study were of analytical grade.

Equipment and methods

The sampling was conducted according to the standard procedures ASTM D4057-19/SR EN ISO3170:04 presenting the conditions for obtaining liquid/semi-liquid products/hydrocarbons from a reservoir, respectively from a pipeline by manual means, with the help of a harvester of oil samples, and in glass containers, respectively [18].

The High Frequency Reciprocating Rig (HFRR) is a microprocessor-controlled reciprocating friction and wear test system which supplies a fast, repeatable assessment of the performance of fuels and lubricants. This method has become the industry standard test for diesel fuel and is conforms ASTM D6079 [19], ASTM D7688 [20] and ISO 12156 [21]. The operating mechanism of the

HFRR device consists of a mechanical arm that simulates the vibration and friction and wear conditions in a pump or in an injector. In the HFRR test, a small sample of test fuel is placed in a temperature-controlled bath, joining contact between a steel ball and a flat steel disc. The temperature is set at 60 ^{0}C and the humidity is controlled and displayed. The ball is then lightly loaded with 2N and moved back and forth (reciprocating) across the disc at setted stroke and frequency. Friction coefficient, fuel temperature and electrical contact resistance are checked during the test. After 75 minutes, the wear scar diameter of the ball is measured using an optical microscope in the sliding direction (Y) and perpendicular to the sliding direction (X), and the average values on both axes are automatically displayed, according to figure 1 [22].

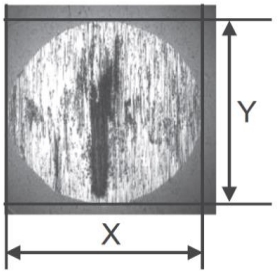

Fig. 1. Wear scar image of the ball after a test captured through the camera attached to the microscope [22]

The measure unit for lubrication is *μm* and it is reported that "WSD-method A" a with approximation of 10μm.

In figure 2, it is shown the schematic diagram of the HFRR device [23].

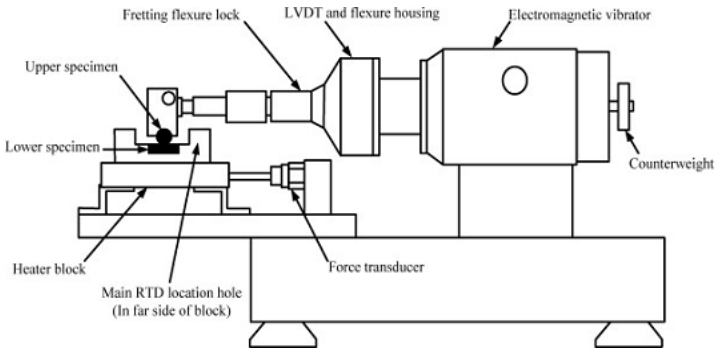

Fig. 2. Schematic diagram of the mechanical unit of HFRR device [23]

In figure 3, it is shown the principle of the lubrication test mechanism in the HFRR device [24].

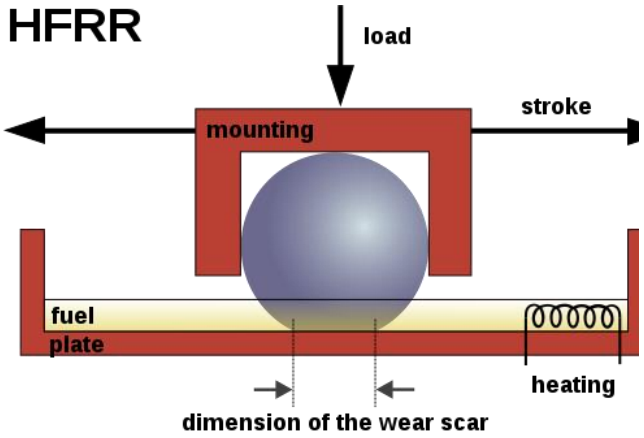

Fig. 3. The principle of the lubrication test mechanism in the HFRR device [24]

The determination of sulphur and nitrogen content is one of the most important properties that ensures the quality and performance of diesel fuel, especially when considering the effect on air pollution and the lubrication capacity of the mechanical components in the engine. So, the sulphur and nitrogen content were determined according to the standard procedures ASTM D5453-12 [25] with the sulphur analyser and ASTM D5762 [26] with the nitrogen analyser, respectively. Both tests are based on the same determination principle, the combustion at the high temperature in a combustion tube with oxides formation followed by quantifying by fluorescence.

Determination of the diesel quality before and after the additivation is performed. In addition to sulphur and nitrogen content, other properties are determined: the water content according to SR EN ISO 12937:01, the density according to ASTM D450-18a, the cetane number according to ASTM D613-05, the flash point according to ASTM D93-13, the calorific power according to ASTM D240-19, the viscosity according to ASTM D445-06 and the corrosion according to ASTM D130-12.

3. Results and discussions

The determination of active polar compounds (content of sulfur and nitrogen) in diesel fuel is conducted on five samples, one being the gas oil proceeding from crude oil primary distillation, before being processed in the hydrotreating process and four hydrotreating types of gas oil fractions obtained the refinery. Results obtained from the sulfur and nitrogen content determinations of the five gas samples are shown in table 1.

Table 1

Sulfur and nitrogen contents in gas oil fractions

Sample	The sulfur content (ppm)	The nitrogen content (ppm)
Atmospheric distillation gas oil (AD)	1093.0	90.04
Diesel from Mild Hydrocracking unit (MHC)	3.0	26.9
Hydrotreated vacuum distillate (VDH)	12.9	7.5
Hydrotreated diesel (PDH)	10.6	23.1
Hydrotreated diesel from (KDH) process	13.1	47.3

In table 1, a considerable disproportionality can be seen between the two types of diesels, the untreated with hydrogen and the hydrotreated ones. Thus, the primary distillation gas oil presented a sulfur content of 1093.0 ppm and nitrogen of 90.04 ppm, compared to the other four gas oils in which the sulfur content varied between 3.0 and 13.1 ppm, and the nitrogen content varied between 26.9 and 47.3 ppm.

To evaluate the impact of active polar compounds on diesel lubrication, the five samples are tribologically analysed with the HFRR device. The results are presented in table 2 and are related to the sulphur and nitrogen content. The characteristics considered in the analysis of diesel lubrication are the diameter of the wear scar (WDS), the percentage of film formation and the digital image of the scar.

The results show quite a significant difference between the lubricating power of diesel not yet subject to hydrorefining and the other four hydrotreated, first benefiting from exceptionally good lubrication. It was noted the proportionality between the content of polar compounds and the lubricity of diesel fuels. Thus, higher the content of polar species, the better lubricating properties of fuels. Also, these polar compounds promote the formation of the tribofilm protecting the metal surfaces in contact.

At the same time, the causality of poor lubrication is showed, namely the hydrorefining process, through which the polar actives species are removed from diesel and with them disappearing the potential natural lubrication.

The results of this study are consistent with the fundamental ideas of Wei and Spike [1] and previous researchers [4-5, 27-28].

Table 2

Lubricity of gas oil fractions, before and after hydrorefining

Sample	Lubricating power (WSD) [μm]	The percentage of film formation [%]	Wear scar image
Atmospheric distillation gas oil (AD)	186	95	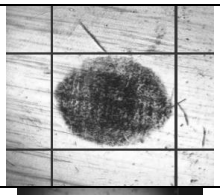
Diesel from Mild Hydrocracking unit (MHC)	523	13	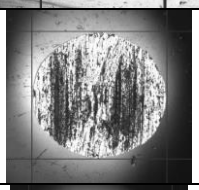
Hydrotreated vacuum distillate (VDH)	704	7	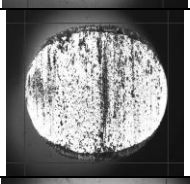
Hydrotreated diesel (PDH)	502	40	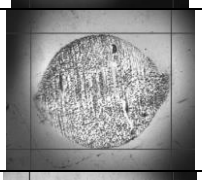
Hydrotreated diesel from (KDH) unit	489	12	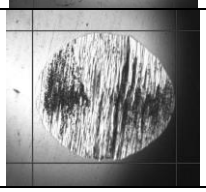

Further, the characterization of two diesel mixtures: M1 and M2 were carried out in terms of the lubricity. Finally, the choice of one of them followed, according to the lowest lubrication power to accentuate the effects of the additives. Table 3 shows the results obtained.

According to the results show in table 3, it is found that the diesel mixture M1 from the PDH, VDH and MHC plants has weaker lubrication properties, having a larger wear scar diameter, 625μm, compared to the wear scar of the diesel mixture M2 from the KDH, VDH and MHC plants, which has a diameter of 560 μm, so

that the poorest mixture M1 was subject to a study about the effect of four commercial lubricity additives on it.

Table 3

Lubricity of two samples of diesel mixture

Sample		Lubricating power (WDS) [μm]	Wear scar image
Mixture	Components		
Diesel M1	Hydrotreated diesel (PDH)	625	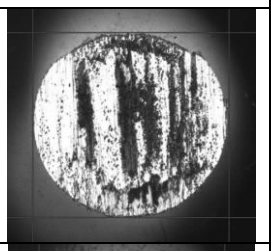
	Hydrotreated diesel (VDH)		
	Diesel from Mild Hydrocracking unit (MHC)		
Diesel M2	Diesel from (KDH) unit	560	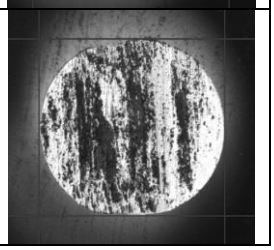
	Hydrotreated diesel (VDH)		
	Diesel from Mild Hydrocracking unit (MHC)		

The mixture M1 is added with four commercial lubricity additives (additive I, additive II, additive III and additive IV) in various concentrations. At this point, the evaluation and qualitative differentiation of the four additives was made, to find their lubrication power. Four mixtures of M1 were additivated with 50, 10, 150 and 200 ppm additive, respectively. Table 4 shows the results obtained.

According to the results presented in table 4, an increase in lubricity can be observed for all four additive diesels, starting from a wear of 625μm of the mixture M1 without additives. It is observed that the lubricating power of the diesel mixture M1 increased with each 50-ppm portion of additive added. The wear scar decreased to a minimum value of 355μm for the Additive IV added in 200 ppm proportion, hence the conclusion that this additive has the greatest effect on the lubrication of the diesel mixture M1 and, therefore it was evaluated as the most effective of the four tested additives. These results agree with the previous studies that were carried out to characterize anti-wear additives [3,6,7,8,17,29,30], thus classifying the Additive IV as adequate and effective in restoring the lubricating properties of the diesel mixture M1.

Table 4

Qualitative evaluation of the additives on diesel lubricity

The diesel mixture M1	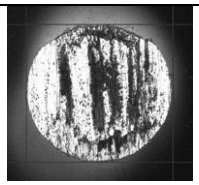 625µm			
Additive	Additive I	Additive II	Additive III	Additive IV
50 ppm	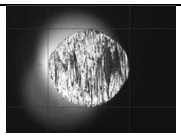 550µm	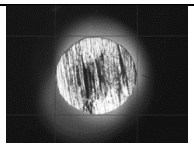 538µm	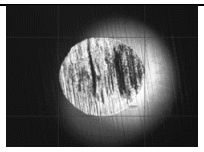 510µm	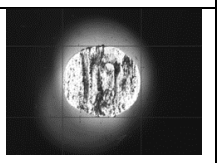 503µm
100 ppm	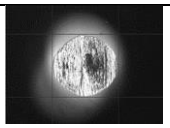 528µm	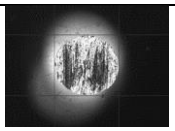 492µm	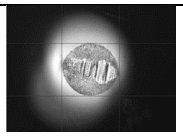 475µm	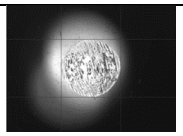 472µm
150 ppm	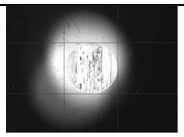 458µm	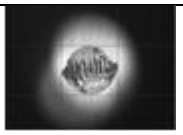 442µm	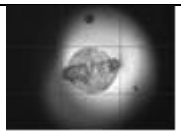 447µm	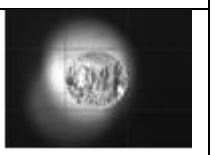 441µm
200 ppm	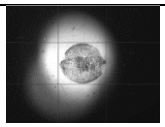 378µm	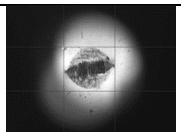 362µm	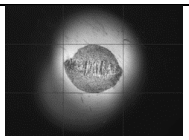 385µm	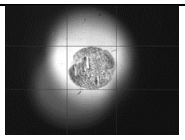 355µm

To evaluate the possibility of the Additive IV modifying other properties of the diesel mixture M1, certain analytical determinations were performed regarding the quality of the diesel fuel before and after additive adding. The properties were: sulfur and nitrogen content, the water content, the density, the cetane number, the flash point, the calorific power, the viscosity, and the corrosion, in accordance with standards [18-21,25-26].

Table 5

The properties of the diesel mixture M1 before and after Additive IV added

Mixture / Properties	The diesel mixture M1	The diesel mixture M1 + 100 ppm Additive IV
Density at 15°C, (g/cm^3)	0.8353	0.8355
The sulfur content, (ppm)	9.36	9.41
The nitrogen content, (ppm)	17.65	17.70
The water content, (ppm)	89.0	90.4
Cetane number	51.2	51.2
The flash point, (°C)	59.0	59.0
Calorific power, (kcal/kg)	10389.8	10389.9
The viscosity at 40°C, (mm^2/s)	2.325	2.327
Corrosiveness to Copper (3 h at 50°C)	1a	1a

According to the results of table 5, there is an insignificant difference between the properties of the diesel mixture M1 before and after additive adding, this indicating that the additive does not significantly affect the quality and performance of the diesel fuel, other than lubricity.

The diesel mixture M1 added with 100 ppm of Additive IV was subject to monitoring over an interval of eight weeks to estimate the stability over time of its lubrication properties (WDS and the film formation). Table 6 shows the results obtained.

Table 6

Monitoring results

Week	0	1	2	3	4	5	6	7
Lubricating power (WDS) [µm]	472	475	479	483	487	490	494	499
Wear scar image				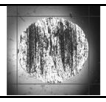	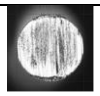	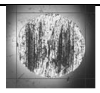	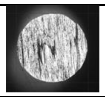	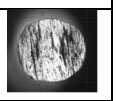

The results presented in Table 6 show that a minor increase can be noticed in wear, in the diesel mixture M1 and implicitly a reduction in lubricity. Comparing the initial result with the one from the eight weeks, a difference of 33µm is noted. This value is related to the time interval allocated to the statistical study, but it exceeds the maximum limit of the lubrication power allowed by the European regulations, namely 460µm, always complying with USA regulation - 560µm, respectively. The differential variation of diesel lubricity from week to week is noted, with values fluctuating between 3 and 6µm. It is observed that the additive in the composition of diesel shows a variable stability over time, almost linear according to the figure 4.

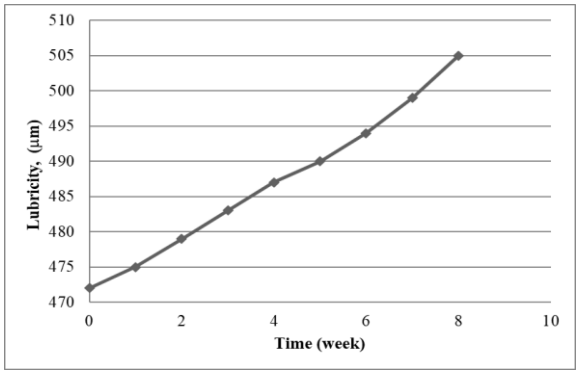

Fig. 4. The variation of the lubricity of the diesel mixture over a period of eight weeks

4. Conclusions

Due to the new fuel quality regulations regarding the upper content of sulphur of 10 ppm, the hydrotreating processes have seen aggressive and obvious progress. This severity was observed early in the implementation of the new extremely low sulfur content in the fuel, due to failures in pumps and injectors. These issues led to the deduction of problems and implicitly to their development and solution. Hydrotreating processes are the cause of poor lubricity in diesel fuel, due to the removal of polar compounds together with sulfur ones. Lubrication analyses appeared as a solution to these complications, with a role in reducing friction and preventing wear. Lubrication is a tribological term based on the ability of a fluid to provide good hydrodynamics to a metal contact. Lubrication is based on the formation of a tribofilm responsible for the actual sliding, due to intra- and intermolecular interactions of a physical or chemical nature. The most effective method of evaluating the lubrication of diesel fuel it turned out to be HFRR and the lubrication is evaluated by the wear scar diameter, this being inversely proportional to the lubrication. Improving the lubricity of diesel fuel was achieved using chemical or bio additives. Among the four additives used in this study, Additive IV presented the greatest positive impact on the lubricating properties. Studies like this one can serve to make the selection of the most effective lubricity additive for a specific crude oil processed in the oil refinery.

REFERENCES

[1] Spikes, H. A., Wei, D. P., *The lubricity of diesel fuel. Wear, Petroleum Refining Research Institute*, Beijing (China), Imperial College of London, Department of Mechanical Engineering, Tribology Section, London (UK), *Elsevier Sequoia Publishing*, 1986, 217-235
[2] ***ASTM D6079-18, https://www.astm.org/Standards/D6079,

[3] Agarwal, S, Chhibber, V. K., Bhatnagar, A. K., Tribological behavior of diesel fuels and the effect of anti-wear additives, *Elsevier INC., Fuel 106*, (2013), 21-29
[4] M. Matzeke, A. Jess, U. Litzow, Polar nitrogen-containing aromatic compounds as carriers of natural diesel lubricity, Elsevier Ltd., *Fuel 140* (2015), 770-777
[5] G. Anastopoulos, E. Lois, D. Karonis, S. Kalligeros, F. Zannikos, Impact of oxygen and nitrogen compounds on the lubrication properties of low sulfur diesel fuels, National Technical University of Athens, Elsevier Ltd., Athens, Greece, *Energy 30*, (2005), 415-426
[6] M. F. Fox, Development of the diesel fuel additive lubricity model, Engineering Tribology, Vol. 221, Institut of Tribology, University of Leeds, Leeds, Great Britain, 2007, 161-164
[7] M. F. Fox, A model for diesel fuel additive lubricity, Elsevier B.V., University of Montfort, Leicester, Great Britain, *Life Cycle Tribology*, (2005), 585-591
[8] D. Claydon, the use of lubricity additives to keep fuel quality in low sulfur diesel fuel, *Afton Chemical*, Great Britain, (2014), 342-353
[9] M.W. Sulek, A. Kulczycki, A. Malysa, Assessment of lubricity of compositions of fuel oil with biocomponents derived from rapeseed, Elsevier Inc. *Wear 268*, (2010), 104-108
[10] M. Muñoz, F. Moreno, C. Monné, J. Morea, J. Terradillos, Biodiesel improves lubricity of new low sulphur diesel fuels, Elsevier Ltd., *Renewable Energy 36*, (2011), 2918-2924
[11] Yufu Xu, Qiongjie Wang, Xianguo Hua, Chuan Li, Xifeng Zhu, Characterization of the lubricity of bio-oil/diesel fuel blends by high frequency reciprocating test rig, Elsevier Ltd, *Energy 35*, (2010), 283-287
[12] M. A. Hazrat, M. G. Rasul, M. M. K. Khan, Lubricity Improvement of the Ultra-low Sulfur Diesel Fuel with the Biodiesel, Elsevier Ltd., *Energi Procedia 75*, (2015), 11-117
[13] Titipong I, Dalai AK, Desai P., Evaluating esters derived from mustard oil as potential diesel additives, *Journal of American Chemical Society*, (2011), 391-402
[14] Drown D.C, Harper K, Frame E., Screening vegetable oil alcohol esters as fuel lubricity enhancers, *Journal of American Chemical Society*, (2001), 579-584
[15] Subongkoj T, Nuwong C., Biodiesel as a lubricity additive for ultra-low sulfur diesel. *Songklanakarin Journal Scientific Technology*, (2010), 153-156
[16] The Diesel Place & Spicer AD, Arlen Spicer. *Diesel fuel lubricity additives study results*, 2007,
[17] Delgado, J., Gadea, M., Esarte, C., Peláez, A., HFRR and SL-BOCLE Lubricity of Paraffinic Diesel Fuels Considering Different Origins and Final Formulations with Biodiesels and Additives, American Chemical Society, *Energy and Fuels*, 34, (2020), 2654-2664
[18] https://buildideas.co/2021/12/21/astm-d-4057-95-reapproved-2000-pdf-free-download
[19] https://pdfcoffee.com/astm-d6079dvfr3720pdf-pdf-free.html
[20] https://www.astm.org/d7688-18.html
[21] https://www.sis.se/api/document/preview/80007413/
[22] https://pcs-instruments.com/wp-content/uploads/2014/03/HFRR-Brochure-2019-v1.pdf
[23] Sukjit, E., Dearn, K.D., Enhancing the lubricity of an environmentally friendly Swedish diesel fuel MK1, University of Birmingham, Birmingham, Great Britain, Elsevier Inc., *Wear 271*, (2011), 1772-1777
[24] https://en.wikipedia.org/wiki/HFRR#/media/File:HFRR_en.svg
[25] https://www.astm.org/Standards/D5453.htm
[26] https://www.astm.org/Standards/D5762.htm
[27] Hammock, B.J., Schimd, S.R., Jacobs, B.O., *Fundamentals of Fluid Film Lubrication, Second Edition*, Marcel Dekker Inc., New York, S.U.A., 2004
[28] Onion, G., Generation, and properties of boundary films formed by diesel fuel at a steel/steel conjunction, *Tribol. Ent.*, 17, (1984), 277 – 287

[29] Kolm, R., Gebeshuber, I.C., Kensey, E., *Life Cycle Tribology, Tribochemistry of mono molecular additive films on metal surfaces, investigated by XPS and HFRR*, Elsevier B.V., Vienna, Austria, 2005, 269-281
[30] Srivastava, P., Hancsok, J., *Fuels and fuel-additives*, John Wiley&Sons, Inc. Hoboken, New Jersey, 2014, 229-233

PARAMETERS ESTIMATION IN NEW KINETIC MODEL FOR MILD-HYDROCRACKING PROCESS

Cosmin COJOCARU[1] and Claudia I. KONCSAG[1*]

[1]Ovidius University of Constanța, 124, Mamaia Blvd., Constanța, 900527

Abstract

This paper aims to estimate the kinetic parameters of a 5-lump model for the mild-hydrocracking process reactions. Using industrial process data, an original kinetic model is developed using the computer simulation environment Berkeley Madonna. Afterwards, the model is simplified to eliminate irrelevant reaction paths. The kinetic parameters for the given reactions are estimated with routine compiled in MATLAB. Using a non-linear approach to optimize the results, the absolute error between the real product yields and the estimated ones is minimized. The order of magnitude for the kinetic parameters is the same with the one cited by other specialists and the relative error of predicting the yield of the Diesel oil is 4%.

Key words: mild-hydrocracking; parameter estimation; original; kinetic model; non-linear; hydrocarbon lumps.

1. Introduction

Toughening of the sulfur limit toleration in fuels, corroborated with squeezing the bottom barrel, lead to the decision of mild-hydrocracking unit integration, as the preferred upgrade for the typical European refinery. Keeping in mind high operational cost as severe reaction conditions are required, this chemical process must be improved so that to provide high return and flexibility in operation. Efficient technology and operation of the unit isn't always reflected in the economical results, having been registered even worsening results at changing the feedstock quality or at the start/end of the catalytic cycle. The complete control over a hydrocarbon conversion unit can be achieved using a good model for yields prediction based on the reaction kinetics.

A wide palette of kinetic models developed in the last years is presented by Thybaut and Marin [1]. Given the difficulty of characterizing crude fractions as feed and products of the process, the simplest method is to consider the discrete lumped models.

Discrete lumped models can be based on distillation ranges [2] or on pseudo-components (basically hydrocarbon classes) [3]. In literature, the preferred method was that based on distillation range. The models evolved from simply three-lump [4] (Maya residue, light oils and gases) to four-lump [5], or six-lump

*Corresponding author: email address: ckoncsag@yahoo.com

[6,7], in case of vacuum oil feed. Sometimes, the network is simplified afterwards, to reduce the complexity without increasing the model error [5, 6]. Their common characteristic is that each model is optimized and adapted for an individual process, without standardization. Depending on the severity of the process conditions, an extra coke lump (formed on the catalyst) or various middle distillates such as kerosene and light/heavy naphtha can be included [8].

Another lumping method is based on continuous kinetics, by assuming that the product distribution changes continuously and calculating the reaction rate accordingly, in simulations and optimization routines [9, 10].

Single event micro-kinetics models, describing in detail the chemistry of the process is another category gaining attention [11]. This method requires extensive computational work and should be used complementary, in conjunction with the continuous lumping model, for better results [12].

Among these methods, the lumped method based on the fraction boiling points seems simplistic but proved to be reliable especially when corroborated with accurate input data. After the characterization of the components, a kinetic network is established to simulate the chemical reactions taking place during the passage of the feedstock through the reactors. More accurate results are obtained using more lumps, hence more kinetic parameters to estimate. These networks can become very complex, having to simulate first/second order reactions, irreversible reactions and assume hydrocracking, thermal cracking, and coke formation reactions [3].

The kinetic parameters of the model serve to predict the yields of the process component fractions at the end of the reaction section. Estimation of these parameters is complex, due to high number of unknown or insufficient available equations. Various studies show successful results in using non-linear methods of estimation [6, 7].

To achieve minimum error, the model is optimized using of the least squares method [12] or a non-linear optimization one, such as particle swarm [13].

In this paper, a 5-lump kinetic model is proposed, for a custom mild-hydrocracking process. Industrial operating data have been used to start from the real reaction conditions. The model implies the estimation of the parameters of a 15 irreversible hydrocracking reactions network. The model is simulated with Berkeley Madonna [14], where the reactions in time evolution are followed and mass balance can be expressed. The initial values for the kinetic parameters are taken from studies above mentioned [2, 6, 7].

To fit the actual yields to the output data from simulated kinetics, the data generated by Berkeley Madonna software [14] are used in a non-linear parameter estimation software written in MATLAB [15,16]. The obtained results are optimized with each iteration, having as an objective function the minimization of error between real and predicted component yields. To reduce the errors, the

kinetic network is reduced to 6 reactions, by eliminating the reactions with low impact, due to their irrelevant reaction rate.

2. Experimental

2.1. Experimental setup and data collection

The experimental data were collected in an industrial mild hydrocracking unit with two reactors in series, cumulating 592 m^3 NiCoMo catalyst in their fixed beds.

The feed during the test was mixed vacuum gas oil (VGO) with heavy gas oil proceeding from the coke unit. The main product is the Diesel (D) with less than 10 ppm wt sulphur. Also, two fractions of naphtha with low sulphur are obtained, and gases. The residue is further processed in a FCC unit.

Thirty sets of running data were selected in three campaigns: first 10 sets for medium values parameters, when the performance was measured as 2.7-2.8 ppm sulphur in gasoil, the following 10 sets for performance of 1.1-1.2 ppm sulphur in GO, when the unit ran in more severe conditions and the last 10 sets for 3.3-6.1 ppm sulphur, when the regime was milder. The data sets are not temporally consecutive but collected in different days and chosen following the main performance (sulphur content in Diesel), thus ensuring that the kinetic model is independent of acquisition time. The data were collected over a 3-month period, served to calibrate the kinetic model, then this one was validated with experimental data in the very next month, so that catalyst deactivation doesn't affect the kinetic parameters. The test period corresponds to a normal running, in the midst of the catalyst cycle, with the catalyst unaffected by deactivation. For different conditions, the model should be re-calibrated.

The feed had a constant quality on long-term running, with a specific gravity 0.948 (ASTM D1298), distillation range 265-565^{o}C (ASTM D-1160), sulphur 1.73% wt (ASTM D-2622), and Conradson coke 0.49% wt (ASTM D-4530).

The products are: C_1- C_4 gases, light naphtha (specific gravity 0.725, distillation range 38-137^{o}C), heavy gasoline (specific gravity 0.737, distillation range 65-219^{o}C) and Diesel (specific gravity 0.866, distillation range 169-364^{o}C).

The main parameters in the reaction unit are presents in Table 1. Since there are two reactors in series, the reaction unit is represented as a single plug flow reactor.

Table 1

Main parameters of reaction unit

#	Feed flowrate (m^3/h)	LHSV, h^{-1}	Reactor temperature (°C)	
			Inlet	Outlet
1	145.4	0.25	355.5	368.9
2	147.7	0.25	355.0	367.4
3	98.2	0.17	340.7	351.7
4	229.0	0.39	385.6	395.0
5	150.0	0.25	355.9	369.1
6	207.5	0.35	379.4	389.7
7	214.7	0.36	380.7	390.6
8	234.0	0.40	383.3	392.9
9	235.1	0.40	383.3	392.6
10	240.2	0.41	384.5	393.9
11	240.0	0.41	384.6	393.8
12	241.4	0.41	384.7	394.0
13	240.0	0.41	384.5	393.9
14	239.0	0.40	384.5	393.9
15	228.9	0.39	385.5	394.8
16	222.9	0.38	385.2	394.4
17	220.0	0.37	384.1	393.5
18	212.6	0.36	383.2	392.6
19	211.7	0.36	383.4	392.8
20	224.7	0.38	378.1	388.0
21	244.0	0.41	384.7	394.4
22	244.0	0.41	384.8	394.4
23	233.9	0.40	383.3	392.7
24	242.6	0.41	384.9	394.4
25	243.4	0.41	385.0	394.5
26	231.9	0.39	382.8	392.3
27	230.2	0.39	378.4	389.0
28	244.8	0.41	385.0	394.7
29	145.5	0.25	355.6	368.5
30	205.2	0.35	371.5	381.9

2.2. The proposed kinetic model

A 5-lump kinetic model is proposed, by adapting the 6-lump kinetic model of Sadighi *et al* [6] to the actual process which doesn't produce kerosene, as in their work. The kinetic scheme is presented in Fig.1.

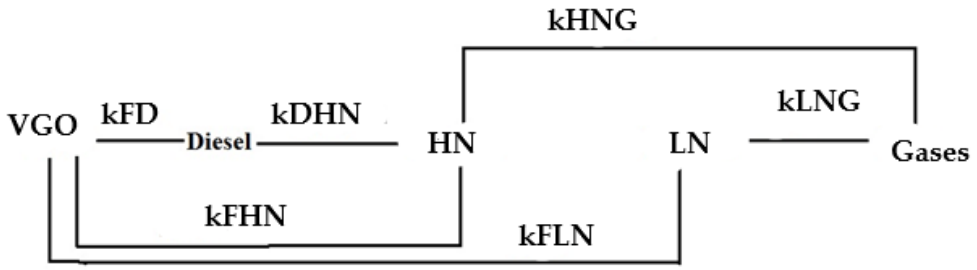

Fig. 1. The proposed 5-lump kinetic scheme

The symbols in the Fig.1 are the following: VGO (vacuum gas oil) is also denoted as F (feed) so kFD is the kinetic constant for the reaction Feed (F)→Diesel (D); HN is the heavy naphtha and LN is light naphtha, gases are denoted as G. The symbols for the rest of the kinetic constants in Fig.1 can be easily deducted.

In the kinetic equations, the parameters were taken from [6], for the initialization of the model. These are presented in Table 2.

Table 2

Kinetic parameters used for model initializing

Reaction	Frequency factor, k_0 (hr^{-1})	Activation energy, E (kcal/mol)
F → D	4.84	12.06
F – HN	6010.61	25.37
F – LN	14.955	16.29
D – HN	0.003	24.19
HN – G	0.304	8.71
LN – G	0.044	8.28

Taking into account these parameters, the kinetic constants of the reactions were calculated with the Arrhenius equation, e.g. for the F→D reaction, with Eq.1:

$$k_{FD} = k_{0FD} \cdot exp(\frac{-E_{FD}}{RT}) \quad (1)$$

Where T is the process temperature, calculated as the average between inlet and outlet temperature, and R is the universal constant of gases.

The reaction rate is then calculated taking into consideration the producing/consumption of the component in the reactions, as an algebraic sum, e.g. for Diesel (Eq.2):

$$R_D = k_{FD} \cdot C_F - k_{DHN} \cdot C_D \quad (2)$$

Where C_F and C_D are the concentrations of components expressed as weigh fraction in the reaction mass, so the reaction rate is expressed in h^{-1}.

2.3. Mass balance

The mass balance equations are prepared having in view the calculation of effluent composition. These equations constitute the mathematical model used in simulations.

The volume of catalyst, ω, is considered constant and evenly distributed in the reactor. The catalyst quantity crossed by effluent in the infinitesimal time interval dt is $d\omega$. Considering a stationary regime and a plug flow, the material balance around the infinitesimal volume element is, as in Fig 2 and Eq. 4:

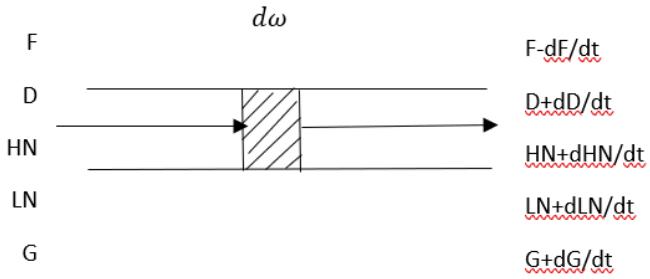

Fig.2. Material balance around the infinitesimal volume elements

$$\frac{dF}{dt} = \frac{dD}{dt} + \frac{dHN}{dt} + \frac{dLN}{dt} + \frac{dG}{dt} \quad (3)$$

At the initial moment, t_0, the mass fraction of the VGO (feed) is considered 1, and for all products is 0:

$$C_F = 1$$
$$C_D = 0$$
$$C_{HN} = 0$$
$$C_{LN} = 0$$
$$C_G = 0 \quad (4)$$

For integration purpose, the time increment is dt= 0.1 s. With every 0.1 s passing, the catalyst quantity crossed by fluid increases with $d\omega$ such as in the final moment, all the catalyst volume ω is used. The final reaction time is the residence time calculated from the volumetric LHSV and the catalyst volume. The final mass fraction of feed and products

2.4. The simulation of the hydrocracking reactor

In order to solve such numerous differential equations, the specialized programme Berkeley Madonna was utilized [14]. This one includes iterative methods for solving the differentials.

Because the reaction time and the temperature are different for each set of experimental data, there is a separate file with these data from which the main programme is fed.

The listing of the programme in Berkeley Madonna, is the following:

```
[Start]
METHOD AUTO

DT =0.1       ; time increment
i = 1  ; i is the running constant - changing manually
from 1,2,3 ... 30 during run
```

```
STOPTIME= #IndexReactiontime(i); separate file from
this programme code- it represents the reaction time
corresponding to i dataset.
TC = #IndexTempReactors(i); separate file from this
programme code-it represents the medium temperature in
the reaction zone.

R=0.0019872041 ; universal constant of gases,
cal/(K*mol)

; activation energy (kcal/mol):

EFD=12.06
EFHN=25.37
EFLN=16.29
EDHN=24.19
EHNG=8.71
ELNG=8.28

; frequency factors (h-1):

k0FD=4.84
k0FHN=6010.61
k0FLN=14.955
k0DHN=0.003
k0HNG=0.304
k0LNG=0.044

; initial conditions

INIT F=1
INIT D=0
INIT HN=0
INIT LN=0
INIT G=0

TK=R*(TC+273.15) ; represents the pre-calculated RT
value with temperature in K, to be used in Arrhenius
equation

; reaction system
```

```
D/DT(F)=RF
D/DT(D)=RD
D/DT(HN)=RHN
D/DT(LN)=RLN
D/DT(G)=RG

kFD=k0FD*EXP(-EFD/TK)
kFHN=k0FHN*EXP(-EFHN/TK)
kFLN=k0FLN*EXP(-EFLN/TK)
kDHN=k0DHN*EXP(-EDHN/TK)
kHNG=k0HNG*EXP(-EHNG/TK)
kLNG=k0LNG*EXP(-ELNG/TK)

RF=-(kFD*F+kFHN*F+kFLN*F)
RD=kFD*F-kDHN*D
RHN=kDBG*D+kABG*F-kBGG*HN
RLN=kFLN*F-kHNG*LN
RG=kHNG*HN+kLNG*LN

RF=RD+RHN+RLN+RG

; the mass balance condition is satisfied, otherwise
the programme displays error.
[End]
```

3. Results and discussions

3.1. Results of simulation

After simulations in Berkeley-Madonna with initial kinetics parameters, for the 30 sets of data, the conversion of the feed and products yields are obtained. They are presented in Table 3 and synthetically, in Fig.3.

Table 3

The results of reactor simulations

TIME	A:30	D:30	BG:30	BU:30	G:30
0	1	0	0	0	0
0.1	0.999746	2.05E-04	2.48E-05	2.37E-05	2.58E-09
0.2	0.999492	4.11E-04	4.97E-05	4.74E-05	1.03E-08
0.3	0.999239	6.16E-04	7.45E-05	7.10E-05	2.32E-08
0.4	0.998985	8.21E-04	9.93E-05	9.47E-05	4.13E-08
0.5	0.998731	0.001026	1.24E-04	1.18E-04	6.45E-08
……	……	…….	……..	……..	…….
1249.0	0.728629	0.219501	0.023729	0.024738	0.003402
1249.1	0.728444	0.219651	0.023743	0.024755	0.003407
1249.2	0.72826	0.2198	0.023757	0.024771	0.003412
1249.31	0.728202	0.219847	0.023762	0.024776	0.003414

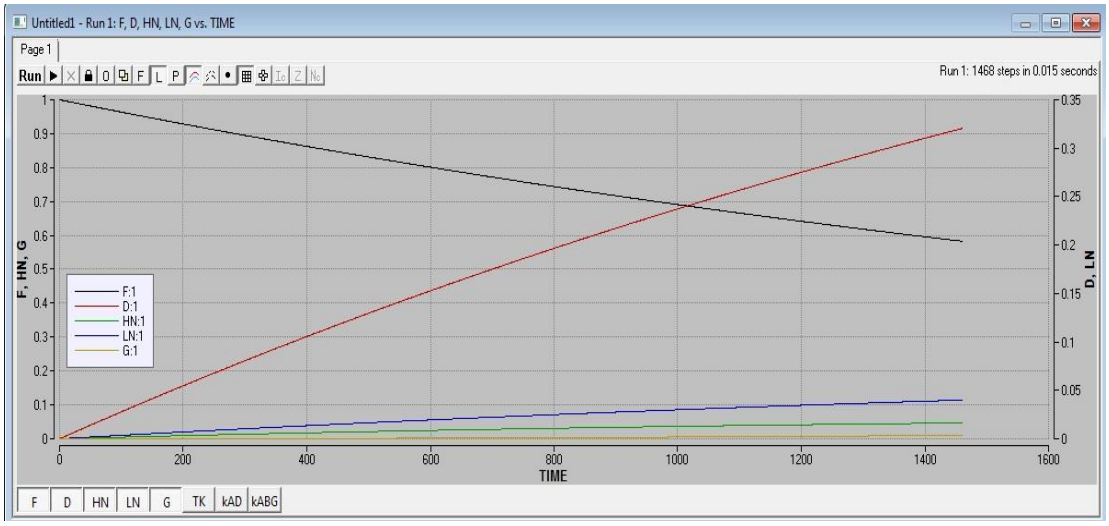

Fig.3. The dynamic of conversion and yields in the reactor

The relative errors between the actual products yields and those obtained by simulations with the kinetic data from literature (Table 2) are calculated in Table 4.

Table 4

Model errors. Predicted yields vs. actual yields

#	D			HN			LN			Gases		
	Pred.	**Act.**	**Err. (%)**	**Pred.**	**Act.**	**Err (%)**	**Pred.**	**Act.**	**Err (%)**	**Pred.**	**Act.**	**Err. (%)**
1	13.55	11.86	-14.3	0.12	1.00	87.8	1.43	1.37	-4.4	0.11	1.67	93.7
2	13.59	13.55	-0.3	0.12	0.72	83.2	1.43	1.11	-28.8	0.11	1.89	94.4
3	7.16	14.92	52.0	0.05	0.58	91.6	0.69	0.91	-29.2	0.11	2.09	95.0
4	27.89	30.69	9.1	0.36	1.09	67.1	3.33	3.26	24.5	0.66	2.48	73.3
5	14.00	16.85	16.9	0.13	0.75	83.1	1.48	1.01	-2.2	0.11	1.49	92.4
6	24.27	32.92	26.3	0.29	1.18	75.2	2.84	3.28	-47.1	0.46	2.27	79.8
7	25.27	32.68	22.7	0.31	1.12	72.6	2.97	3.35	13.6	0.51	2.53	79.9
8	27.81	33.39	16.7	0.35	1.19	70.8	3.29	3.28	11.4	0.64	2.30	72.0
9	27.89	33.39	16.5	0.35	1.19	70.8	3.30	3.28	-0.3	0.65	2.30	71.8
10	28.67	33.17	13.6	0.36	1.08	66.6	3.40	3.33	-0.5	0.70	2.27	69.3
11	28.63	33.09	13.5	0.36	1.13	68.2	3.40	3.35	-2.1	0.69	1.74	60.1
12	28.81	33.17	13.1	0.36	1.08	66.4	3.42	3.33	-1.4	0.71	2.27	69.0
13	28.64	32.80	12.7	0.36	1.09	67.1	3.40	3.37	-2.6	0.69	2.25	69.1
14	28.54	33.86	15.7	0.36	1.05	65.8	3.39	3.36	-0.9	0.69	2.25	69.4
15	27.87	30.14	7.6	0.36	1.01	64.6	3.33	3.20	-0.8	0.66	2.17	69.5
16	27.18	30.87	11.9	0.35	1.02	65.8	3.24	3.31	-3.8	0.62	2.44	74.5
17	26.68	30.52	12.6	0.34	1.01	66.3	3.17	3.30	2.0	0.59	2.44	75.7
18	25.69	31.24	17.8	0.32	1.01	68.0	3.05	3.23	3.7	0.54	2.37	77.2
19	25.69	31.24	17.8	0.32	1.01	68.0	3.05	3.23	5.6	0.54	2.37	77.2
20	25.51	28.35	10.0	0.30	1.09	72.5	2.96	2.93	5.6	0.51	2.27	77.7
21	29.12	31.31	7.0	0.37	1.04	64.8	3.46	3.25	-1.0	0.72	2.31	68.6
22	29.14	31.63	7.9	0.37	0.98	62.7	3.46	3.15	-6.6	0.73	2.30	68.5
23	27.79	30.89	10.0	0.35	1.21	71.5	3.29	3.17	-9.9	0.64	2.36	72.7
24	29.02	31.08	6.6	0.37	1.07	65.8	3.45	3.25	-3.6	0.72	2.29	68.6
25	29.13	31.31	7.0	0.37	1.04	64.6	3.46	3.25	-6.1	0.73	2.31	68.5
26	27.49	32.12	14.4	0.34	1.29	73.5	3.25	3.27	-6.7	0.63	2.56	75.6
27	26.16	30.76	14.9	0.31	1.37	77.6	3.04	2.74	0.6	0.54	2.02	73.5
28	29.30	31.34	6.5	0.37	1.08	65.6	3.49	3.19	-10.8	0.74	2.24	67.1
29	13.55	16.85	19.6	0.12	0.75	83.7	1.43	1.01	-9.4	0.11	1.49	92.9
30	21.98	25.76	14.7	0.24	0.76	68.6	2.48	2.20	-42.3	0.34	1.63	79.1
Av. Err	13.34%			71.34%			4.59%			75.87%		

The average relative errors were the highest for the gases (75.87%) and for heavy naphtha (71.34%). These high errors are due mainly to the very low yields of these products (0.72- 1.37% for the HN and 1.49-2.56% for gases) and also because the gases quantities are measured approximately from three sources in the industrial unit (from the low-pressure separator vessel and from other two distillation columns). Better results were obtained for the LN (average error 4.59%) and for the hydrotreated VGO (the uncracked feed) with 5.4% error (not included in the Table 4). For the main product, the Diesel, the average error is pretty high (13.34%) and this is related to the differences between the kinetic parameters from literature used in simulations and the true values of these parameters.

The programme also calculates the constants of reaction rate, for the 30 sets of experimental data shown in Table 5.

Table 5

Constants of reaction rate calculated by Berkeley Madonna programme

k_{FD}	k_{FHN}	k_{FLN}	k_{DHN}	K_{HNG}	K_{LNG}
1.67E-04	1.61E-05	1.79E-05	6.77E-12	1.50E-04	3.06E-05
1.65E-04	1.57E-05	1.76E-05	6.59E-12	1.49E-04	3.03E-05
1.25E-04	8.76E-06	1.21E-05	3.78E-12	1.22E-04	2.51E-05
2.47E-04	3.66E-05	3.04E-05	1.48E-11	1.99E-04	4.00E-05
1.68E-04	1.62E-05	1.80E-05	6.82E-12	1.51E-04	3.07E-05
2.29E-04	3.13E-05	2.75E-05	1.27E-11	1.89E-04	3.80E-05
2.33E-04	3.23E-05	2.80E-05	1.31E-11	1.91E-04	3.84E-05
2.41E-04	3.47E-05	2.93E-05	1.41E-11	1.95E-04	3.93E-05
2.40E-04	3.46E-05	2.93E-05	1.40E-11	1.95E-04	3.93E-05
2.44E-04	3.56E-05	2.98E-05	1.44E-11	1.97E-04	3.96E-05
2.43E-04	3.55E-05	2.98E-05	1.44E-11	1.97E-04	3.96E-05
2.44E-04	3.57E-05	2.99E-05	1.45E-11	1.97E-04	3.97E-05
2.44E-04	3.56E-05	2.98E-05	1.44E-11	1.97E-04	3.96E-05
2.43E-04	3.55E-05	2.98E-05	1.44E-11	1.97E-04	3.96E-05
2.47E-04	3.66E-05	3.04E-05	1.48E-11	1.99E-04	4.00E-05
2.46E-04	3.62E-05	3.02E-05	1.47E-11	1.98E-04	3.99E-05
2.43E-04	3.54E-05	2.97E-05	1.43E-11	1.97E-04	3.96E-05
2.40E-04	3.45E-05	2.92E-05	1.40E-11	1.95E-04	3.92E-05
2.40E-04	3.45E-05	2.92E-05	1.40E-11	1.95E-04	3.92E-05
2.25E-04	3.00E-05	2.67E-05	1.22E-11	1.86E-04	3.75E-05

2.45E-04	3.59E-05	3.00E-05	1.45E-11	1.98E-04	3.98E-05
2.45E-04	3.60E-05	3.00E-05	1.46E-11	1.98E-04	3.98E-05
2.40E-04	3.46E-05	2.93E-05	1.40E-11	1.95E-04	3.93E-05
2.45E-04	3.60E-05	3.01E-05	1.46E-11	1.98E-04	3.98E-05
2.45E-04	3.61E-05	3.01E-05	1.46E-11	1.98E-04	3.98E-05
2.39E-04	3.42E-05	2.91E-05	1.39E-11	1.95E-04	3.91E-05
2.26E-04	3.05E-05	2.70E-05	1.24E-11	1.87E-04	3.77E-05
2.46E-04	3.63E-05	3.02E-05	1.47E-11	1.99E-04	3.99E-05
1.67E-04	1.61E-05	1.79E-05	6.76E-12	1.50E-04	3.06E-05
2.05E-04	2.484E-05	2.37E-05	1.02E-11	0.00017436	3.53E-05

These constants are to be adjusted, to minimize the model's errors.

3.2. Adjustment of the kinetic model

Considering that the activation energy values are trustworthy, the variables that can be adjusted are the constants of reaction rate.

A method was used for the identification of experimental kinetic parameters when the theoretical model is known. The used programme, PARES (Parameter Estimator), was made available, by courtesy of dr. Mehmet Yuceer from Inonu University, Turkey, and this was successfully used previously in other works [15,16]. This programme solves differential equation systems by iteration. The programme includes a selection of optimization methods for different objective- functions.

For this application, the programme performs correlations between the kinetic constants and the actual yields. With these adjusted values, new frequency factors are to be calculated.

The programme is initialized under MATLAB. The equations system (5) is defined as follows:

```
F=[parm(1)*x(1)+parm(2)*x(1)+parm(3)*x(1);
  parm(1)*x(1)-parm(4)*x(2);
   parm(4)*x(2)+parm(2)*x(1)- parm(5)*x(3);
   parm(3)*x(1)- parm(6)*x(4);
   parm(5)*x(3)+parm(6)*x(4)];                    (5)
```

Where *F* is the name of the system, *parm (i)* represents the parameter to be estimated and *x* is the weight fraction of the product in the reaction mass, as in (6):

$$\begin{aligned} parm(1) &= k_{FD} \\ parm(2) &= k_{FHN} \\ parm(3) &= k_{FN} \\ parm(4) &= k_{DHV} \\ parm(5) &= k_{HNG} \\ parm(6) &= k_{LNG} \end{aligned} \qquad \begin{aligned} x(1) &= C_F \\ x(2) &= C_D \\ x(3) &= C_{HN} \\ x(4) &= C_{LN} \end{aligned} \tag{6}$$

The next step requires the initial values to start iteration, and lower/upper values of parameters as in Fig.4.

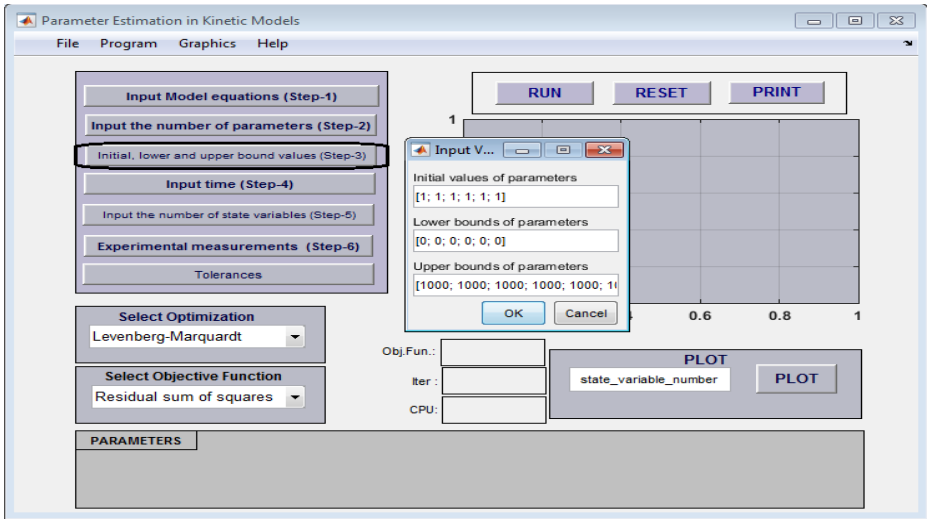

Fig.4. Initialization of PARES programme

The reaction time is then introduced in programme, for each set of experimental data; it is different from one set of data to another, depending on LHSV. The experimental values of four products are used as input variable. For

accuracy and a reasonable running time, a tolerance of 0.001 of the estimated parameter is accepted.

Then, the chosen optimization method was SQP(Sequential Quadratic Programming) Constraint, a non-linear method based on setting the confidence interval. The method finds the minimum of the objective-function. The objective-function is, in this case, the residual sum of squares (RSS). Used together, SQP and RSS represent a reliable instrument for solving an equations system when the number of equations is insufficient for linear programming.

In case of a single set of data, 54 iterations were needed, with a duration of approx.12 minutes. The results (adjusted kinetic parameters), shown in Table 6, are average values for the 30 sets of data.

Table 6

Adjusted kinetic parameters find with PARES programme

Reaction	Frequency Factor	Activation energy
FD	2.92	12.06
FHN	8416.03	25.37
FLN	7.577	16.29
DHN	0.0015	24.19
HNG	1.5320	8.71
LNG	0.0220	8.28

As seen, the frequency factors are different from the literature data (Table 2) since the activation energy is the same because it is supposed trustworthy, from the beginning, as previously mentioned. New simulations are performed with these values and experimental data from 15 consecutive running days, for the validation of the new model. In this period with a normal regime, small variation of parameters was noticed: the temperature varied in range 384.99 – 387.28 °C, and flowrate from 185.3 to 208.4 m^3/h. The predicted values computed with new constant vs. actual yields are presented in Table 7.

Table 7

Validation of the new model. Predicted yields vs. actual yields

#	VGO			D		
	Predicted	**Actual**	**Error,%**	**Predicted**	**Actual**	**Error,%**
1	63.34	63.13	-0.33	29.83	30.38	1.84
2	63.67	62.86	-1.29	29.86	30.68	2.67
3	63.72	62.48	-1.98	29.82	30.69	2.83
4	63.35	63.48	0.20	30.12	30.14	0.09
5	63.25	63.24	-0.03	30.20	30.13	-0.24
6	63.09	62.37	-1.16	30.33	30.87	1.73
7	65.68	62.99	-4.27	28.28	30.86	8.37
8	65.74	62.74	-4.79	28.24	30.52	7.48
9	65.18	63.24	-3.07	28.67	30.07	4.63
10	63.19	62.14	-1.68	30.17	31.25	3.45
11	66.72	65.73	-1.51	27.49	27.79	1.08
12	66.93	68.07	1.68	27.27	25.52	-6.85
13	67.37	66.03	-2.02	26.93	27.38	1.63
14	66.47	66.81	0.52	27.58	26.44	-4.33
15	65.11	68.02	4.28	28.73	25.42	-13.03
Average error,%			**1.92**			**4.02**

Table 7(continued)

#	HN			LN			G		
	Predicted	**Actuall**	**Predicted**	**Real**	**Error,%**	**Real**	**Predicted**	**Real**	**Error,%**
1	1.14	1.01	-12.71	3.00	3.22	6.99	2.32	2.27	-2.38
2	1.11	1.03	-7.65	3.00	3.23	6.90	2.33	2.20	-5.72
3	1.11	1.09	-2.58	3.00	3.26	7.95	2.32	2.48	6.46
4	1.14	1.01	-12.65	3.03	3.20	5.47	2.36	2.17	-9.07
5	1.14	1.00	-14.04	3.04	3.24	6.36	2.37	2.40	1.03
6	1.11	1.02	-9.58	3.05	3.31	7.78	2.39	2.44	1.89
7	1.12	0.99	-13.52	2.83	3.24	12.77	2.09	1.92	-8.62
8	1.12	1.01	-11.09	2.82	3.30	14.29	2.08	2.44	14.77
9	1.12	1.02	-9.80	2.87	3.24	11.21	2.15	2.42	11.44
10	1.17	1.01	-15.34	3.06	3.23	5.33	2.42	2.37	-1.94
11	1.11	1.02	-8.68	2.75	3.15	12.76	1.98	2.31	14.19
12	1.11	1.08	-2.89	2.73	3.15	13.42	1.96	2.18	10.24
13	1.11	1.10	-0.44	2.69	3.17	15.19	1.91	2.32	17.89
14	1.11	1.18	5.72	2.76	3.28	15.64	2.00	2.29	12.58
15	1.12	1.12	-0.23	2.88	3.25	11.39	2.15	2.19	1.63
Average error,%			**8.46**			**10.23**			**7.99**

As seen in Table 7, the computed values of the feed conversion and products yields with adjusted kinetics parameters (Table 6) are closer to the actual values then with older parameters. The relative errors are between 1.92% and 10.23%, much lower than in case of old model, and it is noticeable that for the higher yields' products, the relative errors are lower.

4. Conclusions

The present work proposes a new 5-lump kinetic model for the mild hydrocracking of VGO, on NiCoMo catalyst in the midst of its running cycle. The model proceeds from adapting a 6-lump model [6] to an industrial process with fewer products. Old kinetic parameters in Arrhenius equation prove to give some inacceptable errors when processing the experimental data in Berkley Madonna. The kinetic parameters were adjusted, by means of PARES programme [15] and the errors were mitigated. The validation of model was performed on a new set of data and proved to be a reliable one.

REFERENCES

[1] Thybaut J.W., Marin G.B., Hydrocracking: From reaction mechanism over catalysts to kinetics and industrial application, Chapter Two in: C.S.Song, *Advances in Catalysis volume 59*, Academic Press, Cambridge MA, SUA, p.167-197, 2016.

[2] Martinez J., Ancheyta J, Kinetic model for hydrocracking of heavy oil in a CSTR involving short term catalyst deactivation, *Fuel*, 100, (2012), 193-199**.**

[3] Pellegrini L., Bonomi S., Gamba S., Calemma V., Molinary D., The "all components hydrocracking model", *Chemical Engineering Science*, 62, (2007), 5013-5020.

[4] Callejas M.A., Martinez M.T.- Hydrocracking of a Maya residue. Kinetics and product yield distributions, *Industrial&Engineering Chemistry Research*, 38, (1999), 3285-3289.

[5] Sadighi S. Ahmad A., Rashidzadeh, M., 4-Lump kinetic model for vacuum gas oil hydrocracker involving hydrogen consumption, *Korean Journal of Chemical Engineering*, 27, (2010), 1099-1108.

[6] Sadighi S. Ahmad A., Mohadeccy S.R.S., 6-Lump Kinetic Model for a Commercial Vacuum Gas Oil Hydrocracker, *International Journal of Chemical Reactors Engineering*, 8, (2010), 1-8.

[7] Asaee S., Vafajoo L., Khorasheh F., A new approach to estimate parameters of a lumped kinetic model for hydroconversion of heavy residue, *Fuel*, 134, (2014), 343–353.

[8] Hua Zh., Lu J., Cao Zh., Shi Zh., Pan M.L.W., Jiang Q., Modeling and optimization of an industrial hydrocracking unit to improve the yield of diesel or kerosene, *Fuel*, 90, (2011), 3521–3530.

[9] Becker P.J., A continuous lumping model for hydrocracking on a zeolite catalysts: model development and parameter identification, *Fuel*, 164, (2016), 73-82

[10] Gambaro C., Calemma V., Molinari D., Denayer J.-Hydrocracking of FischerTropsch waxes: kinetic modeling via LHHW approach, *American International Chemical Engineering Journal*, 57, (2011), 711-723.

[11] Guillaume D., Valery E., Verstraete J. J., Surla K., Galtier P., Schweich D., Single event kinetic modelling without explicit generation of large networks: Application to hydrocracking of long paraffins, *Oil&Gas Science and Technology*, 66, (2011), 399–422.
[12] Becker P., Serrand N., Celse B., Guillaume D., Dulot H., Comparing hydrocracking models: Continuous lumping vs. single events, *Fuel*, 165, (2016), 306–315.
[13] Kumar V. Balasubramanian P., Kinetic parameter estimation in hydrocracking using hybrid particle swarm optimization, *Fuel*, 88, (2009), 2171–2180.
[14] Ingham J., Dunn I, J, Heinzle E., Přenosil J.E., Snape J.B., Chemical Engineering Dynamics (with floppy disk containing Berkeley-Madonna programme), Ed.WILEY-VCH, Weinheim, Germany, 2007.
[15] Yuceer M., Atasoy I., Berber, R., A software for parameter estimation in dynamic models, *Brazilian Journal of Chemical Engineering*, 25, (2008), 813-821.
[16] Esposito W., Floudas Ch.A., Global optimization for the parameter estimation of differential-algebraic systems, *Industrial&Engineering Chemistry Research*, 39, (2000), 1291-1310

RHEOLOGICAL STUDY ONROMANIAN TYPES OF OILS

Timur CHIS[1*], Ancaelena Eliza STERPU[1], Olga Valerica SAPUNARU[1]

[1]Ovidius University of Constanța, 124, Mamaia Blvd., Constanța, 900527

Abstract

The crude oil extracted from the Romanian oil fields was reclassified by the National Agency of Mineral Resources in eight categories: heavy crude oil, medium-heavy crude oil, medium crude oil, medium-light crude oil, light crude oil, very light crude oil, ultra-light and condensed crude oil, depending on density and sulfur content. But in Order 137 / 13.02.2019, no reference is made to the viscosity of crude oil and the freezing point. This work's goal is to characterize the Romanian oils from the viewpoint of viscosity variation with temperature. Mathematical correlations were established, useful in the transport of oil through pipes. Also, the parameters of Walter correlation from literature were found by processing experimental data.

Key words: Dynamic viscosity, Romanian Oil, Mathematical modeling

1. Introduction

The viscosity of a fluid is that property through which tangential stresses arise within it, opposing the movement of the layers during their movement, relative to each other [1].

In the laminar flow of liquids, the tangential stresses are directly proportional to the velocity difference between two layers and inversely proportional to the distance between them, measured in the direction of flow.

The proportionality factor that intervenes in this relationship is the dynamic viscosity [2].

In the oil and gas industry, knowing the dynamic viscosity and kinematic viscosity (which is defined by the ratio of dynamic viscosity to liquid density, at the temperature and pressure of determination), is very important in transporting crude oil and groundwater through pipelines and more, are chosen in the establishment of processing recipes (blend type mixtures), in order to obtain specialized petroleum products for industrial applications [3].

*Corresponding author: email address timur.chis@gmail.com

The analysis of the crude oil extracted from the associated crude oil and gas deposits, created the possibility to establish their classification techniques, the first classification being elaborated by Professor Creangă (the Carpathian classification).

In determining the crude oil grades, the Carpathian classification took into consideration the hydrocarbon classes in the fraction with distillation range between 250°C and 300°C, the percentage of paraffin in the oils, and the asphalt content.

This classification of Romanian crude oil highlighted 7 classes, 7 groups and 12 subgroups of crude oil [4].

But a new classification entered into force in Romania after1995, in order to tax the oil royalty in accordance with the international price of Brent crude oil, which takes into account only the density and sulphur content of crude oils.

Table 1

Crude Oil Classes in Romania [5]

Clasa	Density API,	Density g/cm^3 (medium values)	Density API (medium values)	Sulphur %, (medium values)
1-Heavy Crude oil	≤20	0.95	17.45	0.31
2- Medium-heavy crude oil	20-25	0.92	22.30	0.36
3- Medium crude oil	25-30	0.89	27.49	0.35
4- Medium-light crude oil	30-35	0.86	33.03	0.32
5- Light crude oil	35-40	0.84	36.95	0.24
6- Crude oil very light	40-46	0.81	43.19	0.16

7- Ultra light crude oil	46-50	0.786	48.53	0.105
8-Condensate	≥50	0.756	55.67	0.038

But this classification does not take into consideration the viscosity of crude oil and the paraffin content.

The viscosity of crude oil depends on its composition, pressure, and temperature.

At constant pressure, the viscosity of the crude oil varies with temperature according to Walter's equation (ASTM) [6]:

$$lg[\lg(\upsilon + 0{,}8)] = a + b\ lgT \quad (1)$$

Where:

- υ is the kinematic viscosity, cSt,
- T is the temperature of determination, K.

With this equation, having the viscosity value of the product at two temperatures, one can determine the values of the constants *a* and *b* and then deduce the viscosity values at the desired temperature.

In the case of crude oil with high viscosity, the above relationship can be simplified in form of Eq.2[7]:

$$lg[\lg(\upsilon)] = a + b\ lgT \quad (2)$$

Thorn and Rogers determined another relationship between the viscosity of a product and the temperature of determination (Eq.3):

$$\upsilon = \frac{1}{C+At+Bt^2}, \quad (3)$$

Where:

- υ, este is the kinematic viscosity, cSt;
- *A,B,C* are constants ;
- *t* is the temperature of determination, ºC.

2. Experimental

The analysed crude oils were collected from deposits (Table 2), aiming to cover all existing types of crude oil in Romania.

The samples were collected and analysed according to current standards.

The crude oil density was determined according to ASTM D5002-19 - Standard Test Method for Density, Relative Density, and API Gravity of Crude Oils by Digital Density Analyzer, using the DMA 4100M Densimeter from Anton Paar.

The device has an accuracy of 0.001 g/cm^3 (at a temperature of 0.3 ºC).

The kinematic viscosity was determined using the apparatus produced by Anton Paar type SMV 3001, according to the standard ISO 3104: 2020, Petroleum Products-Transparent and Opaque Liquids-Determination of kinematic viscosity and calculation of dynamic viscosity.

The measurement error is maximum 0.35% at a density of 0.0005 g/cm^3.

Water and dry air were used to calibrate the devices.

3. Results and discussions

The measured values of the viscosity *vs.* temperature are given in **Figures 1-8** for all types of Romanian crude oils samples.

Equations of behaviour were determined for all the curves drawn. The constant values *a, b*in the Eq.1were also determined.

The accuracy of viscosity estimation was evaluated in terms of average absolute deviation (AAD%) calculated by Eq.4:

$$AAD = \frac{100}{N}\sum_{i=1}^{N}\frac{|\upsilon_{exp,i}-\upsilon_{cal,i}|}{\upsilon_{exp,i}} \quad (4)$$

Where:

- $\upsilon_{exp,i}$, experimentally determined kinematic viscosity, cSt;
- $\upsilon_{cal,i}$, calculated kinematic viscosity, cSt.

In Table 2, the rheological equations are written but also, the density and paraffin content, for complete characterization.

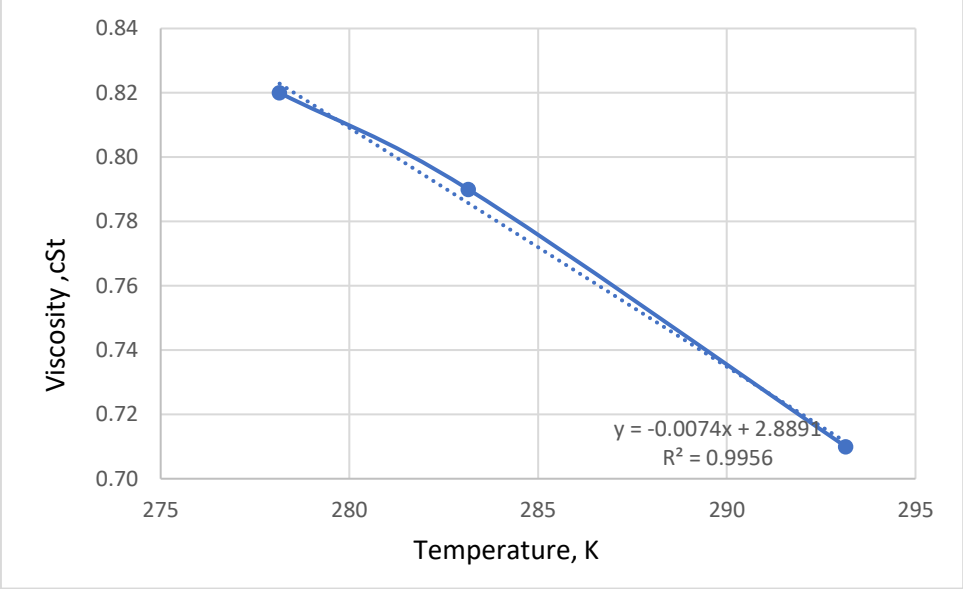

Fig. 1. Viscosity variation with temperature for crude oil condensed -Căpreni

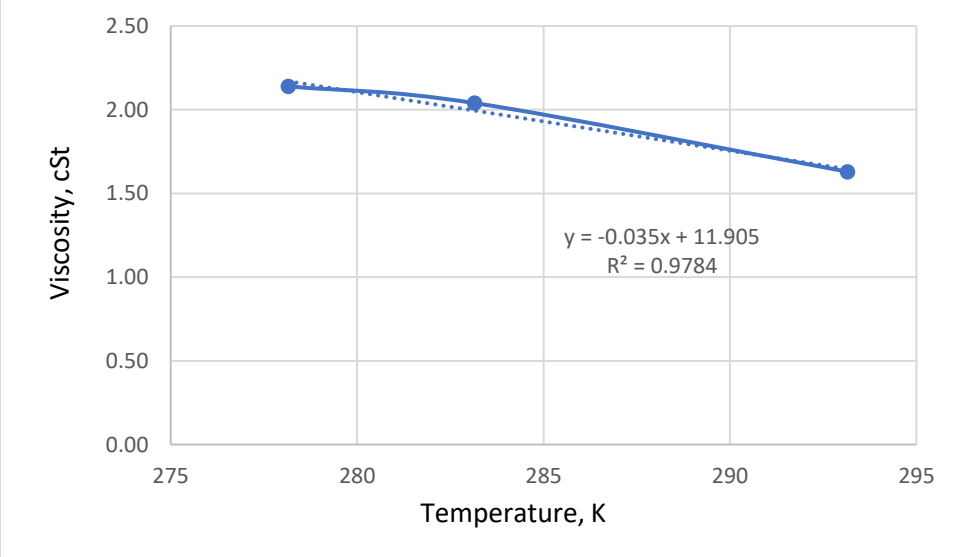

Fig. 2. Viscosity variation with temperature for Ultra light crude oil-Mădulari

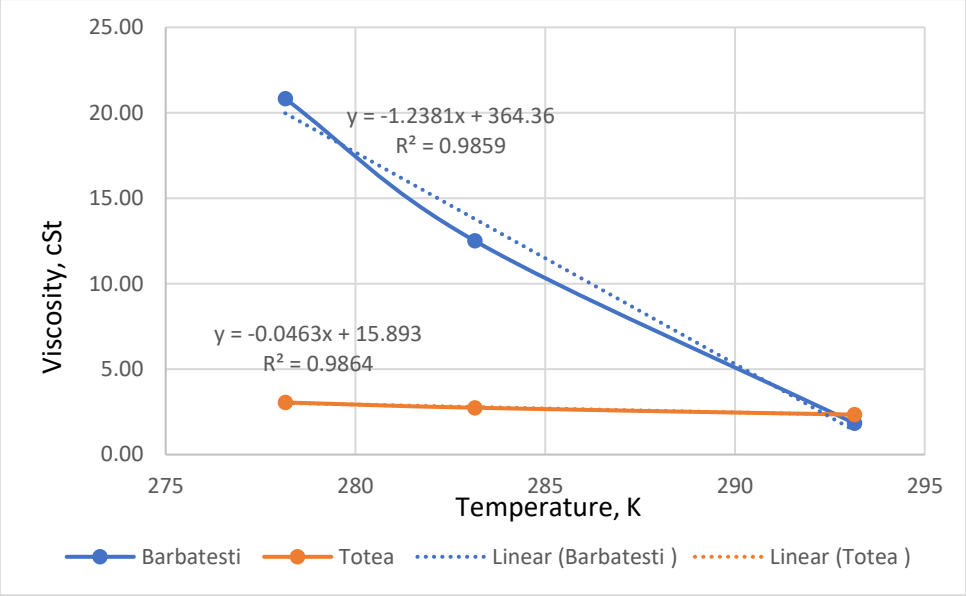

Fig. 3. Viscosity variation with temperature, for Crude oil very light- Bărbătesti and Totea

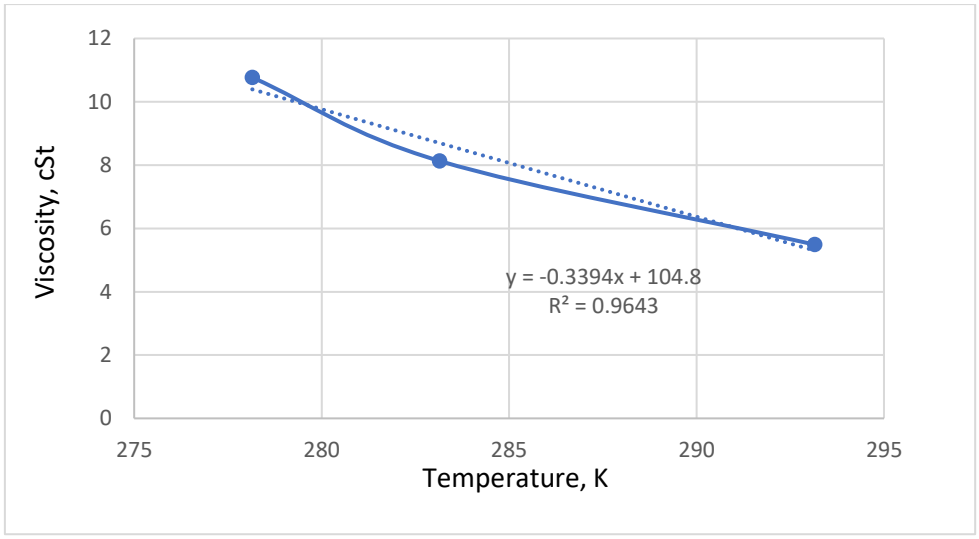

Fig. 4. Viscosity variation with temperature for Light crude oil-Icoana

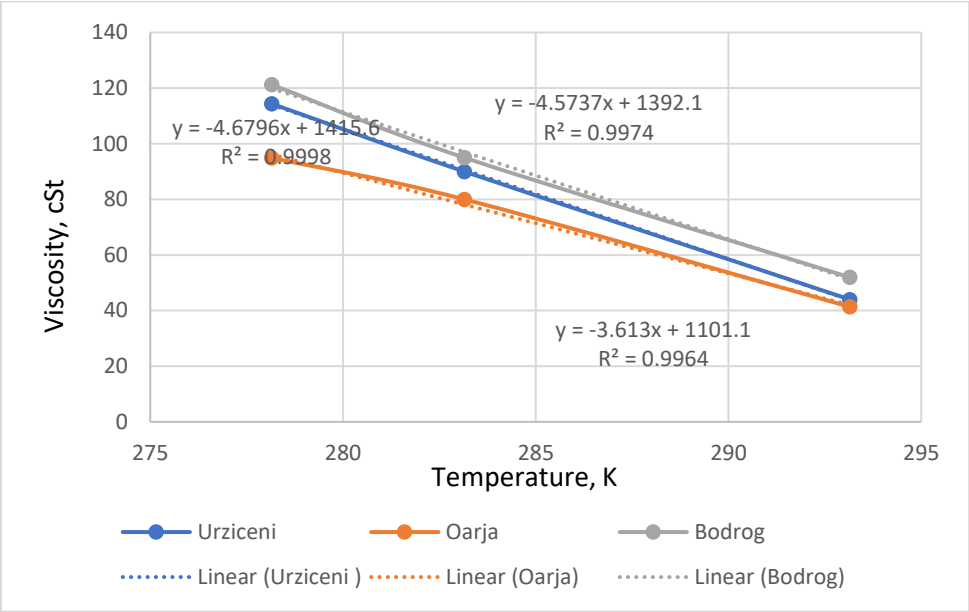

Fig. 5. Viscosity variation with temperature for Medium-light crude oil-Poiana Lacului and Ghercești

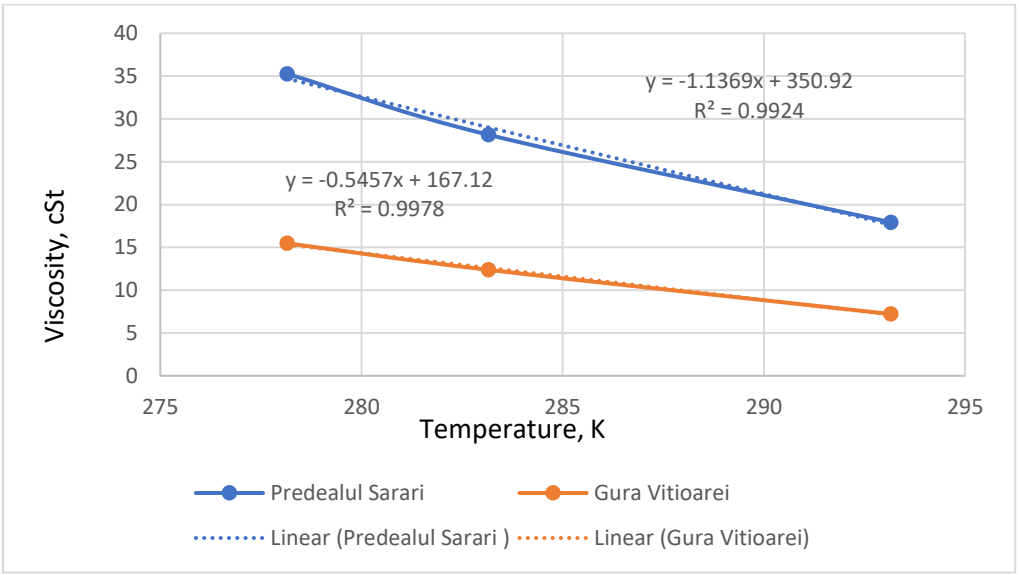

Fig. 6. Viscosity variation with temperature for Medium crude oil- Predealu Sărari and Gura Vitioarei

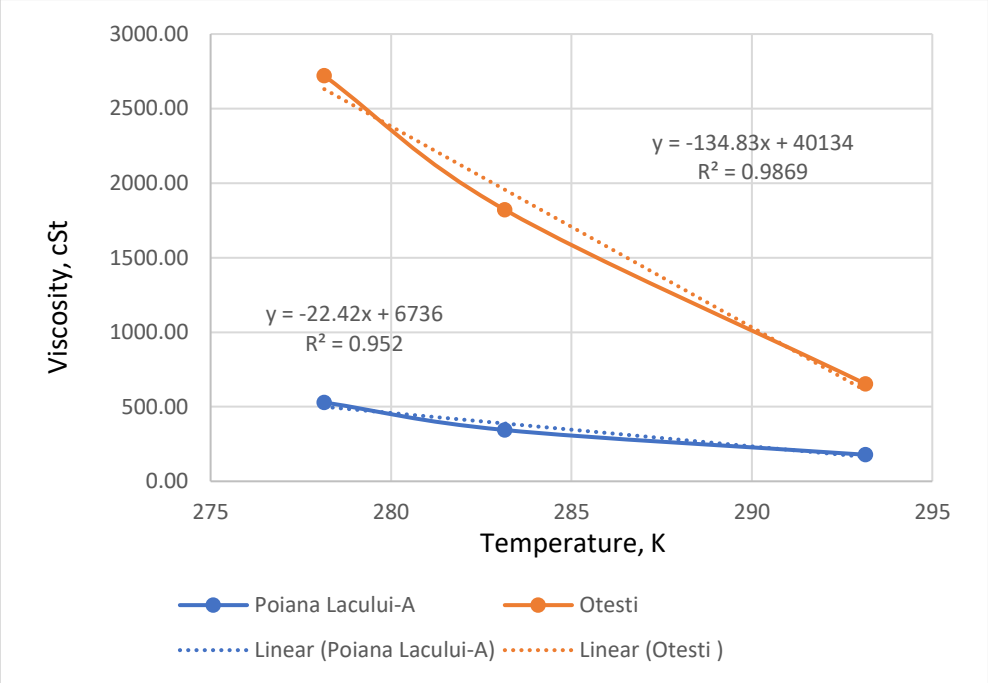

Fig. 7. Viscosity variation with temperature for Medium-heavy crude oil- Urziceni and Oarda

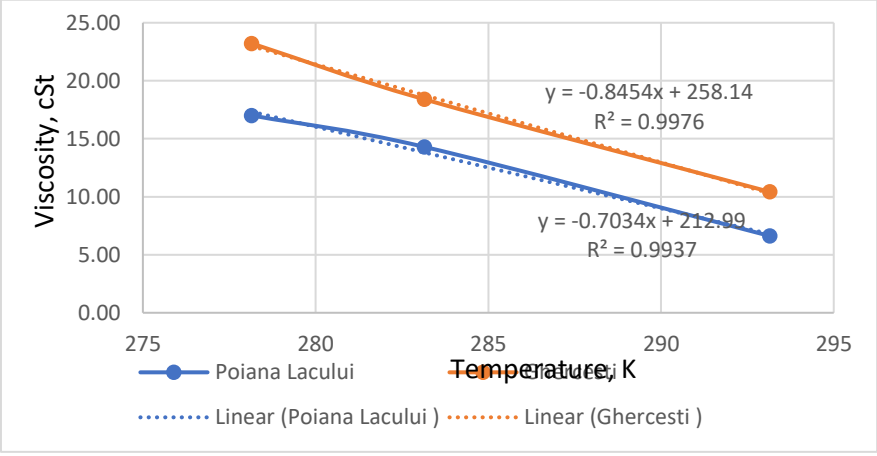

Fig. 8. Viscosity variation with temperature for Heavy Crude oil- Poiana Lacului and Otești

Table 2

Equations of viscosity function by temperature variation

Crude oil collection location	Oil classes	Equations of viscosity function of temperature -y is viscosity in cSt -x is temperature, K	Density g/cm^3	Paraffin content %,wt.
Otești	1-Heavy Crude oil	y= -0,8454x + 258,14	0,9976	-
Poiana Lacului	1-Heavy Crude oil	y = -0,7034x + 212,99	0,9937	
Bodrog	2- Medium-heavy crude oil	y = -4,5737x + 1392,1	0,9974	0,450
Urziceni	2- Medium-heavy crude oil	y = -4,6796x + 1415,6	0,9998	0,500
Oarja	2- Medium-heavy crude oil	y = -3,613x + 1101,1	0,9964	0,506
PredealuSărari	3- Medium crude oil	y = -1,1369x + 350,92	0,9924	1,8
GuraVitioarei	3- Medium crude oil	y = -0,5457x + 167,12	0,9978	6,2
Ghercesti	4- Medium-light crude oil	y = -0,8454x + 258,14	0,9976	6,5
Poiana Lacului	4- Medium-light crude oil	y = -0,7034x + 212,99	0,9937	8,4
Icoana	5- Light crude oil	y = -0,3394x + 104,8	0,9643	12
Barbatesti	6- Crude oil very light	y = -1,2381x + 364,36	0,9859	26,2

Totea	6- Crude oil very light	y = -0,0463x + 15,893	0,9864	2,5
Madulari	7- Ultra light crude oil	y = -0,035x + 11,905	0,9784	2
Capreni	8-Condensate	y = -0,0074x + 2,8891	0,9956	0

Table 3

The values of a and b in Equation 1

Crude oil picking location	Oil classes	a	b	AAD
Otesti	1-Heavy Crude oil	10,16	-10,02	0,025
Poiana Lacului A	1-Heavy Crude oil	10,25	-10,05	0,065
Bodrog	2- Medium-heavy crude oil	7,48	0,095	0,022
Urziceni	2- Medium-heavy crude oil	7,41	-2,90	0,017
Oarja	2- Medium-heavy crude oil	7,45	-4,03	0,019
PredealuSărari	3- Medium crude oil	10,83	-4,41	0,026
GuraVitioarei	3- Medium crude oil	10,85	-6,61	0,17
Ghercesti	4- Medium-light crude oil	0,14	-10,15	0,06
Poiana Lacului	4- Medium-light crude oil	0,10	-10,65	0,025
Icoana	5- Light crude oil	17,28	-7,06	0,029
Barbatesti	6- Crude oil very light	14,08	-9,96	0,50
Totea	6- Crude oil very light	0,050	-28,31	0,007
Madulari	7- Ultra light crude oil	4,94	-1,83	0,36
Capreni	8-Condensate	6,65	-2,99	0

By analysing the variation of the viscosity of Romanian crude oil with temperatures (Fig.1-8) corroborated with density and paraffin content (Table 2), the following can be observed:

- The viscosity of crude oil at 278.15 K depends on their density and the amount of paraffin content.
- Heavier the crude oil would be, higher its viscosity is.
- Thus, the kinematic viscosity increases from the condensate (0.82 cSt) to medium oil (35 cSt) then heavy oil (2500 cSt).
- Also, higher the paraffin content would be, higher the viscosity is.
- This is obvious when comparing two oils belonging to the same class but with very different paraffin content such as Poiana Lacului (8.4% wt. paraffin, 23 cSt) and Ghercești (6.5 % wt. paraffin, 17 cSt), both belonging to medium light class or, more obvious, Bărbătești (26.8 % wt paraffin, 21 cSt) and Totea (2.5% wt paraffin, 3.5 cSt), both belonging to very light class of oils.

In the case of paraffinic crude oils, due to the presence of paraffin, this leads to high viscosity when the temperature is low (278.15), because the solution approaches tothe freezing point.

Without regard to the chemical composition of the oil, the viscosity decreases with temperature, as in case of all liquids. What is specific to the crude oils, this decreasing is accentuated on small interval of temperature at low temperature (Δt =278.15-293.15 K), and especially for the paraffinic oils (ex. Very light Bărbătești, or medium light Poiana Lacului).

4. Conclusions

The present work gathered all types of Romanian crude oils in a rheological study, intending to characterize them also related to their density and the paraffin content.

The rheological behaviour at low temperature (278.15 K) disclosed the dependency of the viscosity on density and paraffin content, as heavier oils have much higher viscosity than the lighter ones and paraffin rich oils are more viscous than those poor in paraffin.

For the variation of the viscosity with temperature, the linear equation describes satisfactorily the rheological behaviour with a good coefficient of determinationR^2 = 0,992…-0,999….

Constants *a* and *b* in Walter's correlation were found for all analysed oils.

The mathematical correlations viscosity vs. temperature determined here are useful for the transport of oil through pipes calculations.

REFERENCES

[1] Nita I., Osman S., Iulian O., Dynamic viscosity dependence on temperature for fuels used for diesel engine, *Ovidius University Annals of Chemistry*, 32, 1, 98-103, 2021.

[2] Randová A., Bartovská L., Densimetric and viscometric study of liquid systems alkane + alcohol, *Journal of Molecular Liquids*, 242 (2017) 767-778.

[3] Chis T., Sterpu A.E., Koncsag C.I., Dumitru A.. Ease the Transport of Viscous Crude Oil by Pipeline through Performing Right Blending Recipes**,** *14 th International Scientific Conference*, SGEM 2014, Varna, Bulgaria, 17-25 June 2014, Proceedings Conference ISSN 1314-2704.

[4] Chis T., The Roumanian Oil Clasification**,** *11 th International Scientific Conference*, SGEM 2011, Varna, Bulgaria, 20-24 June 2011, Proceedings Conference ISSN 1314-2704.

[5] Order on the approval of the methodology for establishing the reference price for crude oil extracted from Romania, nr. 137/13.02.2019, ANRE București.

[6] Sánchez-RubioM., Chinas-CastilloF.,Ruiz-AquinoF., Lara-RomeroJ., A new focus on the Walther equation for lubricant viscosity determination, *Lubrification Science*, https://onlinelibrary.wiley.com/doi/pdf/10.1002/ls.9.

[7] Ebna A.F.M., Poh-Seng L., Chou S.K., Wenming Y., Yap C., Experimental study and empirical correlation development of fuel properties of waste cooking palm biodiesel and its diesel blends at elevated temperatures, *Renewable Energy*, 68 (2014) 282-288.

METALS DETECTION IN ABANDONED OIL TANK FARM

Timur CHIS[1]*, Ancaelena Eliza STERPU[1], Olga Valerica SAPUNARU[1]

[1]Ovidius University of Constanța, 124, Mamaia Blvd., Constanța, 900527

Abstract

The primary processing of crude oil consists in the separation of gas and field water from crude oil. This activity takes place in extraction areas. But during the processing of crude oil, there is a possibility that the phenomenon of environmental pollution may occur, due to the evacuation of gases from the safety valves or the accidental leakage of oil and groundwater. In Romania, the extraction areas abandoned until 2000 are depolluted from public funds and that is why, the level of hydrocarbons in the soil is measured and if the allowed maximum amount is overcome, the area enters in the process of rehabilitation.

In this paper, the level of metals is analyzed (Cu, Pb, Zn, Ag, Ni, Mn, As, Cd, V, Cr, S) from the samples collected from an abandoned extraction park. The crude oil extraction and treatment park is in the Moinești area, Romania, and the oil processing facilities are decommissioned. A natural pasture was created on the territory of this park.

Correlations between concentration of the main pollutant in the soil (crude oil) and different metals concentration were established which could serve to the prediction of metals pollution in other abandoned oil tank farms.

Key words: Oil pollution, Metals pollution, Soil pollution, Risk Assesment

1. Introduction

The Moinești area has been producing crude oil since 1440 [1]. The oil exploration has led to accidental pollution over the years. These incidents were reported to the Bacău Environmental Protection Agency only after 1990. But the analysis reports refer only to the hydrocarbon content in the soil. No level of pollution with heavy metals or radioactive elements has been established in this area. The city of Moineşti is in the NW part of Bacău County (46º26'N, 26º29'E).

The analyzed area is located on the border between the Eastern Carpathians and the Subcarpathian Depression of the Tazlau. It is an agricultural area, used for grazing.

From the analyzes performed on the soils polluted with oil, a change of the physico-chemical and biological properties of the soil was found. At the same time, there is an increase in the concentration of heavy metals and radioactive elements in the soil.

*Corresponding author: email address: timur.chis@gmail.com

It also affects flora and fauna, endangering the safety of ecosystems and the health of the population due to the circulation of pollutants through food chains [2,3].

In the analyzed area, there were few interventions regarding the depollution of the affected land (mostly the soil was replaced with the contribution of material brought from elsewhere). That is why the analysis of metallic elements in the soil is part of the study of their influence on human activity and spontaneous flora (the area being a public pasture).

Crude oil is a solution consisting of hydrocarbons, metals, non-metals, water [4].

If determined the chemical elements in oil, we would discover almost all the common metals in the periodic table. The metals detected in the crude oil analyzed in different parts of the globe are Na, Li, Be, Mg, Ca, Ba, Sr, Cu, Ag, Zn, Cd, Fe, Co, Ni, Ti, V, Mn [1,4,5].

Metals presence provide us with data on the crude oil migration process from the formation rocks in the storage basins and may have different concentrations even in the same deposit (at different extraction layers).

Studies of various types of crude oil have identified their presence [5, -10], as:

-metalloporphyrin chelates (V, Ni);
- metallic complexes, small tetradentate ligands (V, Ni, Fe, Cu, Cr, Co);
-carboxylic acid salts of the functional polar groups of resins (Mo, Zn, Ge);
-colloidal minerals (silica and NaCl);
-organometallic compounds (Hg, Sb, As).

2. Materials and Methods

The extraction of oil took place between 1960-2000, after which the field was abandoned.

No soil physico-chemical decontamination has been carried out in the analyzed area, as the hydrocarbon content in the soil is less than 1000 mg/kg dry matter and the land is included in the areas accepted not to be depolluted. From the area affected by the location of the oil and gas depot, 12 sets of soil samples were taken at a depth of 100 mm.

The samples were dried in an oven at 100°C, after which it was crushed and homogenized. After drying the soil samples, the oil content was analyzed using infrared absorption spectroscopy (FTIR).

For calibration, two samples were taken from an unpolluted area in Moinești and from a municipal area (Cluj Napoca).

Also, to obtain the spectra, the method of measuring the absorption of infrared diffuse reflection using a diamond crystal Attenuated Total Reflectance (ATR) unit was used.

The Bruker Tensor 27 IR Spectrometer with Golden Gate interface was used for measurements. The spectrophotometer was used to determine the metals in the soil and the total hydrocarbon content, in the spectral range corresponding to the wave numbers from 4000 cm^{-1} to 700 cm^{-1} with a spectral resolution of 2 cm-1 as an average of 64 scans. Each determination was performed in triplicate, the relative error being max.0.05%.

The exploitation of crude oil is a set of operations that can lead to soil and groundwater pollution. The interest of researchers to study the risk of environmental pollutants is well known, the research works being focused on determining the hydrocarbon content in soil and plants and less on those dedicated to qualitative and quantitative analysis of soil and plant metal content [1,4,11] as shown in **Table 1**.

The studies focused on the development of a model for assessing the risk of pollutants determined from oil, for certain study areas.

A model for assessing the risk in exploitation of the land affected by pollution, on the Bayesian model was developed by Aguilera content [3,12-14] and developed by Diana Mariana Cocârță [15].

Usually, an analysis of a land which must be returned to use after the completion of onshore operations should include in addition to determining the content of petroleum products, the determination 14 elements of the periodic table, namely Cu, Pb, Zn, Ag, Ni, Mn, As, Cd, V, Cr and S [16] (see **Table 2**).

An analysis of the effects of metals found in soils in areas where oil mines existed, was performed by A. R. Karbassi [17]. After a pollution, the analyzes must indicate if there are traces of petroleum product (THP), radioactive elements and especially metals.

For the analysis of the environmental impact of metal pollution from the exploitation of oil fields, a variant of risk composition based on Baysian networks is proposed [18, 19], starting from the relation 1:

$$P(x) = P(X_1, X_2, X_3, \dots, X_n) = \prod_{i=1}^{n} P(\frac{X_i}{X_{j(i)}}) \quad (1)$$

Where $X_{j(i)}$ are data taken from the acyclic graph of the variables X_i.

Muller designed a pollution index also called Igeo index [18-20] and defined by equation 2:

$$Igeo = log2 \frac{C_n}{1{,}5 \cdot B_n} \quad (2)$$

Where:

- C_n is the metal concentration in the sample collected;
- B_n is the reference metal concentration;

- 1,5 –calculation factor.

Table 1.

Concentration of metals (picogram/gram) in crude oil from various regions

Chemical Elements	Oil extracted by Moinești	Oil export from		
		California, USA	Libya	Alberta, Canada
Na	2.0	13.3	13.0	3.62
Ni	5.0	98.4	49.1	9.38
Cu	0.17	0.93	0.19	0
Fe	9.8	68.9	4.94	10.8
Mn	0.1	1.20	0.79	0.01
Zn	0.4	9.76	62.9	0.046
Cd	0	0.004	0	0

Another model for determining pollution classes is described by relation 3 [19,20], as Enrichment factor:

$$EF = \frac{\left(\frac{C_n}{C_{Mn}}\right)analysis\ sample}{\left(\frac{C_n}{C_{Mn}}\right)sample\ analysis-soil\ notpollution} \quad (3)$$

Where C_{Mn} is the concentration of manganese in the soil sample.

Tables 3 and **Table 4** show the pollution classes for the two mathematical models presented above.

Another method of determining ecological risk measurement levels is represented by the relationships 4 and 5 for the ecological risk description and the risk index [19,20].

$$E_r^i = T_r^i \cdot \frac{C_i}{C_0} \quad (4)$$

$$RI = \sum_{i=1}^{n} T_r^i \cdot \frac{C_i}{C_0} \quad (5)$$

Where:

- C_i is the metal concentration in the analyzed sample;
- C_0 – the metal concentration in the control sample;
- T_r^i – toxicity factor, (toxicity factor for different elements are: *As = 10, Cu = Pb = Ni = 5, Zn = Mn = 1, Cr = 2);*
- E_r^i it is the ecological risk factor;
- RI represents the risk index of the presence of metals in the soil.

Table 2.

Concentration of approved metals in soil pollution (mg/kg dry matter) [19,20]

Metals	Normal values	Threshold sensitive area alert/less sensitive	Intervention threshold sensitive areas/less sensitive
Cu (mg/kg)	20	100-250	200-500
Pb (mg/kg)	20	50-250	100-1000
Zn (mg/kg)	100	300-700	600-1500
Ag (mg/kg)	2	10-20	20-40
Ni (mg/kg)	20	75-200	150-500
Mn (mg/kg)	900	1500-2000	2500-4000
As (mg/kg)	5	15-25	25-50
Cd (mg/kg)	1	3-5	5-10
V (mg/kg)	50	100-200	200-400
Cr (mg/kg)	30	100-300	300-600
S (mg/kg)	-	400-5000	1000-20000

Table 3.

Pollution classes according to the Igeo Index [21]

Igeo Index	Pollution type
Igeo≤0	Reduced pollution
Igeo=0-1	Normal values
Igeo=1-2	Sensitive area alesrt threshold
Igeo=2-3	Less sensitive area alert threshold
Igeo=3-4	Intervention threshold sensitive area
Igeo=4-5	Intervention threshold less sensitive area
Igeo≥5	Extreme pollution

Table 4.

Pollution classes according to the Enrichment Index [21]

Level EF	Pollution level
EF ≤0	Reduced pollution
EF =0-1	Normal values
EF =1-2	Sensitive area alert threshold
EF =2-3	Less sensitive area alert threshold
EF =3-4	Intervention threshold sensitive area
EF =4-5	Intervention threshold less sensitive area
EF ≥5	Extreme pollution

The pollution classes used in the method of determining the levels of ecological risk measurement are expressed in **Table 5**.

Table 5.

Pollution classes according to the E_r and RI index [21]

Level E_r	Value E_r	Risk	Level RI	Risk
0	<40	Reduced	<110	Reduced
1	40-80	Moderate	110-200	Moderate
2	80-160	Considerable	200-400	Considerable
3	160-320	Big	>400	Big
4	>320	Catastrophic		

Oil exploration can also create accidental pollution with heavy metals.

Even if the concentration of total hydrocarbons in the soil is within the limits and not requiring intervention for depollution, rather high concentrations of metals have been found. The analyzes showed that the metals were adsorbed by the soil even in the control sample collected from more than 1 km away from the crude oil exploitation area.

Crude oil extraction areas are usually located at long distances from human settlements, but the presence of metals in the soil can lead to their leaching in transitional waters (groundwater).

Usually, when the soil contains metals, in the plant samples, metals are found too, making it necessary to determine the metallic elements in case of an oil exploitation area under ecological reconstruction. The plants situated in the control area should contain heavy metals which could be taken from the air (particles), then transferred to the soil. For the treatment of the soil in the analyzed area, marigolds and lettuce were used as remediation crops. In the absence of analyses, it is recommended not to use these vegetable products.

Table 6.

Soil samples position

Nr. crt.	Measurement point
1.	Parking area for workers and contractors
2.	Vertical tank contained oil and water 250 mc,
3.	Buried tank contained oil and water 250 mc,
4.	Vertical tank 200 m^3 contained salt water
5.	Vertical tank 20 m^3 contained oil and water
6.	Vertical tank 20 m^3 contained oil and water
7.	Oil, gas and water pipelines keyboard
8.	Vertical separator oil, water, gas 3,85 m^3 - 8 bar
9.	Vertical separator oil, water, gas
10.	Vertical separator oil, water, gas 3,85 m^3 - 8 bar

Nr. crt.	Measurement point
11.	Vertical separator oil, water, gas
12.	Oil, gas and water pipelines blending area

It was observed that the pollution with metals, coming from crude oil, is present in the extraction area, being over 10 times bigger than in a residential area (Figure 1 and Figure 2).

All collected samples had concentrations of metals within the control limits. Zinc pollution is present in areas where gas leaks have occurred, the area being at moderate risk in operation.

Depollution intervention is not recommended but maintaining agricultural crops that naturally remove the metals would be a good option.

Lead pollution is present especially around the biphasic separator, where the elimination of gases in the atmosphere, due to the opening of the safety valve and the slight tightening of the valves created the possibility to remove metals in the exhaust gases. This is an alert threshold.

Also, the risk analysis in operation by the two spectrophotometric methods is very useful, the results being similar comparatively.

The variation of metallic elements depending on soil pollution was analyzed too.

In monitoring point 1, it was observed that the pollution was not only with crude oil but also with petrol and diesel (being a car park), therefore these data were excluded from the statistical analysis.

By statistical analysis, it was possible to determine the equations of variation for the heavy metal elements in the soil, as a function of oil pollution level (mg/kg) (Figure 3 and Table 12).

Table 7.

Metals contents in the analyzed area (mg/kg)

Location	Oil contents in soil	Pb	Ni	V	Cd	Zn	Ag	Cu
1	92	6	105	81	0,23	121	1,25	110
2	998	80	195	199	0,93	245	4,7	198
3	953	78	185	167	0,85	233	4,1	189
4	50	15	110	92	0,01	88	1,2	102
5	987	79	188	175	0,87	241	4,4	195
6	820	65	171	157	0,68	197	3,8	188
7	740	61	155	151	0,50	177	2,9	172
8	890	69	173	177	0,71	199	4,5	189
9	75	23	115	102	0,09	91	1,5	109
10	72	21	111	99	0,05	89	1,4	108
11	93	28	120	111	0,13	102	1,6	113
12	99	29	121	114	0,15	115	1,8	115
Min	50	15	110	92	0,01	88	1,2	102

Max	998	80	195	199	0,93	245	4,7	198
Mediate	489	46,1	145	135	0,43	158	2,7	149
Dispersion	159336	763	2276	2426	0,11	4283	2,0	2558
Standard Deviation	399	27,6	47,7	49,2	0,33	65,4	1,41	50,5
Coefficient of variation	7,9	2,7	0,23	0,38	0,32	0,83	0,72	0,94
Control sample value	50	10	95	88	0,008	60	0,9	93
Cluj City Value	10	0,8	10	70	0,005	4,21	0,01	0,75

Table 8.

Pollution Index to Pb and Ni

Locație	Pb	Igeo	E_r	Ni	Igeo	E_r
1	6	- 1,32	3,00	105	- 0,44	5,53
2	80	2,42	40,00	195	0,45	10,26
3	78	2,38	39,00	185	0,38	9,74
4	15	-	7,50	110	-0,37	5,79
5	79	2,40	39,50	188	0,40	9,89
6	65	2,12	32,50	171	0,26	9,00
7	61	2,02	30,50	155	0,12	8,16
8	69	2,20	34,50	173	0,28	9,11
9	23	0,62	11,50	115	- 0,31	6,05
10	21	0,49	10,50	111	- 0,36	5,84
11	28	0,90	14,00	120	- 0,25	6,32
12	29	0,95	14,50	121	- 0,24	6,37
Control sample value	10			95		
RI	277			92,05		

Table 9.

Pollution Index to V and Cd

Locație	V	Igeo	E_r	Cd	Igeo	E_r
1	81	- 0,70	4,60	0,23	4,26	143,75
2	199	0,59	11,31	0,93	6,28	581,25
3	167	0,34	9,49	0,85	6,15	531,25
4	92	-0,52	5,23	0,01	- 0,26	6,25
5	175	0,41	9,94	0,87	6,18	543,75
6	157	0,25	8,92	0,68	5,82	425,00
7	151	0,19	8,58	0,5	5,38	312,50
8	177	0,42	10,06	0,71	5,89	443,75
9	102	-0,37	5,80	0,09	2,91	56,25
10	99	-0,42	5,63	0,05	2,06	31,25

11	111	-0,25	6,31	0,13	3,44	81,25
12	114	-0,21	6,48	0,15	3,64	93,75
Control sample value	88			0,01		
RI	92,33			3250		

Table 10.

Pollution Index to Zn and Ag

Locație	Zn	Igeo	E_r	Ag	Igeo	E_r
1	121	0,43	10,08	1,25	- 0,11	6,94
2	245	1,44	20,42	4,7	1,80	26,11
3	233	1,37	19,42	4,1	1,60	22,78
4	88	- 0,03	7,33	1,2	- 0,17	6,67
5	241	42	20,08	4,4	1,70	24,44
6	197	1,13	16,42	3,8	1,49	21,11
7	177	0,98	14,75	2,9	1,10	16,11
8	199	1,14	16,58	4,5	1,74	25,00
9	91	0,02	7,58	1,5	0,15	8,33
10	89	- 0,02	7,42	1,4	0,05	7,78
11	102	0,18	8,50	1,6	0,25	8,89
12	115	0,35	9,58	1,8	0,42	10,00
Control sample value	60			0,90		
RI	158			184		

Table 11.

Pollution Index to Cu

Locație	Cu	Igeo	E_r
1	110	-0,34	5,91
2	198	0,50	10,64
3	189	0,43	10,16
4	102	-0,45	5,48
5	195	0,48	10,48
6	188	0,43	10,10
7	172	0,30	9,24
8	189	0,43	10,16
9	109	-0,35	5,86
10	108	-0,36	5,80

11	113	-0,30	6,07
12	115	-0,27	6,18
Control sample value	93		
RI	96		

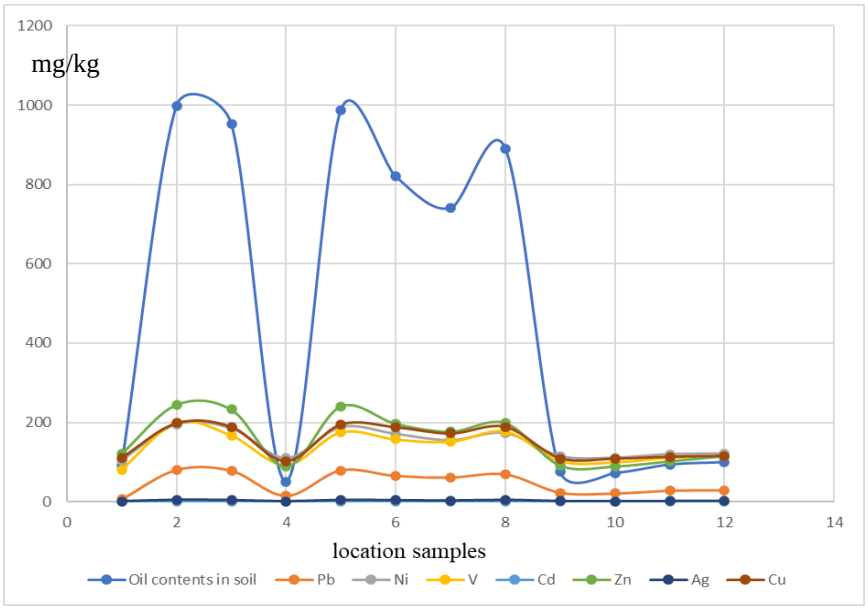

Fig. 1. Metals in soil sample by polluted areas (mg/kg)

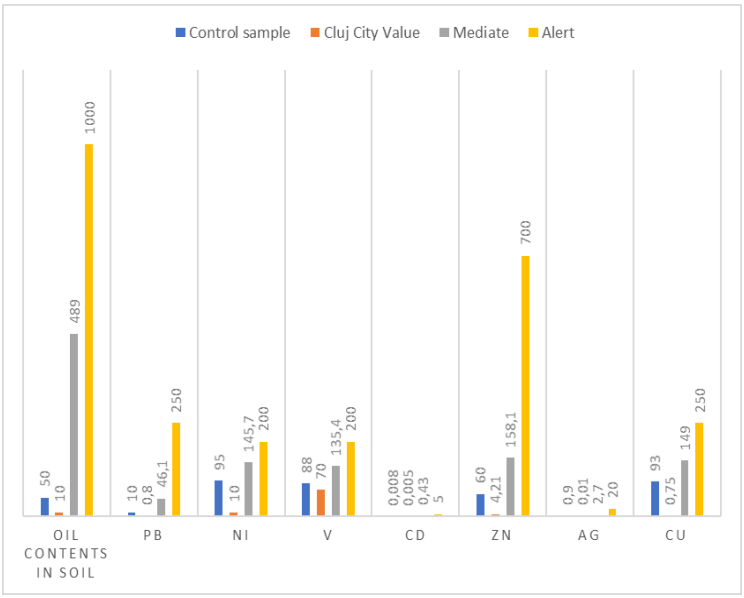

Fig. 2. Metals in soil sample by polluted areas, Cluj City Area , Control sample area and alert threshold (mg/kg)

Table 12.

Equation of variation of metals (mg/kg) (Y) in the soil from the content of hydrocarbons (mg/kg) in the soil (X)

Y (Metals contents in soil (mg/kg))	Equation	R^2
Zn	$y = 4E\text{-}14x^6 - 1E\text{-}10x^5 + 2E\text{-}07x^4 - 0{,}0001x^3 + 0{,}0384x^2 - 3{,}2593x + 170$	0,9955
Pb	$y = -3E\text{-}15x^6 + 8E\text{-}12x^5 - 8E\text{-}09x^4 + 4E\text{-}06x^3 - 0{,}0015x^2 + 0{,}4571x - 4{,}7455$	0,9993
Ni	$y = 2E\text{-}14x^6 - 6E\text{-}11x^5 + 8E\text{-}08x^4 - 4E\text{-}05x^3 + 0{,}0105x^2 - 0{,}7061x + 123{,}63$	0,9972
V	$y = 4E\text{-}14x^6 - 1E\text{-}10x^5 + 2E\text{-}07x^4 - 1E\text{-}04x^3 + 0{,}024x^2 - 1{,}7204x + 130{,}27$	0,9779
Cd	$y = 1E\text{-}16x^6 - 4E\text{-}13x^5 + 4E\text{-}10x^4 - 2E\text{-}07x^3 + 3E\text{-}05x^2 + 0{,}0005x - 0{,}0827$	0,9973
Zn	$y = 4E\text{-}14x^6 - 1E\text{-}10x^5 + 2E\text{-}07x^4 - 0{,}0001x^3 + 0{,}0384x^2 - 3{,}2593x + 170$	0,9955
Ag	$y = 1E\text{-}15x^6 - 4E\text{-}12x^5 + 5E\text{-}09x^4 - 3E\text{-}06x^3 + 0{,}0005x^2 - 0{,}0352x + 1{,}9024$	0,9935

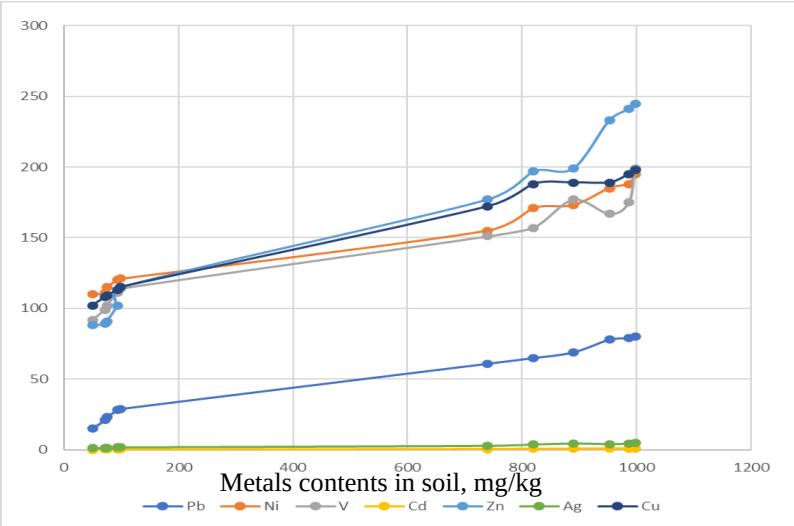

Fig. 3. Metals in soil sample oil contents in soil (mg/kg)

4. Conclusions

This work deals with the monitoring of pollutants (hydrocarbons and heavy metals) in a abandoned oil tanks farm with the aim to assess the risk in agricultural exploitation of the land. It was supposed that the agricultural use would remediate naturally the land, concerning the hydrocarbon, but it was of interest to evaluate the metal pollution as well.

It was concluded that metals concentrations determined correspond to threshold sensitive area alert/less sensitive; this level of metal concentration is considered as average pollution, however this is much higher than in a municipality area of about 100,000 inhabitants.

Also, in this study, correlations between the concentration of main pollutant in the soil (crude oil) and the different metals concentration were established which could serve to the prediction of metals pollution in other abandoned oil tank farms.

REFERENCES

[1] Petrache St., Environmental risk management at the end of onshore oil operations, Ph.D. Thesis, Oil and Gas University, 2021, pp.190-220, Ploiesti.

[2] Michael A. M., Ojha T. P., Principles of agricultural engineering Jain Brother, New Delhi, 2006, pp.90-210.

[3] Chis T, Petrache St. Jugastreanu C., Oil pollution of groudwater in Dobruja Area, Quest *Journal of Research in Environmental and Earth Sciences*, 7(2021), 50-61.

[4] Koncsag C.I., Fizico-chimia petrolului (Petroleum physico-chemistry), Ovidius University Press, Constanta, Romania, 2003, pp 45-90, in Romanian

[5] Hagen J., Industrial Catalysis. A practical approach, Second Edition, WILEY-VCH Verlag GmbH & Co. KGaA, Weinheim, Germany, 2006, pp. 197–207.

[6] Speight J.J. Petroleum Chemistry and Refining, Taylo&Francis, U.S.A, 1997, pp. 202-222.

[7] Yen T.F., Structure of Petroleum Asphaltene and Its Significance, *Energy Sources*,1(1974), 447-463.

[8] Muniyappan R., Porphyrins in petroleum, *Journal of Chemical Education*, 32 (1955), 277-290.

[9] Lash T.D., Almejbel A.S., Synthesis of 2-bromo- and 2-phenyl-neo-confused porphyrins", *Organic & Biomolecular Chemistry*, 37 (2000). DOI: 10.1039/D0OB01642J

[10] Fakher S., Ahdaya M., Elturki M., Critical review of asphaltene properties and factors impacting its stability in crude oil, *Journal Petrol Explor Prod Technol*, 10 (2020), 1183–1200.

[11] Zali M.A., Ananthy R., Ng C.,Wan K., Wan A., Concentration of heavy metals in virgin, used, recovered and waste oil: A spectroscopic study, *Procedia Environmental Sciences*, 30(2015), 201-204.

[12] Albuquerque M.T.D., Gerassis S., Sierra C., Taboada J., martin J.E., Antunes I.M.H.R., Gallego J.R., Developing a new Bayesian Risk Index for risk evaluation of soil contamination, *Sci. Total Environ*., (2017), 603–604

[13] Aguilera P.A., Fernández A., Fernández R., Rumí R., Salmerón A., Bayesian networks in environmental modelling, *Environ. Model. Softw*., 26 (2011), 1376-1388.

[14] Bazlamaçci C.F., Hindi K.S.,Minimum-weight spanning tree algorithms. A survey and empirical study, *Comput. Oper. Res*., 28 (2001), 767-785.
[15] Cocârță D. M., Stoian M. , Karademir A., Crude Oil Contaminated Sites: Evaluation by Using Risk Assessment Approach, *Sustainability*, 9(2017),1365. **https://doi.org/10.3390/su9081365**
[16] Wang Y., Hu J., Xiong K., Huang X., Duan S.,Distribution of Heavy Metals in Core Sediments from Baihua Lake, *Procedia Environ. Sci*.,16 (2012), 51–58.
[17] Karbassi A.R., Abduli M. A., Mahin E., Abdollahzadeh A., Sustainability of energy production and use in Iran, *Energy Policy*, 35(2007), 5171-5180
[18] Alyazichi Y.M., Jones B.G, Mclean E., Pease J., Brown H. Geochemical Assessment of Trace Element Pollution in Surface Sediments from the Georges River, Southern Sydney, Australia, *Arch. Environ. Contam. Toxicol.*, 72 (2017), 247–259.
[19] Ma L., Yang Z., Li L., Wang L., Source identification and risk assessment of heavy metal contaminations in urban soils of Changsha, a mine-impacted city in Southern China, *Environ. Sci. Pollut. Res*., 23 (2016), 17058–17066
[20] Chai L., Li H., Yang Z., Min X., Liao Q., Liu Y., Men S., Yan Y, Xu J., Heavy metals and metalloids in the surface sediments of the Xiangjiang River, Hunan, China: Distribution, contamination, and ecological risk assessment, *Environ. Sci. Pollut. Res.* 24 (2017), 874–885.

SYNTHETIC DYES ADSORPTION FROM AQUEOUS SOLUTIONS. OVERVIEW ON PROCESS IMPROVEMENT BY ULTRASOUND ASSISTANCE

Cristina G. GRIGORAȘ[1], Andrei I. SIMION[1,*], Lucian GAVRILĂ[1*]

[1]"Vasile Alecsandri" University of Bacău, Faculty of Engineering,
Department of Chemical and Food Engineering, 157 Calea Mărășești, Romania

Abstract

Dye wastewater treatment is mandatory in order to reduce its negative impact on the environment. This review begins with a short classification of synthetic dyes, their uses and effects. It is then directed to a brief discussion of the most known technologies involved in the removal of colored compounds from water. Several biological, chemical and physical methods along with their performance, features, advantages and disadvantages are emphasized. The present paper accentuates the possibility of using ultrasound to enhance the results obtained by adsorption – one of the most convenient techniques focused on the elimination of persistent contaminants from aqueous media. Finally, it concludes on revealing the utmost interest lately due to the advantages of the cavitation phenomenon on accelerating the adsorption process.

Key words: adsorption, synthetic dyes, ultrasound, wastewater treatment

1. Introduction

Synthetic dyes are organic molecules able to bind on substrates in order to confer them color. Their coloring properties are connected to the presence of chromophore groups and depend on the capacity of absorbing the radiations in the visible range of the electromagnetic spectrum [1].

Dyes are classified in several different classes according to various criteria. A depiction based on the nature of the chromophore groups is given in Figure 1. Azo dyes are characterized by the presence within the molecule of an azo functional group uniting two alkyl or aryl groups generally based on the azobenzene skeleton [2]. Anthraquinone dyes are, from a commercial point of view, the most important ones after azo dyes. Their general formula derived from anthracene shows that the chromophore is a quinone nucleus with attached hydroxyl or amino groups [3]. Indigoid dyes derive from indigo. Selenium, sulfur

* Corresponding authors: e-mail address: asimion@ub.ro, lgavrila@ub.ro

and oxygenated counterparts of indigo blue cause significant hypsochrome effects with colors ranging from orange to turquoise [4]. Xanthenoid dyes, the best-known compound of which is fluorescein, have intense fluorescence. Less used as dyes, they are established markers during maritime accidents or as flow tracers for underground rivers, waste streams etc. [5, 6]. The phthalocyanines are planar aromatic macrocycles formed by four iso-indole groups linked in position 1-3 by an azone bridge. Nitro and nitroso dyes form a very limited class in number and relatively old. They are currently still used, because of their price very moderate linked to the simplicity of their molecular structure characterized by the presence of a nitro group (-NO_2) in the ortho position of a group electron donor (hydroxyl or amino groups) [7]. Triphenylmethanes are derivatives of methane for which the atoms of hydrogen are replaced by substituted phenyl groups of which at least one is carrying an oxygen or nitrogen atom para to the methane carbon. Triphenylmethane and its homologues are the fundamental hydrocarbons from which derive a whole series of coloring compounds [8].

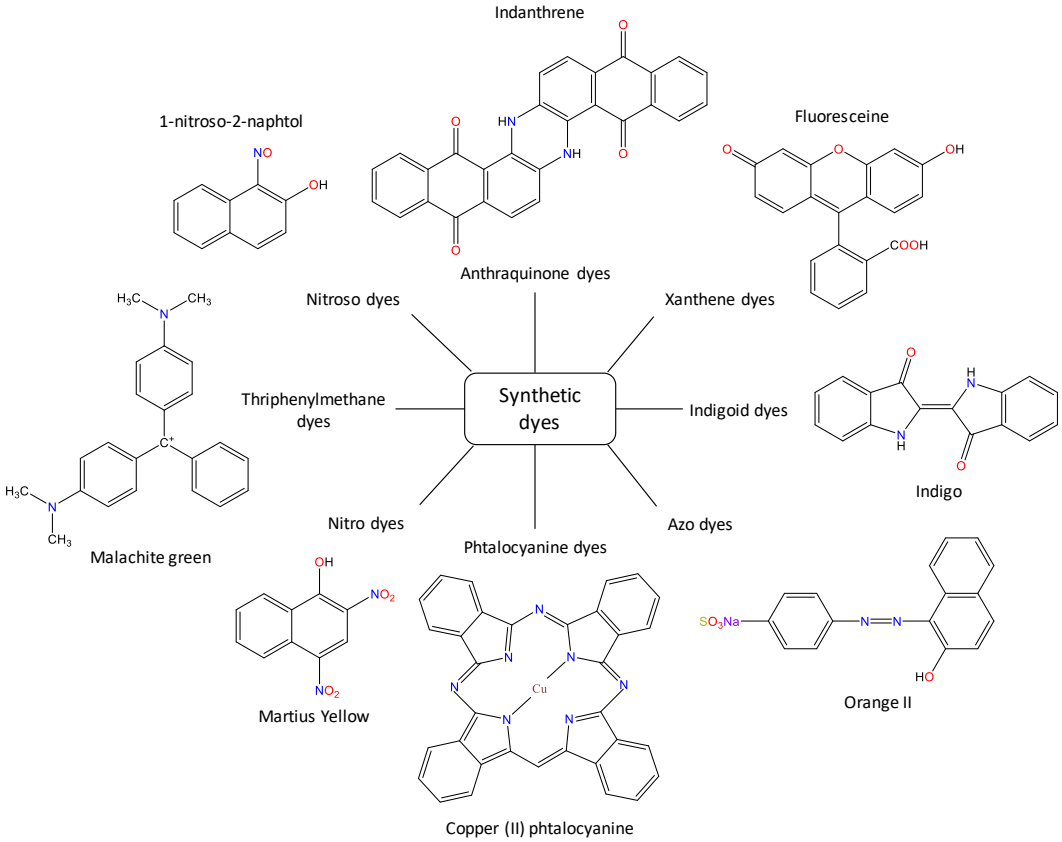

Fig. 1. Synthetic dyes chemical classification

Another classification of dyes can be made taking into consideration the application fields. Different categories defined this time by the auxochromes can be identified. Mordants are soluble dyes possessing the particularity to form complexes with metallic ions through two hydroxyl groups close to each other. They are used for wool and cotton dyeing [9]. Acid dyes are made up of a chromophore group and one or more sulfonates groups allowing their solubilization in water. This class includes azo, anthraquinones or triphenylmethanes dye widely used for silk, cotton, wool, polyamide, or food coloring [10-12]. The basic dyes are derived from organic bases and ionize in water. They are usually in the form of salts and belong to different chemical classes such as diphenylmethane, triarylmethane, oxazine, xanthene etc. being utilized in cotton and wool dyeing. Reactive dyes are soluble anionic compounds that are covalently bound to the substrate, their application being facilitated using electrolytes. The reactivity levels are improved by various reactive groups (trichloropyrimidine, sulphatoethylsulphone, dichlorotriazin etc.). This category of dyes is employed in dyeing cellulose, silk, and wool fibers [13, 14]. Direct dyes are molecules that are loosely bound to support and can be easily removed at temperatures higher than 100 °C. They have a strong affinity for cellulose fibers, but are also used for coloring paper products [15]. Disperse dyes are water-insoluble, non-ionic, and volatile dyes used for polyester, polyamide or cotton dyeing [16]. Vat dyes have better colorfastness and excellent brightness properties. They are primarily soluble in hot water and some of them in sodium carbonate and color cellulose fibers, nylon [17, 18].

Synthetic dyes are produced annually in millions of tones [19] and besides their intensive use in textile industry [20], they are also involved in multiple other sectors.

In paper manufacturing process [21], they are used in making bright colored handmade paper.

In cosmetic and pharmaceutical industries, they color beauty and personal care products and drugs [22-24].

In food industry, they are responsible for the attractive appearance, they compensate the loss of natural colors that are destroyed during processing and storage, and they improve the products properties making them more appealing for consumers [25, 26].

Despite their extensive presence, they can be blamable for skin and mucous membrane irritation and burns, carcinogens, allergic reactions, respiratory problems [27]. Hyperactivity, aggressiveness, urticaria, bronchoconstriction, asthma, eczemas etc. can be listed as undesirable consequences of dyes on human health [28]. The high consumption of synthetic dyes leads to discharge of significant volumes of polluted wastewaters [29] which raises serious concerns both for humans and aquatic life and for the environment.

2. Treatment of dye polluted wastewater

Considering the above related aspects, decolorization of dye effluents receives a special attention and biological, chemical, and physical methods of treatment are incessantly developed for this purpose (Table 1).

Biological processes are among the most convenient clean, green, and sustainable technologies used for wastewater treatment. They employ bacteria, fungi, yeasts, algae, and enzymes in aerobic, anaerobic, or mixed conditions and they do not produce toxic compounds. These processes are largely effective in handling suspended solids, biochemical oxygen demand, and color. Even though, they present drawbacks such as the fact that they require long time to degrade dyes, their reduced performance, the need of large operational space, and the generation of important amounts of sludge [2].

Table 1

Processes used in dye removal

Treatment process	Materials	Studied dyes	Removal efficiency	Reference
Biological treatment	- Bacteria strains of *Micrococcus yunnanensis*	- Methyl orange	98 %	[30]
Biological treatment	- Phyco-composite material composed of *Spirogyra* sp. and *Rhizoclonium* sp.	- Basic red 46	96 %	[31]
Biological treatment	- Soybean peroxidase - Luffa peroxidase	- Methyl orange	75.3 % - 81.4 %	[32]
Ozonation	- Ozone with sodium sulfate, sodium carbonate or sodium hydroxide	- Reactive black 5	100 %	[33]
Ozonation	- Ozone	- Nova cron super black K and terasil red ww 3BS	92.2 %	[34]
Photocatalysis	- Nanocomposites of molybdenum disulfide and titanium dioxide	- Methylene blue	100 %	[35]
Photocatalysis	- Titanate nanosheets - Titanate nanotubes - Platinum doped titanate nanomaterials	- Methylene blue - Rhodamine B - Methyl orange - Naphtol blue-black	60 % - 100 %	[36]
Photocatalysis	- Hybrid material composed of copper (II) oxide and tungsten oxide	- Methylene blue	90.1 %	[37]
Photocatalysis	- Layered double hydroxide materials (ZnCr-Cl, ZnCr-SO_4, ZnCr-CO_3)	- Acid orange 7	25 % - 49.5 %	[38]

Electro - Fenton	- Hydroxyl radicals produced from Fenton reaction	- Reactive red 195	100 %	[39]
Electro - Fenton	- Electro-Fenton process in the presence of iron-doped mesoporous silica	- Rhodamine B	97 %	[40]
Coagulation-flocculation followed by ultrafiltration	- Natural coagulant prepared from *Moringa oleifera* Lam extract with calcium chloride	- Reactive black 5	100 %	[41]
Coagulation	- Magnesium hydroxide	- Reactive red - Reactive yellow	95.7 % - 96.7 %	[42]
Forward osmosis	- Nanocomposite polymer hydrogels	- Rhodamine B	99.9 %	[43]
Forward osmosis	- Nanohybrid agent containing poly[2-dimethylamino)ethyl methacrylate on gas-responsive magnetic nanoparticles	- Rhodamine B	99.99 %	[44]
Forward osmosis	- Thin-film composites membranes with polysulfone substrate and polyamide	- Reactive black 5 - Acid red 114 - Acid red 88	98.2 % - 99.7 %	[45]
Forward osmosis	- Multifunctional active layer membrane prepared with sulfamethoxazole and trimethroprim	- Methyl orange - Acid fuchsin - Congo red	90 % - 95.5 %	[46]

Advanced oxidation processes (AOPs) are chemical techniques able to destroy dyes with the help of reactive species as hydroxyl, sulfate, or superoxide radicals. Different methods are included in the generic appellation of AOPs.

Ozone, for example, is a powerful oxidant that can destroy synthetic dyes directly by electrophilic attack, or indirectly by attack of hydroxyl radicals resulted from its decomposition. Ozonation application diminishes the sludge quantities formed in the wastewater treatment but implies the disadvantage of being difficult to control since the ozone is highly unstable and easily decomposable [47]. Photocatalysis (particularly the heterogeneous one) has proved to be able to degrade dyes by using the sunlight in the presence of a semiconductor photocatalyst. Firstly, the target substrate is adsorbed from the environment on the semiconductor surface. Then, the light with photon energy larger than the band gap energy of the photocatalyst is absorbed leading to the production of photogenerated electron (e^-)-hole (h^+) pairs. E^- and h^+ migrate to semiconductor surface and the redox reaction and recombination of some photogenerated carriers from the surface and the inside of the photocatalyst occur simultaneously. In another step, molecules of water and oxygen are oxidized and reduced to hydroxyl and superoxide radicals by photons in the valence band and by electrons in the conduction band respectively while water contaminants are degraded to small molecules. Finally, the degraded compounds desorb from the

interface to the bulk solution, and photoreaction continues [48, 49]. Another AOPs is the electro-Fenton one. It relies on the hydrogen peroxide electro generated by the two-electron oxygen reduction reaction. The obtained H_2O_2 reacts with the catalyst to produce hydroxyl radicals which are responsible for the mineralization and elimination of synthetic dyes. The process is economically reliable, environmentally friendly and it requires simple equipment but it has a narrow operating range and it demands a low current density and a low conductivity [50].

In terms of physical processes dedicated to the treatment of wastewater containing colored compounds, many techniques are also available. Coagulation-flocculation is based on the use of materials which are put in contact with the contaminated water, destabilize the dyes and force their agglomeration; the formed flocs sediment and are removed by filtration [51]. The process reduces the chemical oxygen demand, turbidity, diminishes the content of suspended solids and organic matter [52]. Forward osmosis implies an osmotic pressure gradient that makes the water pass through the membrane from feed to draw solution and ensures high water flux and reduced fouling with low energy consumption [53].

3. Decontamination of dye polluted wastewater by adsorption

Adsorption process

Dyes adsorption is considered an easily affordable and simple to operate method which leads to high volumes of treated effluents and does not produce harmful substances.

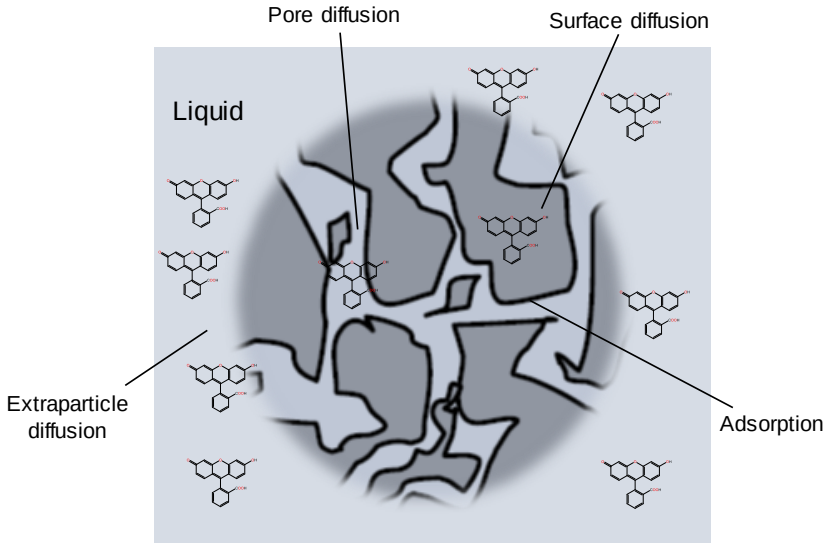

Fig. 2. Schematic illustration of adsorption process

The process refers to the accumulation of a molecule (called adsorbate) at the interface between a liquid phase in which this molecule is often encountered and a solid phase (named adsorbent).

The target compound will pass from the fluid to the adsorbent by mass transfer from the liquid to the surface of the adsorbent particle through the limit film surrounding the particle followed by internal diffusion into the adsorbent pores and adsorption on the particle surface (Figure 2).

Adsorption usually occurs at the same time as reversible physisorption (represented by weak van der Waals and hydrogen bonds, dipole-dipole interactions), and as irreversible chemical adsorption (taking place as a monolayer and being caused by chemical associations between the adsorbate and the adsorbent) [54, 55].

Adsorbent materials

A wide variety of adsorbents with noticeable porosity, important surface area, and high pore size are available. As exposed in Table 2, they can be included in different classes namely activated carbon, waste materials from agriculture and industrial sectors, bioadsorbents, nanomaterials, nanocomposites, metal-oxide based polymers etc. all of them showing very good results in eliminating dyes from wastewater.

Table 2

Adsorbents used in dye removal

Adsorbent	Adsorbed dyes	Tested parameters*	Removal efficiency	Reference
Activated carbon prepared of apricot stones	- Methylene blue - Methyl orange	- C_0: 5 - 100 mg/L - Solution pH: 3 - 10 - Ads. dose: 0.02 - 0.2 g/L - Contact time: 0 - 280 min - Temperature: 20 - 40 °C	99 %	[56]
Activated carbon prepared of coconut leaves	- Methylene blue	- C_0: 30 - 400 mg/L - Solution pH: 3 - 11 - Ads. dose: 0.2 - 2.5 g/L - Contact time: 0 - 180 min - Temperature: 30 - 50 °C	100 %	[57]
Powder of exhausted ground coffee	- Rhodamine B - Rhodamine 6G	- Ads. dose: 1 g/L - Contact time: 180 min - Temperature: 5 °C; 19 °C	91 %	[58]
Leaves of *Platanus orientalis*	- Methylene blue	- C_0: 20 - 180 mg/L - Solution pH: 2 - 12 - Ads. dose: 1.6 g/L - Contact time: 5 - 70 min - Temperature: 25 - 60 °C	76 %	[59]

Diatomite	- Rhodamine B - Methylene blue	- C_0: $2.09 \cdot 10^{-5}$ - $3.13 \cdot 10^{-5}$ mol/L - Solution pH: 3 - 11 - Ads. dose: 0.2 g/L - Contact time: 0 - 240 min - Temperature: 30 °C; 45 °C	94 % - 100 %	[60]
Peach seed powder	- Acid blue 25	- C_0: 25 - 150 mg/L - Ads. dose: 1 g/L - Contact time: 200 min - Temperature: 25 - 50 °C	86 %	[61]
Shrimp shell	- Acid blue 25	- C_0: 50 - 110 mg/L - Solution pH: 2 - 11 - Ads. dose: 0.1 - 0.4 g/L - Contact time: 0 - 60 min - Temperature: 25 - 50 °C - Particle size: 53 - 500 µm - Salinity: 0 - 40 g/L	68 %	[62]
Hybrid material (iron-carbon) magnetic nanosheets	- Methylene blue - Congo red	- Ads. dose: 0.4 g/L - Solution pH: 2; 8 - Contact time: 24 min	96 %	[63]
Graphene oxide	- Methylene blue	- C_0: 125 - 500 mg/L - Solution pH: 2 - 12 - Contact time: 0 - 1800 min - Temperature: 0 - 50 °C	99 %	[64]
Composite of chitosan and sepiolite	- Methylene blue - Reactive orange 16	- C_0: 25 - 400 mg/L - Solution pH: 3 - 11 - Ads. dose: 1 - 3 g/L - Contact time: 0 - 100 min	95 % - 99 %	[65]
Nanohybrid layered double hydroxides	- Amaranth - Diamine green B - Brilliant green	- C_0: 0.061 - 6.62 mmol/L - Solution pH: 4 - 10 - Ads. dose: 1 g/L - Contact time: 0 - 3000 min	84 % - 93 %	[66]
Nanoparticles of magnetite modified with humic acid	- Malachite green	- C_0: 20 - 60 mg/L - Solution pH: 2 - 12 - Ads. dose: 3 - 7 g/L - Contact time: 10 - 100 min - Temperature: 25 - 50 °C	84.4 % - 98.8 %	[67]
Porous microspheres of zinc oxide – aluminum oxide	- Congo red	- C_0: 50 mg/L - Ads. dose: 0.5 g/L - Contact time: 720 min - Temperature: ambient	94.3 %	[68]
Zirconium-based metal-organic frameworks	- Cristal violet - Rhodamine B	- C_0: 10 - 90 mg/L - Solution pH: 3 – 11 - Ads. dose: 1 g/L - Contact time: 0 - 540 min - Temperature: ambient	98.4 %	[69]

Nanocomposites of polypyrrole or polyaniline	- Sunset yellow - Congo red	- C_0: 50 mg/L - Solution pH: 2 - 11 - Ads. dose: 0.0001 - 0.05 g/L - Contact time: 0 - 30 min - Temperature: ambient	98 % - 99 %	[70]
Composite magnetic-adsorbent prepared from spinel ferrite in chitosan	- Acid orange 7	- C_0: 50 mg/L - Solution pH: 6.2 - Ads. dose: 2 g/L - Temperature: 25 °C - Contact time: 0 - 360 min	98.01 %	[71]

*C_0 – initial dye concentration; Ads. dose – adsorbent dose

Adsorption enhancement by ultrasound assistance

Ultrasounds are mechanical waves that exceed the human perception threshold (20 Hz - 20 kHz). They propagate through the material or to its surface at a speed depending on the nature of the waves and the material being treated.

The effect of ultrasound on liquid systems is largely due to the cavitation phenomenon. These waves propagate in the form of a series of compression-rarefaction cycles induced in environmental molecules as pictured in Figure 3.

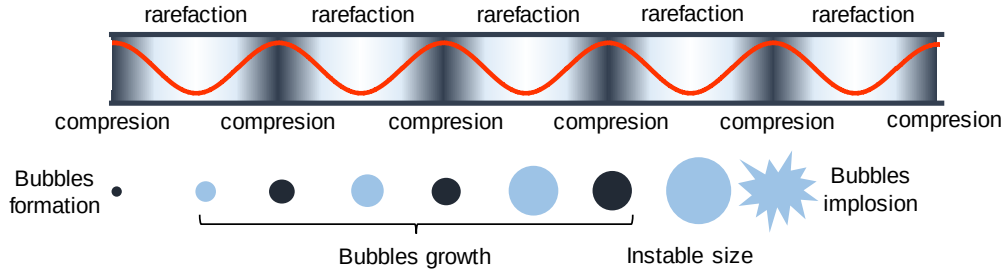

Fig. 3. Cavitation bubbles generation under ultrasound effect

At a sufficiently high intensity, the thinning cycles can exceed the attractive forces of the molecules conducting to the appearance of bubbles formed by the gas nuclei existing in the liquid subjected to the action of ultrasound. These bubbles, randomly distributed in the liquid, grow over several cycles to a critical size, become unstable and break violently. The implosion of cavitation bubbles leads to the accumulation of energy generating extremely high temperatures and pressures which in turn cause turbulence in the cavitation area [72]. The combination of these factors (pressure, heat, and turbulence) has many effects on ultrasonicated systems. The energy and intensity of ultrasound along with the viscosity of the environment, the surface tension, the nature and concentration of dissolved gases, the presence of solid particles and the temperature and pressure of the treatment determine the expansion of the cavity. An additional phenomenon

that derives from the variation of the size of the bubbles and their implosion is represented by the development of strong micro-jets associated with high-speed gradients that alter the characteristics of the propagation medium. Some of the acoustic energy can be absorbed in the form of heat. Another important effect is that water molecules can be broken down, leading to the generation of highly reactive free radicals ($\cdot OH^-$) that can react with other molecules [73].

In the removal of synthetic dyes from wastewater by adsorption, ultrasound can be used to successfully improve the process.

Dastkhoon *et al.* [74] investigated this possibility for the elimination of malachite green. They prepared a material by applying zinc sulfide and copper nanoparticles on activated carbon and put it in contact with dye solution under sonication. They designed an experimental program based on Response Surface Methodology and established that at in a solution of 20 mg/L concentration and pH 6, with an adsorbent dose of 0.02, after 3 min of ultrasound action, the synthetized adsorbent had an adsorption capacity of 168.1 mg/g.

Other researchers [75] report that a simultaneously and competitive removal of auramine-O, erythrosine and methylene blue is obtained when an adsorbent produced also from copper-doped zinc sulfide nanoparticles loaded on activated carbon and an ultrasound tank with heating system and a frequency of 40 kHz are employed.

Acid yellow 36 and acid blue 74 were retained on graphene oxide nanoplatelets embedded in chitosan. The appropriate time for ultrasound exposure was in this case of only 6.48 min. In the experimental conditions, 0.5 g/L adsorbent removed more than 98 % of the contaminants [76].

The effect of parameters such as pH, sonication time (1 - 5 min), adsorbent amount (activated carbon loaded with nanoparticles of manganese saturated with zinc sulfide), dyes solutions concentration was established by Asfaram *et al.* [77] by central composite design. At the end, the authors discovered that the first three mentioned factors have the greatest impact on the target malachite green and methylene blue removal. Their results reveal efficiencies of at least 98 % when the solutions have concentrations of 15 mg/L and pH 7, an amount of 0.025 g of adsorbent is used and the process is assisted 3 min by ultrasound.

In other paper [78], activated carbon modified with Mn@ CuS/ZnS-NC was able to eliminate methylene blue and malachite green from their binary mixture in aqueous solution. pH, adsorbent quantity, sonication time and dyes solutions concentration were considered as independent variables affecting the process while the dyes removal percentages were investigated as responses. The optimized value for applying ultrasound was of 3 min.

Dashamiri *et al.* [79] conducted a study on the elimination of eosin Y, methylene blue and phenol red from aqueous solutions by activated carbon loaded with copper hydroxide particles. The removal almost complete (99.20 % ± 1.48)

was obtained at pH 6.0, ultrasound time 2.5 min with a mass of adsorbent of 20 mg for initial dye concentration of 5 mg/L for methylene blue and eosin Y and of 12.5 mg/L for phenol red.

In the research conducted by Ghaedi *et al.* [80], rose Bengal, safranin O and malachite green were removed from aqueous media by using a material resulted from the immobilization of copper oxide nanoparticles on activated carbon. Sonication time was among the various factors tested. Based on the results recovered by using Response Surface Methodology, under the optimized conditions 94.26%, 71% respectively 76% of dyes were eliminated.

A biochar was produced by Amin *et al.* [81] from *Chlorella* sp. solid waste and its potential of retaining reactive yellow dye-145 was examined. Ultrasound assisted adsorption had an efficiency of 99 % in only 1 min.

According to results published by Sharma and Verma [82], the presence of ultrasound and rare earth ions had a favorable impact for the adsorption of disperse orange 30 and yellow brown S2RFL dyes on titanium oxide.

Ultrasonication can be used also in the preparation of adsorbents affecting consequently indirectly the adsorption process.

Jun *et al*. [83] resorted to ultrasound (frequencies of 28 kHz and 580 kHz) in dispersing an adsorbent of two-dimensional titanium carbide that was used after that to adsorb methylene blue and methyl orange.

Low and Tan [84] treated pomelo peels with ultrasound at 30, 60 and 90 % amplitude in order to improve its ability to remove methylene blue from aqueous solution. The peels adsorption capacity at different solution pH (2 - 10), dye concentration (50 - 250 mg/L), adsorbent dose (0.05 - 0.25 g) and contact time (0.5 - 5 h) was investigated. Recorded data revealed that ultrasound pre-treated pomelo peel needed less time to attain higher saturation limit of adsorption capacity and had highest adsorption capacity compared to the non-treated one.

Modwi *et al.* [85] synthesized a composite material through sonication in methanol followed by evaporation and calcination. 1 g of the prepared adsorbent was able to remove 1250 mg of Congo red and 1791 mg of basic fuchsin.

Table 3 gives an additional outline about other studies having as subject the use of ultrasound as a tool to ameliorate the synthetic dyes adsorption from aqueous media.

Table 3

Studies regarding the implication of ultrasound in dyes adsorption

Process	Adsorbent	Adsorbed dyes	Removal efficiency	Reference
Assisted adsorption	- Exfoliated graphite	- Acid brown 348	90 %	[86]
Assisted adsorption	- Zinc aluminate	- Auramine O - Methylene blue	92.78 % - 97.73 %	[87]

Assisted adsorption	- Activated carbon with cupric sulfide load	- Bromophenol blue - Methylene blue	95 %	[88]
Assisted adsorption	- Activated carbon loaded with nanoparticles	- Methylene blue - Crystal violet	99.8 % - 99.87 %	[89]
Assisted adsorption	- Activated carbon prepared from apple tree wood with load of nanoparticles	- Methylene blue - Janus green	98.7 % - 99.57 %	[90]
Assisted adsorption	- Activated carbon doped with copper and zinc sulfide	- Sunset yellow CFC	97.2 %	[91]
Adsorbent preparation	- Peanut husk powder	- Crystal violet	94.83 %	[92]
Adsorbent preparation and assisted adsorption	- Nanoparticles of zinc oxide doped with chromium	- Malachite green - Eosin yellow - Auramine O	97.24 % - 99.26 %	[93]

4. Conclusions

Latest technological progresses allow the development of different methods and their application for the successful removal of toxic contaminants pour into the water. Among them, adsorption is considered an easily affordable and simple to operate process which leads to high volumes of treated effluents and does not produce harmful substances.

In this regard, we reviewed here the recent research targeting the treatment of water polluted with colored molecules highlighting the fact that combining the adsorption effect with that of ultrasound appears to be encouraging for the elimination of wastewater persistent compounds. According to consulted papers we can conclude that parameters such as ratio between the adsorbent and the adsorbate, pH, temperature etc. can be easily adjusted when joined with ultrasound. The cavitation obtained with the help of these waves is recognized as responsible for temperature raise which causes the augmentation of the diffusion rate and the equilibrium endothermic trend. Moreover, ultrasound presence ensures a better mass transfer of the adsorbate to the adsorbent material, an augmentation of the intraparticle diffusion and a considerable reduction of the time required for a good retention of the pollutants.

REFERENCES

[1] Alsantali R. I., Raja Q. A., Alzahrani A. Y. A., Sadiq A., Naeem N., Mughal E. U., Al-Rooqi M. M., El Guesmi N., Moussa Z., Ahmed S. A., Miscellaneous azo dyes: a comprehensive review on recent advancements in biological and industrial applications, *Dyes and Pigments*, 199, (2022), 110050.

[2] Kapoor R. T., Danish M., Singh R. S., Rafatullah M., H.P.S A. K., Exploiting microbial biomass in treating azo dyes contaminated wastewater: Mechanism of degradation and factors affecting microbial efficiency, *Journal of Water Process Engineering*, 43, (2021), 102255.

[3] Li Y., Cao P., Wang S., Xu X., Research on the treatment mechanism of anthraquinone dye wastewater by algal-bacterial symbiotic system, *Bioresource Technology*, 347, (2022), 126691.

[4] Koren Z. C., Chromatographic and colorimetric characterizations of brominated indigoid dyeings, *Dyes and Pigments*, 95, 3, (2012), 491-501.

[5] Li J., Zhang M., Yang L., Han Y., Luo X., Qian X., Yang Y., "Xanthene" is a premium bridging group for xanthenoid dyes, *Chinese Chemical Letters*, 32, 12, (2021), 3865-3869.

[6] Hirata R., Torii A., Kawano K., Futaki S., Imayoshi A., Tsubaki K., Development of xanthene dyes containing arylacetylenes: The role of acetylene linker and substituents on the aryl group, *Tetrahedron*, 74, 27, (2018), 3608-3615.

[7] Odey J. O., Louis H., Agwupuye J. A., Moshood Y. L., Bisong E. A., Brown O. I., Experimental and theoretical studies of the electrochemical properties of mono azo dyes derived from 2-nitroso-1- naphthol, 1-nitroso-2-naphthol, and C.I disperse yellow 56 commercial dye in dye-sensitized solar cell, *Journal of Molecular Structure*, 1241, (2021), 130615.

[8] Wang H., Le Y., Sun J., Light-driven bio-decolorization of triphenylmethane dyes by a Clostridium thermocellum-CdS biohybrid, *Journal of Hazardous Materials*, 431, (2022), 128596.

[9] Ding Y., Freeman H. S., Mordant dye application on cotton: optimisation and combination with natural dyes, *Coloration Technology*, 133, 5, (2017), 369-375.

[10] Deng Y., Tang B., Zhao H., Xu J., Xiao J., Zhang X., Xu H., Zhang S., Dyeing method and properties of polymaleic acid dyes on cotton, *Coloration Technology*, 129, 2, (2013), 144-149.

[11] Billah S. M. R., Christie R. M., Shamey R., Direct coloration of textiles with photochromic dyes. Part 3: dyeing of wool with photochromic acid dyes, *Coloration Technology*, 128, 6, (2012), 488-492.

[12] Dotto G. L., Pinto L. A. A., Adsorption of food dyes acid blue 9 and food yellow 3 onto chitosan: Stirring rate effect in kinetics and mechanism, *Journal of Hazardous Materials*, 187, 1, (2011), 164-170.

[13] Sun L., Li Z., Fu Z., Li Y., Jiang Z., Tang B., Quan J., Xia Y., Wang M., Wang J., Huang H., Coloration of Calcium Alginate Fiber with Dyes and Auxiliary Derived from Polyvinylamine. Part II. Application of PVAm in Salt-free Dyeing with Reactive Dyes, *Fibers and Polymers*, 22, 10, (2021), 2773-2781.

[14] Smith B., Berger R., Freeman H. S., High affinity, high efficiency fibre-reactive dyes, *Coloration Technology*, 122, 4, (2006), 187-193.

[15] Porter J. J., Dyeing equilibria: interaction of direct dyes with cellulose substrates, *Coloration Technology*, 118, 5, (2002), 238-243.

[16] Penthala R., Oh H., Park S. H., Lee I. Y., Ko E. H., Son Y.-A., Synthesis of novel reactive disperse dyes comprising carbamate and cyanuric chloride groups for dyeing polyamide

and cotton fabrics in supercritical carbon dioxide, *Dyes and Pigments*, 198, (2022), 110003.
[17] Khatri M., Ahmed F., Shaikh I., Phan D.-N., Khan Q., Khatri Z., Lee H., Kim I. S., Dyeing and characterization of regenerated cellulose nanofibers with vat dyes, *Carbohydrate Polymers*, 174, (2017), 443-449.
[18] Burkinshaw S. M., Son Y.-A., The dyeing of supermicrofibre nylon with acid and vat dyes, *Dyes and Pigments*, 87, 2, (2010), 132-138.
[19] Al-Tohamy R., Ali S. S., Li F., Okasha K. M., Mahmoud Y. A. G., Elsamahy T., Jiao H., Fu Y., Sun J., A critical review on the treatment of dye-containing wastewater: Ecotoxicological and health concerns of textile dyes and possible remediation approaches for environmental safety, *Ecotoxicology and Environmental Safety*, 231, (2022), 113160.
[20] Benkhaya S., M' rabet S., El Harfi A., A review on classifications, recent synthesis and applications of textile dyes, *Inorganic Chemistry Communications*, 115, (2020), 107891.
[21] Saakshy, Singh K., Gupta A. B., Sharma A. K., Fly ash as low cost adsorbent for treatment of effluent of handmade paper industry-Kinetic and modelling studies for direct black dye, *Journal of Cleaner Production*, 112, (2016), 1227-1240.
[22] Vázquez-Ortega F., Lagunes I., Trigos Á., Cosmetic dyes as potential photosensitizers of singlet oxygen generation, *Dyes and Pigments*, 176, (2020), 108248.
[23] Guerra E., Alvarez-Rivera G., Llompart M., Garcia-Jares C., Simultaneous determination of preservatives and synthetic dyes in cosmetics by single-step vortex extraction and clean-up followed by liquid chromatography coupled to tandem mass spectrometry, *Talanta*, 188, (2018), 251-258.
[24] Tang Y., Zhang Z., Yang S., Smith G. J., Liu L., Diatomite encapsulated AgNPs as novel hair dye cosmetics: Preparation, performance, and toxicity, *Colloids and Surfaces B: Biointerfaces*, 200, (2021), 111599.
[25] Palianskikh A. I., Sychik S. I., Leschev S. M., Pliashak Y. M., Fiodarava T. A., Belyshava L. L., Development and validation of the HPLC-DAD method for the quantification of 16 synthetic dyes in various foods and the use of liquid anion exchange extraction for qualitative expression determination, *Food Chemistry*, 369, (2022), 130947.
[26] Bogdanova P., Vakh C., Bulatov A., A surfactant-mediated microextraction of synthetic dyes from solid-phase food samples into the primary amine-based supramolecular solvent, *Food Chemistry*, 380, (2022), 131812.
[27] Kausar A., Iqbal M., Javed A., Aftab K., Nazli Z.-i.-H., Bhatti H. N., Nouren S., Dyes adsorption using clay and modified clay: A review, *Journal of Molecular Liquids*, 256, (2018), 395-407.
[28] Pavithra K. G., P S. K., V J., P S. R., Removal of colorants from wastewater: A review on sources and treatment strategies, *Journal of Industrial and Engineering Chemistry*, 75, (2019), 1-19.
[29] Lan D., Zhu H., Zhang J., Li S., Chen Q., Wang C., Wu T., Xu M., Adsorptive removal of organic dyes via porous materials for wastewater treatment in recent decades: A review on species, mechanisms and perspectives, *Chemosphere*, 293, (2022), 133464.
[30] Carolin C. F., Kumar P. S., Joshiba G. J., Sustainable approach to decolourize methyl orange dye from aqueous solution using novel bacterial strain and its metabolites characterization, *Clean Technologies and Environmental Policy*, 23, 1, (2021), 173-181.
[31] Deniz F., Tezel Ersanli E., Removal of colorant from simulated wastewater by phyco-composite material: Equilibrium, kinetic and mechanism studies in a lab-scale application, *Journal of Molecular Liquids*, 220, (2016), 120-128.
[32] Chiong T., Lau S. Y., Lek Z. H., Koh B. Y., Danquah M. K., Enzymatic treatment of methyl orange dye in synthetic wastewater by plant-based peroxidase enzymes, *Journal of Environmental Chemical Engineering*, 4, 2, (2016), 2500-2509.

[33] Colindres P., Yee-Madeira H., Reguera E., Removal of Reactive Black 5 from aqueous solution by ozone for water reuse in textile dyeing processes, *Desalination*, 258, 1, (2010), 154-158.
[34] Wijannarong S., Aroonsrimorakot S., Thavipoke P., Kumsopa c., Sangjan S., Removal of Reactive Dyes from Textile Dyeing Industrial Effluent by Ozonation Process, *APCBEE Procedia*, 5, (2013), 279-282.
[35] Chandrabose G., Dey A., Gaur S. S., Pitchaimuthu S., Jagadeesan H., Braithwaite N. S. J., Selvaraj V., Kumar V., Krishnamurthy S., Removal and degradation of mixed dye pollutants by integrated adsorption-photocatalysis technique using 2-D MoS2/TiO2 nanocomposite, *Chemosphere*, 279, (2021), 130467.
[36] Nguyen C. H., Juang R.-S., Efficient removal of cationic dyes from water by a combined adsorption-photocatalysis process using platinum-doped titanate nanomaterials, *Journal of the Taiwan Institute of Chemical Engineers*, 99, (2019), 166-179.
[37] Dursun S., Koyuncu S. N., Kaya İ. C., Kaya G. G., Kalem V., Akyildiz H., Production of CuO–WO3 hybrids and their dye removal capacity/performance from wastewater by adsorption/photocatalysis, *Journal of Water Process Engineering*, 36, (2020), 101390.
[38] El Mersly L., El Mouchtari E. M., Moujahid E. M., Forano C., El Haddad M., Briche S., Alaoui Tahiri A., Rafqah S., ZnCr-LDHs with dual adsorption and photocatalysis capability for the removal of acid orange 7 dye in aqueous solution, *Journal of Science: Advanced Materials and Devices*, 6, 1, (2021), 118-126.
[39] Elbatea A. A., Nosier S. A., Zatout A. A., Hassan I., Sedahmed G. H., Abdel-Aziz M. H., El-Naggar M. A., Removal of reactive red 195 from dyeing wastewater using electro-Fenton process in a cell with oxygen sparged fixed bed electrodes, *Journal of Water Process Engineering*, 41, (2021), 102042.
[40] Jinisha R., Gandhimathi R., Ramesh S. T., Nidheesh P. V., Velmathi S., Removal of rhodamine B dye from aqueous solution by electro-Fenton process using iron-doped mesoporous silica as a heterogeneous catalyst, *Chemosphere*, 200, (2018), 446-454.
[41] Beluci N. d. C. L., Mateus G. A. P., Miyashiro C. S., Homem N. C., Gomes R. G., Fagundes-Klen M. R., Bergamasco R., Vieira A. M. S., Hybrid treatment of coagulation/flocculation process followed by ultrafiltration in TIO2-modified membranes to improve the removal of reactive black 5 dye, *Science of The Total Environment*, 664, (2019), 222-229.
[42] Li H., Liu S., Zhao J., Feng N., Removal of reactive dyes from wastewater assisted with kaolin clay by magnesium hydroxide coagulation process, *Colloids and Surfaces A: Physicochemical and Engineering Aspects*, 494, (2016), 222-227.
[43] Vafaei M. A., Shakeri A., Salehi H., Razavi S. R., Salari N., The effect of nanosheets on polymer hydrogels performance in Rhodamine B dye removal by forward osmosis process, *Journal of Water Process Engineering*, 44, (2021), 102351.
[44] Joafshan M., Shakeri A., Razavi S. R., Salehi H., Gas responsive magnetic nanoparticle as novel draw agent for removal of Rhodamine B via forward osmosis: High water flux and easy regeneration, *Separation and Purification Technology*, 282, (2022), 119998.
[45] Lin C.-S., Tung K.-L., Lin Y.-L., Dong C.-D., Chen C.-W., Wu C.-H., Fabrication and modification of forward osmosis membranes by using graphene oxide for dye rejection and sludge concentration, *Process Safety and Environmental Protection*, 144, (2020), 225-235.
[46] Wen H., Huang W., Liu C., Double-barrier forward osmosis membrane for rejection and destruction of bacteria and removal of dyes, *Desalination*, 529, (2022), 115609.
[47] Rekhate C. V., Srivastava J. K., Recent advances in ozone-based advanced oxidation processes for treatment of wastewater- A review, *Chemical Engineering Journal Advances*, 3, (2020), 100031.

[48] Wang H., Li X., Zhao X., Li C., Song X., Zhang P., Huo P., Li X., A review on heterogeneous photocatalysis for environmental remediation: From semiconductors to modification strategies, *Chinese Journal of Catalysis*, 43, 2, (2022), 178-214.
[49] Karim A. V., Krishnan S., Shriwastav A., An overview of heterogeneous photocatalysis for the degradation of organic compounds: A special emphasis on photocorrosion and reusability, *Journal of the Indian Chemical Society*, 99, 6, (2022), 100480.
[50] Asaithambi P., Govindarajan R., Yesuf M. B., Alemayehu E., Removal of color, COD and determination of power consumption from landfill leachate wastewater using an electrochemical advanced oxidation processes, *Separation and Purification Technology*, 233, (2020), 115935.
[51] Zahrim A. Y., Tizaoui C., Hilal N., Coagulation with polymers for nanofiltration pre-treatment of highly concentrated dyes: A review, *Desalination*, 266, 1, (2011), 1-16.
[52] Abujazar M. S. S., Karaağaç S. U., Abu Amr S. S., Alazaiza M. Y. D., Bashir M. J. K., Recent advancement in the application of hybrid coagulants in coagulation-flocculation of wastewater: A review, *Journal of Cleaner Production*, 345, (2022), 131133.
[53] Wang J., Liu X., Forward osmosis technology for water treatment: Recent advances and future perspectives, *Journal of Cleaner Production*, 280, (2021), 124354.
[54] Yagub M. T., Sen T. K., Afroze S., Ang H. M., Dye and its removal from aqueous solution by adsorption: A review, *Advances in Colloid and Interface Science*, 209, (2014), 172-184.
[55] Dąbrowski A., Adsorption — from theory to practice, *Advances in Colloid and Interface Science*, 93, 1, (2001), 135-224.
[56] Djilani C., Zaghdoudi R., Djazi F., Bouchekima B., Lallam A., Modarressi A., Rogalski M., Adsorption of dyes on activated carbon prepared from apricot stones and commercial activated carbon, *Journal of the Taiwan Institute of Chemical Engineers*, 53, (2015), 112-121.
[57] Jawad A. H., Rashid R. A., Ishak M. A. M., Wilson L. D., Adsorption of methylene blue onto activated carbon developed from biomass waste by H2SO4 activation: kinetic, equilibrium and thermodynamic studies, *Desalination and Water Treatment*, 57, 52, (2016), 25194-25206.
[58] Shen K., Gondal M. A., Removal of hazardous Rhodamine dye from water by adsorption onto exhausted coffee ground, *Journal of Saudi Chemical Society*, 21, (2017), S120-S127.
[59] Peydayesh M., Rahbar-Kelishami A., Adsorption of methylene blue onto Platanus orientalis leaf powder: Kinetic, equilibrium and thermodynamic studies, *Journal of Industrial and Engineering Chemistry*, 21, (2015), 1014-1019.
[60] Du P. D., Danh H. T., Single and Binary Adsorption Systems of Rhodamine B and Methylene Blue onto Alkali-Activated Vietnamese Diatomite, *Adsorption Science & Technology*, 2021, (2021), 1014354.
[61] Ali Rıza KUL A. A., Hasan ELİK, Adsorption of Acid Blue 25 on peach seed powder: Isotherm, kinetic and thermodynamic studies, *Environmental Research and Technology*, 2, 4, (2019), 233-242.
[62] Daneshvar E., Sohrabi M. S., Kousha M., Bhatnagar A., Aliakbarian B., Converti A., Norrström A.-C., Shrimp shell as an efficient bioadsorbent for Acid Blue 25 dye removal from aqueous solution, *Journal of the Taiwan Institute of Chemical Engineers*, 45, 6, (2014), 2926-2934.
[63] Manippady S. R., Singh A., Basavaraja B. M., Samal A. K., Srivastava S., Saxena M., Iron–Carbon Hybrid Magnetic Nanosheets for Adsorption-Removal of Organic Dyes and 4-Nitrophenol from Aqueous Solution, *ACS Applied Nano Materials*, 3, 2, (2020), 1571-1582.

[64] Yang S.-T., Chen S., Chang Y., Cao A., Liu Y., Wang H., Removal of methylene blue from aqueous solution by graphene oxide, *Journal of Colloid and Interface Science*, 359, 1, (2011), 24-29.
[65] Marrakchi F., Khanday W. A., Asif M., Hameed B. H., Cross-linked chitosan/sepiolite composite for the adsorption of methylene blue and reactive orange 16, *International Journal of Biological Macromolecules*, 93, (2016), 1231-1239.
[66] Abdellaoui K., Pavlovic I., Barriga C., Nanohybrid Layered Double Hydroxides Used to Remove Several Dyes from Water, *ChemEngineering*, 3, 2, (2019), 41.
[67] Abate G. Y., Alene A. N., Habte A. T., Addis Y. A., Adsorptive Removal of Basic Green Dye from Aqueous Solution Using Humic Acid Modified Magnetite Nanoparticles: Kinetics, Equilibrium and Thermodynamic Studies, *Journal of Polymers and the Environment*, 29, 3, (2021), 967-984.
[68] Lei C., Pi M., Xu D., Jiang C., Cheng B., Fabrication of hierarchical porous ZnO-Al2O3 microspheres with enhanced adsorption performance, *Applied Surface Science*, 426, (2017), 360-368.
[69] Zhao J., Xu L., Su Y., Yu H., Liu H., Qian S., Zheng W., Zhao Y., Zr-MOFs loaded on polyurethane foam by polydopamine for enhanced dye adsorption, *Journal of Environmental Sciences*, 101, (2021), 177-188.
[70] Aliabadi R. S., Mahmoodi N. O., Synthesis and characterization of polypyrrole, polyaniline nanoparticles and their nanocomposite for removal of azo dyes; sunset yellow and Congo red, *Journal of Cleaner Production*, 179, (2018), 235-245.
[71] Cojocaru C., Samoila P., Pascariu P., Chitosan-based magnetic adsorbent for removal of water-soluble anionic dye: Artificial neural network modeling and molecular docking insights, *International Journal of Biological Macromolecules*, 123, (2019), 587-599.
[72] Bhat A. P., Gogate P. R., Degradation of nitrogen-containing hazardous compounds using advanced oxidation processes: A review on aliphatic and aromatic amines, dyes, and pesticides, *Journal of Hazardous Materials*, 403, (2021), 123657.
[73] Zhang X., Hao C., Ma C., Shen Z., Guo J., Sun R., Studied on sonocatalytic degradation of Rhodamine B in aqueous solution, *Ultrasonics Sonochemistry*, 58, (2019), 104691.
[74] Dastkhoon M., Ghaedi M., Asfaram A., Goudarzi A., Langroodi S. M., Tyagi I., Agarwal S., Gupta V. K., Ultrasound assisted adsorption of malachite green dye onto ZnS:Cu-NP-AC: Equilibrium isotherms and kinetic studies – Response surface optimization, *Separation and Purification Technology*, 156, (2015), 780-788.
[75] Asfaram A., Ghaedi M., Hajati S., Goudarzi A., Bazrafshan A. A., Simultaneous ultrasound-assisted ternary adsorption of dyes onto copper-doped zinc sulfide nanoparticles loaded on activated carbon: Optimization by response surface methodology, *Spectrochimica Acta Part A: Molecular and Biomolecular Spectroscopy*, 145, (2015), 203-212.
[76] Banerjee P., Barman S. R., Mukhopadhayay A., Das P., Ultrasound assisted mixed azo dye adsorption by chitosan–graphene oxide nanocomposite, *Chemical Engineering Research and Design*, 117, (2017), 43-56.
[77] Asfaram A., Ghaedi M., Yousefi F., Dastkhoon M., Experimental design and modeling of ultrasound assisted simultaneous adsorption of cationic dyes onto ZnS: Mn-NPs-AC from binary mixture, *Ultrasonics Sonochemistry*, 33, (2016), 77-89.
[78] Asfaram A., Ghaedi M., Ahmadi Azqhandi M. H., Goudarzi A., Hajati S., Ultrasound-assisted binary adsorption of dyes onto Mn@ CuS/ZnS-NC-AC as a novel adsorbent: Application of chemometrics for optimization and modeling, *Journal of Industrial and Engineering Chemistry*, 54, (2017), 377-388.
[79] Dashamiri S., Ghaedi M., Asfaram A., Zare F., Wang S., Multi-response optimization of ultrasound assisted competitive adsorption of dyes onto Cu (OH)2-nanoparticle loaded

activated carbon: Central composite design, *Ultrasonics Sonochemistry*, 34, (2017), 343-353.

[80] Ghaedi A. M., Karamipour S., Vafaei A., Baneshi M. M., Kiarostami V., Optimization and modeling of simultaneous ultrasound-assisted adsorption of ternary dyes using copper oxide nanoparticles immobilized on activated carbon using response surface methodology and artificial neural network, *Ultrasonics Sonochemistry*, 51, (2019), 264-280.

[81] Amin M., Chetpattananondh P., Khan M. N., Ultrasound assisted adsorption of reactive dye-145 by biochars from marine Chlorella sp. extracted solid waste pyrolyzed at various temperatures, *Journal of Environmental Chemical Engineering*, 8, 6, (2020), 104403.

[82] Sharma J., Sharma S., Soni V., Classification and impact of synthetic textile dyes on Aquatic Flora: A review, *Regional Studies in Marine Science*, 45, (2021), 101802.

[83] Jun B.-M., Kim S., Rho H., Park C. M., Yoon Y., Ultrasound-assisted Ti3C2Tx MXene adsorption of dyes: Removal performance and mechanism analyses via dynamic light scattering, *Chemosphere*, 254, (2020), 126827.

[84] Low S. K., Tan M. C., Dye adsorption characteristic of ultrasound pre-treated pomelo peel, *Journal of Environmental Chemical Engineering*, 6, 2, (2018), 3502-3509.

[85] Modwi A., Khezami L., Ghoniem M. G., Nguyen-Tri P., Baaloudj O., Guesmi A., AlGethami F. K., Amer M. S., Assadi A. A., Superior removal of dyes by mesoporous MgO/g-C3N4 fabricated through ultrasound method: Adsorption mechanism and process modeling, *Environmental Research*, 205, (2022), 112543.

[86] Ya-Li Song J.-T. L., Hua Chen, Removal of acid brown 348 dye from aqueous solution by ultrasound irradiated exfoliated graphite, *Indian Journal of Chemical Technology*, 15, 443-448, (2008).

[87] Hachem K., Bokov D., Farahani M. D., Mehdizade B., Kazemzadeh Farizhandi A. A., Ultrasound-assisted adsorption of dyes and cadmium ion from aqueous solutions by ZnAl2O4 nanoparticles, *Materials Chemistry and Physics*, 276, (2022), 125398.

[88] Mazaheri H., Ghaedi M., Asfaram A., Hajati S., Performance of CuS nanoparticle loaded on activated carbon in the adsorption of methylene blue and bromophenol blue dyes in binary aqueous solutions: Using ultrasound power and optimization by central composite design, *Journal of Molecular Liquids*, 219, (2016), 667-676.

[89] Sharifpour E., Haddadi H., Ghaedi M., Optimization of simultaneous ultrasound assisted toxic dyes adsorption conditions from single and multi-components using central composite design: Application of derivative spectrophotometry and evaluation of the kinetics and isotherms, *Ultrasonics Sonochemistry*, 36, (2017), 236-245.

[90] Khafri H. Z., Ghaedi M., Asfaram A., Safarpoor M., Synthesis and characterization of ZnS:Ni-NPs loaded on AC derived from apple tree wood and their applicability for the ultrasound assisted comparative adsorption of cationic dyes based on the experimental design, *Ultrasonics Sonochemistry*, 38, (2017), 371-380.

[91] Agarwal S., Tyagi I., Gupta V. K., Dastkhoon M., Ghaedi M., Yousefi F., Asfaram A., Ultrasound-assisted adsorption of Sunset Yellow CFC dye onto Cu doped ZnS nanoparticles loaded on activated carbon using response surface methodology based on central composite design, *Journal of Molecular Liquids*, 219, (2016), 332-340.

[92] Low S. K., Tan M. C., Chin N. L., Effect of ultrasound pre-treatment on adsorbent in dye adsorption compared with ultrasound simultaneous adsorption, *Ultrasonics Sonochemistry*, 48, (2018), 64-70.

[93] Jamshidi M., Ghaedi M., Dashtian K., Hajati S., Bazrafshan A. A., Sonochemical assisted hydrothermal synthesis of ZnO: Cr nanoparticles loaded activated carbon for simultaneous ultrasound-assisted adsorption of ternary toxic organic dye: Derivative spectrophotometric, optimization, kinetic and isotherm study, *Ultrasonics Sonochemistry*, 32, (2016), 119-131.

EXTRACTION OF POLYSACCHARIDES FROM *CERAMIUM RUBRUM*

Doinita-Roxana CIOROIU TIRPAN[1*], Cristian RADUCANU[2], Timur CHIS[1], Tănase DOBRE[2]

[1] Ovidius University of Constanta, Chemical and Chemical Engineering Department, 124 Mamaia Blvd., Constanta, 900527, Romania
[2] University "Politehnica" of Bucharest, Chemical and Biochemical Engineering Department, 1-7 Gheorghe Polizu Str., Bucharest, 011061, Romania

Abstract

The aim of this study is to present Ceramium rubrum species from Romanian Black Sea Coast as a sustainable source of polysaccharides. A brief physicochemical characterization of this red macroalgae was performed: dry matter content and chemical structure by functional group identification with a FT-IR spectrometer. The extraction of polysaccharides from Ceramium rubrum species was performed by precipitation with ethanol. A yield of 4.27% polysaccharides on dry matter content was obtained. HPAEC analysis revealed the presence of galactan-type polysaccharides in proportion of 78%.

Key words: *Ceramium rubrum*, polysaccharides, ethanol.

1. Introduction

Modern biotechnologies specific to algae can have important implications in the chemical, food, cosmetic, pharmaceutical and agronomy industries, because they can capitalize biomass to obtain proteins, polysaccharides, polyphenols, etc. [1]. Polysaccharides, widely found in seaweeds, have attracted the scientists' attention due to their bioactive properties [2]. The polysaccharides from red algae represents polymers composed of various monosaccharide molecules [3]. The polysaccharides contained in the highest proportion in red algae are the galactan type. Galactans are used in the food industry as a food additive to thicken or stabilize foods. Galactans can be agar or carrageenan.

Agar is a phycoloid type compound found primarily in the cell walls of red algae. The *Gracilaria* and *Gelidium* species are cultivated industrially to extract agar. Agar is a collective name for complex mixtures of polysaccharides consisting of hybrid structures of two alternative structures: α-L-galactopyranose and β-D-galactopyranose [4, 5]. Agar contains 70–80% polysaccharides, 10–20% water, 1.5–4% mineral substances and has a very high gelling power. Named

*Corresponding author: email address: tirpanroxana@gmail.com

stabilizer E406, it is used as a food additive in the ice cream, jams, and candies preparation. It is also used for technical purposes (production of linoleum, silk, artificial leather, soap, watercolors and very fine photographic films) but also in culture media preparation from bacteriology and pharmaceutical industries [6].

Carrageenan is a natural compound extracted from red macroalgae and is formed by linear polysaccharide chains having sulfated galactans attached to the sugar unit. Carrageenan has gelling properties, structural characteristics of forming viscous solutions and is used in the food industry [4]. In this study, we describe *Ceramium rubrum* macroalgae as a sustainable source in the extraction process of polysaccharides.

Ceramium rubrum species (Phylum *Rhodophyta*, Genus *Ceramium*, Class *Florideophyceae*, Order *Ceramiales*, Family *Ceramiaceae*) is a red alga due to the pigments phycoerythrin and phycocyanin, small, up to 20 cm in height, that dominates the marine vegetation on the Romanian Black Sea coast. The thallus is filamentous, irregular and pseudo-dichotomously branched, most often the branches end with colorless cilia. The species is illustrated in figure 1.

Fig. 1. Young colony of *Ceramium rubrum* floating in sea water

Ceramium rubrum species is an opportunistic macrophyte which is often an epiphyte in its growth on the *Cladophora vagabunda* and *Ulva lactuca* species. The favorable conditions for the development of red algae are determined by the quality and transparency of the water, the lighting regime of the environment, the nutrients of the substrate and the high temperature. The three species are found in

separate colonies but also together. Figure 2 shows the rocks populated by *Ceramium rubrum*, *Ulva lactuca* and *Cladophora vagabunda* algae.

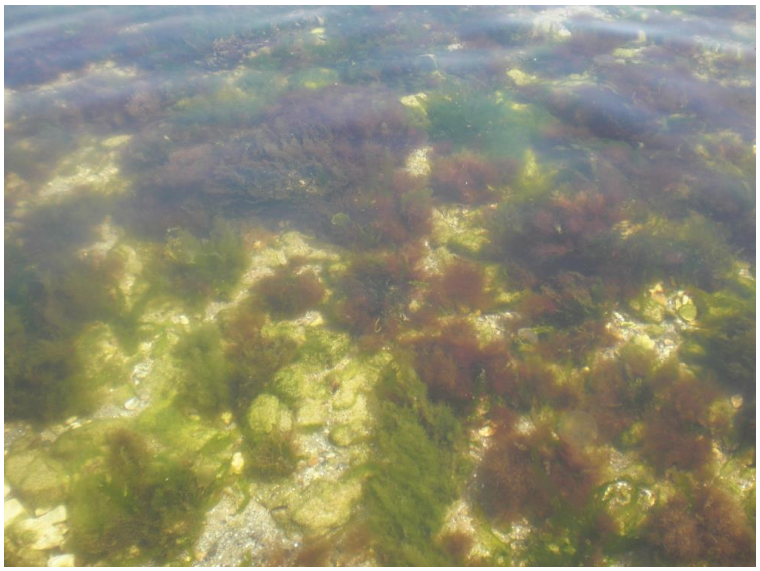

Fig.2. Rocks populated by *Ceramium rubrum*, *Ulva lactuca* and *Cladophora vagabunda* algae

Table 1 presents the composition of this alga according to the three major classes of compounds of interest. The nitrogen content given in this table is an indirect expression of the protein content of this algae species.

This species has a high content of polysaccharides (about 52% by weight), a promising feedstock for the chemical, food, cosmetic and pharmaceutical industries.

Table 1

Chemical composition of *Ceramium rubrum* species [7]

Component	**Content, mass %**
Carbohydrates in D.M.	51.90
Proteins in D.M.	19.94
Lipids in D.M.	3.43
Total volatile solids	75.27
Nitrogen	3.19

D.M. – dry matter

2. Experimental

Materials

Ceramium rubrum species was harvested from the "Modern" beach in Constanta, Romania (Latitude: 44°11'10.5"N; Longitude: 28°39'17.2"E), in the summer of 2021. Denatured ethyl alcohol with 96% purity was purchased from "S.C. Chemical Company S.A.", Romania. Also, for this experiment acetone provided by S.C. Tunic Prod S.R.L., Romania was used.

Equipment and methods

The D.M. content was determined with the OHAUS thermobalance, model MB45, also called humidity analyzer (Figure 3). This was programmed at 180°C for 14 minutes, for wood plants, as recommended by the supplier. The mass loss of the sample allows the determination of moisture content.

Fig.3. OHAUS thermobalance (moisture analyzer)

For the quantitative and qualitative analysis of the functional groups in the structure of algae powder was used Nicolet 6700 FT-IR Spectrometer from Thermo Scientific (Figure 4). The working method used is based on the total reflection attenuation technique (ATR- Attenuator Total Reflectance) in tablet samples [8]. Infrared radiations with long wavelengths and low energies can

produce vibrational and rotational transitions of the molecules of bioactive compounds. Spectral analyzes in FT-IR result by determining the radiation absorbed by an analyte molecule, radiation that disappears from the complex fasciculus of incident radiation [9].

Fig.4. Nicolet 6700 FT-IR Spectrometer -Thermo Scientific

After ethanol precipitation, water-soluble polysaccharides (WSP) were determined using HPAEC (High-performance anion-exchange chromatography) analysis. HPAEC at high pH is one of the most useful techniques for the determination of carbohydrates.

3. Results and discussions

Pretreatment process

Ceramium rubrum algae was freshly harvested from the beach, washed with sea water and transported to the laboratory in plastic containers. The algae was washed with fresh water, distilled water and cleaned of impurities. Then, the seaweed was dried in a dehydrator at 45 °C for 48 hours. The drying process is the first step in the treatment of fresh seaweed harvested from the sea in order to preserve the crude extract and prevent the gelling of the seaweed. Algae was crushed using a mechanical device and sieved through a certified granulometric sieve having a size smaller than 3.15 mm. The moisture content of *Ceramium rubrum* determined with OHAUS thermobalance was measured under the conditions specified above and presented in table 2. The medium moisture content in red algae was 24,17%, respectively 75,82% dry matter (D.M).

Table 2

Moisture content for *Ceramium rubrum* species, dried at 45° C for 48 h

Determination no.	Moisture content, %	Dry Matter (D.M.), %
1	24.63	75.37
2	23.79	76.21
3	24.11	75.89
u_m	**24.17**	**75.82**

FT-IR spectrum of Ceramium rubrum species

With the FT-IR spectrometer, algal powder of *Ceramium rubrum* species was analyzed. The sample was introduced into the apparatus on a germanium selenide crystal (GeSe), to achieve the spectrum in the range of wavelength from 4000 to 600 cm^{-1} and the final spectrum was the average of 135 scans at a resolution of 4 cm^{-1} [10]. In the interpretation of the results, the group frequencies, characteristic of the main organic substances, were considered [8]. The FT-IR spectrum of algal powder from *Ceramium rubrum* species, shown in figure 5, highlights the presence of several characteristic bands, intense, medium or small, specific to different functional groups [8].

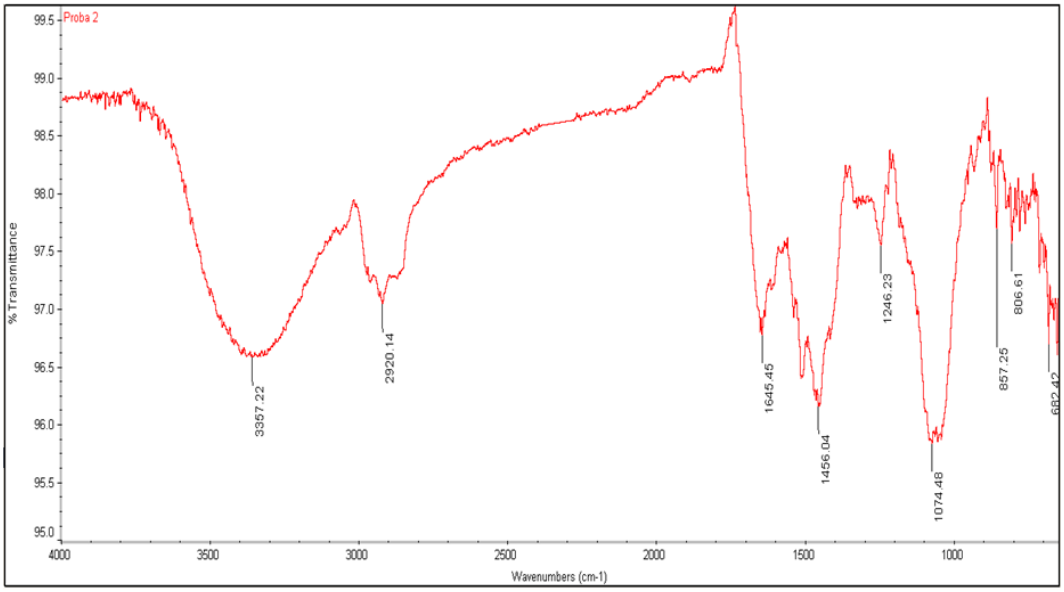

Fig. 5. The FT-IR spectrum of *Ceramium rubrum* algae

The identification of the chemical groups was achieved by comparing the bands with those from the specialized literature. The spectral analysis shows the characteristic bands of the oscillation vibrations of the OH group (3357,22 cm^{-1}), lipids (2920,14 cm^{-1}), amides from the protein structure (1645,45 cm^{-1}), polysaccharides (1074,48 cm^{-1}) and phosphates (1246,23 cm^{-1}).

Procedure for extracting polysaccharides from Ceramium rubrum species

The extraction of polysaccharides from *Ceramium rubrum* species was carried out using 15 g of dried algae with 360 mL of water (solid/liquid ratio: 1/24) at 80 °C for 2 hours. The polysaccharides extraction scheme is presented in the figure 6. After vacuum filtration we obtained 137 g of wet fibers and 120 mL of filtrate. The moistened fibers were dried in an oven at 105 °C for 24 hours. After drying, approximately 9.26 g of dry fibers were obtained. Further, the filtrate was centrifuged at 2000 rpm, at 60 °C for 15 minutes. After centrifugation, we obtained fibers in the top of the tubes and also, 110 mL of supernatant.

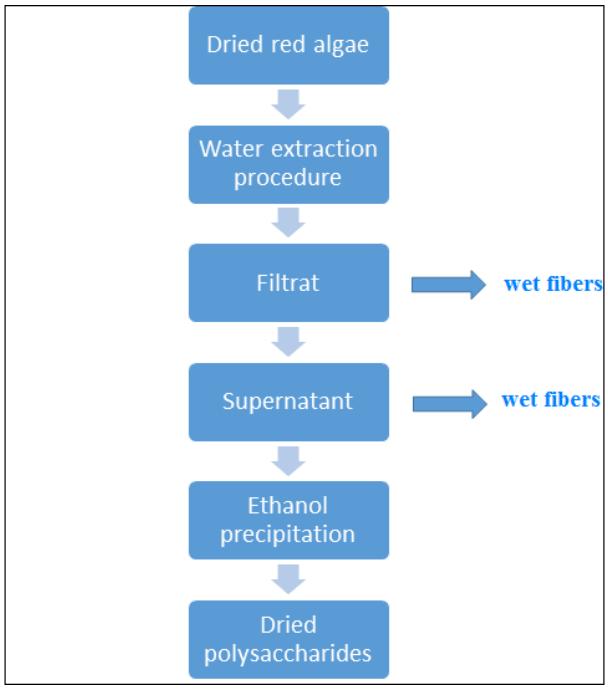

Fig.6. Polysaccharides extraction process from *Ceramium rubrum* species

Polysaccharides were extracted by precipitation with ethanol 96% (Figure 7). 100 mL of ethanol were added to the supernatant, 3 times each. After vacuum

filtration, the polysaccharides were dehydrated with 10 mL of acetone, in 2 rows. The polysaccharides were dried at 50 °C and crushed. 0.64 g of polysaccharides were obtained, corresponding to an extraction yield of 4.27%.

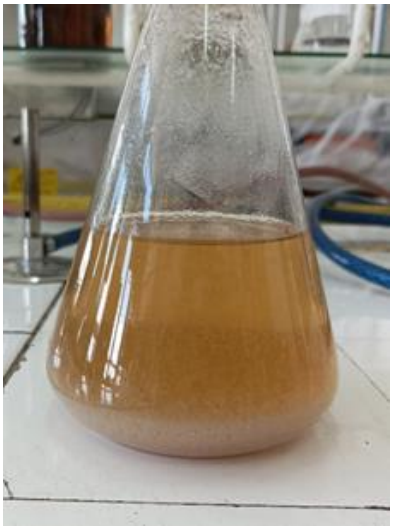

Fig. 7. Polysaccharides purification by ethanol precipitation

After ethanol precipitation, water-soluble polysaccharides were determined using HPAEC analysis. The analysis revealed the presence of galactan type polysaccharides in a proportion of 78%.

4. Conclusions

In this study, a physicochemical characterization of the *Ceramium rubrum* species from Romanian Black Sea Coast was carried out: determination of moisture content of dried algae at 45 °C and determination of chemical composition by FT-IR spectrum. Then, an extraction of polysaccharides was performed by ethanol precipitation. The separation scheme includes wet pellets removal operations, but it does not affect polysaccharides that are obtained in the form of an off-white powder. A yield of 4.27% polysaccharides on D.M. was obtained, demonstrating that *Ceramium rubrum* species is a viable alternative resource in polysaccharide production. HPAEC analysis revealed the presence of galactan-type polysaccharides in proportion of 78%. Galactans (agar and carrageenan) are used in the food industry as a food additive to thicken or stabilize food, but also for technical purposes.

REFERENCES

[1] Corradini C., Cavazza A., Bignardi C., High-Performance Anion-Exchange Chromatography Coupled with Pulsed Electrochemical Detection as a Powerful Tool to Evaluate Carbohydrates of Food Interest: Principles and Applications, *International Journal of Carbohydrate Chemistry*, Vol. 2012, https://doi.org/10.1155/2012/487564
[2] Cioroiu D-R., 2017, Integrated chemical and biochemical processes with the processing of plant products and residues: macrophyte algae, PhD Thesis, University Politehnica of Bucharest.
[3] Zhang T., Guo Q., Xin Y., Liuc Y., Comprehensive review in moisture retention mechanism of polysaccharides from algae, plants, bacteria and fungus, *Arabian Journal of Chemistry*, 32, 10, (2022), 104163.
[4] Trică B.,2019, Valorization of brown seaweed from the Black Sea (*Cystoseira barbata*), PhD Thesis, University Politehnica of Bucharest.
[5] Turvey J., Williams E.L., The agar-type polysaccharide from the red alga *Ceramium rubrum*, *Carbohydrate Research*, 49, (1976), 419-425.
[6]. https://ro.wikipedia.org/wiki/Agar-agar
[7] INCD ―Grigore Antipa, *Research report No.3, Structural characterization of macrophytes on the Romanian sea shore*, Project MACROEVAL, 2010, http://www.rmri.ro/WebPages/MACROEVAL/32-144%20Etapa3.pdf
[8] Horincar V.B., 2012, Extracția și caracterizarea compușilor bioactivi din alge marine, Teza de doctorat, Universitatea „Dunărea de Jos Galaţi, Facultatea Ştiinţa şi Ingineria Alimentelor, Galaţi.
[9] Mare D.A., 2012, Investigaţii structurale ale unor complecşi moleculari de interes biologic, Teza de doctorat, Universitatea Babes-Bolyai, Facultatea de Fizică,Cluj.
[10] Cioroiu Tirpan D.-R., Koncsag C. I., Dobre T., Cellulose fibers extraction from Ulva lactuca from the Black Sea, *Ovidius University Annals of Chemistry*, 31, 2, (2020),158-162.

POULTRY LITTER PYROLYSIS TO ADDRESS AGRICULTURAL AND ENERGY CHALLENGES IN BOTSWANA

Daniel E. BOTHA[1,2,*], Paul S. AGACHI[2,3]

[1]Pyro Carbon Energy PTY LTD, [2]Botswana International University of Science and Technology, [3]University Babeș-Bolyai, Romania

Abstract

Botswana is dry and landlocked, with 16% in extreme poverty and 52.9% unemployed youth. As a net importer of fuel and food, a focus on agriculture, occupying 45.9% of land resources, is crucial to address several sustainable development goals (SDG) that are tied to the agricultural sector. Crop farming production is low due to limited rural energy, poor soil quality, and climate-related challenges while poultry farming has waste management challenges. Poultry Litter (PL) pyrolysis offers solutions and its feasibility to solve Botswana's challenges was investigated. PL pyrolysis kinetics were studied and the PL pyrolysis concept, which was based on an induction heated auger type reactor, was developed into a feasible engineering solution, and through mathematical and financial modelling, design, and construction a 1 ton/day plant was realized to validate laboratory scale experimental results. A full techno-economic feasibility study, which included validation testing of the plant at commercial scale, was performed to evaluate the solution. The reactor's induction heating system, however, did not perform to full capacity (only 6.7kW of 60kW realized, i.e., 11.2% of rated capacity), and limited the product throughput to 25% of design capacity with. By extrapolation, however, it is reasonable to expect full throughput of the plant with an optimized induction system. However, even at these turndown conditions the plant could produce good quality bio-oil, biochar, and gas at typical product yields of >50%, ~20% and <30% respectively. The biofuel is suitable for heavy fuel oil (HFO) power at farms and rural areas, or as a fuel oil in boilers and burners. As soil enhancer, biochar improves soil nutrients, water retention, cation exchange and benevolent microbial activity. Pyroligneous acid will offset the import of its chemical equivalents as organic fertilizer, organic pesticide, and organic herbicide. Simultaneously, it meets End-of-Waste objectives while addresses health and environmental risks, and Botswana's drive towards renewable energy. Actual capital expenses of building a commercial scale plant and operating expenses, provided accurate financial model input data, resulting in 39% internal rate of return (IRR). The absence of disqualifying aspects regarding statutory feasibility, together with the benefits of biochar as soil enhancer further contributed towards favorable feasibility. The conversion of PL, a biohazardous agricultural waste product, into high value products using pyrolysis is therefore proven feasible, thereby

* Corresponding author: daniel.botha@pyrocarbonenergy.com

addressing soil quality and climatic challenges in the agricultural sector as well as contributing to the national energy goal, and especially in rural communities.

Key words: pyrolysis, waste to energy, biochar, biofuel, circular economy, drought abatement, end-of-waste, food security.

1. Introduction

Botswana, a landlocked arid to semi-arid country, is a developing and upper-middle-income country[1], of which 30% live in rural areas [2]. Sixteen percent of its people are living in extreme poverty and 52.9% of the urban youth are unemployed. A focus on the country's energy situation, as well as the agricultural sector, which occupies 45.9% of Botswana's land resources, using pyrolysis of poultry litter (PL), a biohazardous agricultural waste product, is crucial to the address several sustainable development goals (SDGs), including: No Poverty (SDG 1), Zero Hunger (SDG 2), Affordable and Clean Energy (SDG 7), Responsible Consumption (SDG 12), and Life on Land (SDG 15) [2].

The global gross domestic product (GDP) recently exceeded the highest level ever to above $100 trillion, a figure that was only expected in 2024[3]. With almost 70% of the projected increase in global energy demand being in emerging markets and developing economies, these drove energy demands back above 2019 levels after the covid pandemic [4]. The recovery was reported to be stronger in 2021 than expected, and a world growth of 4.2% is expected in 2022 [3]. The acceleration in world GDP growth in 2021 has strengthened the fossil fuel prices and although ever increasing use of renewables may reduce demand, investment in new sources is expected to be reduced by higher demand, and the prices were predicted to remain at around $70 per barrel [3]. However, the Russia-Ukraine war has rendered all predictions void and oil is now at over $100 per barrel [5]. Similar trends are expected with coal and natural gas [4]. Global, electricity demand grew by 6% in 2021, pushing up power prices and emissions to record levels and putting power systems under strain [6]. A rapidly growth in renewables is expected during 2022-2024, contributing more than 90% of net demand growth. Nuclear-based generation is expected to grow 1% per year, meeting 4% of global total demand growth [7]. The primary energy economy in Southern Africa is dominated by local coal supply, which comprises 60% of energy consumption, while imported crude oil constitutes 13% of energy consumption. The balance of energy supply is made up from nuclear, hydro, renewable and other sources. Renewable energy from non-biological and biological waste such as poultry litter has the potential to contribute to the primary energy supply in Southern Africa, especially the rural areas.

Fuel is imported through South Africa at an average rate of approximately 21,000 barrels per day (BPD) [8] and constitutes 14.5% of all imports into

Botswana [9] with an increasing trend, any form of local fuel production is arguably one of the highest priorities of the country. Only 66% of the population have access to electricity [10] of which 81% reside in urban areas. The country's energy consists of oil products (35%), coal (44%), (traditional) biofuels and waste (19%) and imported electricity (2%), totaling 2.9 Mtoe (mega tons of oil equivalent) in 2017. Electricity is produced mainly from coal and (to a lesser degree) from petroleum products [2]. In 2021, the Botswana Parliament adopted the Botswana National Energy Policy, a strategic instrument for the successful and economic development of its local energy sector with a key objective being to achieve substantive penetration of new and renewable energy sources in Botswana's energy mix. The goal is to achieve sufficient economic energy self-sufficiency and security, as well as working towards becoming a regional net exporter, especially in the electricity sector. Increased energy efficiency and the use of renewable energy have been recognized as key drivers for the transition to a clean energy future [2]. An increase of electricity consumption in Botswana over the long and short term is driven by the positive economic growth, financial development, increasing industrialization and urbanization [11]. With the GDP almost tripling since 2000 while the total final energy consumption (TFEC) only increased by 45% (and while the country is still recovering from its economic downturn in 2015 due to decline in diamond exports, severe drought, and energy shortages), the Government of Botswana has adopted an Economic Stimulus Program to boost growth and promote both economic diversification and job creation [2]. As with most countries in the Southern African Development Community (SADC), Botswana's electricity supply is unreliable due to lack of investment, poor maintenance, and high service costs. Although the situation has improved hugely where more than 80% of the national electricity demand was imported from South Africa [12], Botswana still, after much improvement with the ongoing recovery of the Morupule B plant, imports approximately 15% of its power needs from the Southern Africa Power Pool (SAPP) and when these are not available, Botswana Power Corporation (BPC) must resort to costly diesel power plants. Only 69% of the electricity demand is met by local generation [10]. Nevertheless, Botswana's total primary energy supply (TPES) is fossil-based (oil products and coal), and to a lesser degree by biomass and waste energy. However, a significant proportion of TFEC (27.8%), remains biomass energy based (i.e., biofuel) in the form of traditional residential wood fuel. With very high renewable energy potential (yet unexploited), in the form of solar, wind and bioenergy the country has plans to integrate renewable energy into its energy system. The goals of the Integrated Resource Plan (IRP), launched in December 2020, is for renewable energy to account for at least 15% of the energy mix by 2030. Morupule B power station is expected to reach full capacity in 2023, and with no more additional capacity from coal power stations available, other sources

of energy will be required as the baseline energy demand continually rises. In any case, the emergency (diesel) power generation is extremely expensive and should be avoided, which makes an even larger case for other sources, of which non-variable renewable energy is a real opportunity. The electrification rate in Botswana was 62.8% in 2017 (World Bank Data Portal, 2017) compared to 49% in 2008 and 26% in 2004 and [12]. Rural areas, however, only account for 24.2%, which is an area needing serious action. Under the "SEforAll Initiative" the Government of Botswana has set a national electricity access target of 100% by 2030.

The poultry industry of Botswana is currently the dominant meat producing industry in the country, making Botswana self-sufficient in poultry meat (and also eggs) [13], estimated at P1 billion in 2010 (excluding ostriches) [14]. Poultry farming in Botswana can be categorized into traditional farming (family poultry) and commercial enterprise, which can be further categorized into large-scale (>50,000 birds), medium-scale, and small-scale (≤20,000 birds) [15]. The poultry industry in Botswana is under strain due to the rising cost of poultry feed and shortages caused by import restrictions [16]. Broiler farming in the commercial sector produces significant amounts of poultry litter (PL), an agricultural waste product for which no feasible safe disposal solution currently exists. PL is therefore commonly disposed of by means of land application with detrimental effects on the environment, including oversupply of nitrogen, resulting in nitrate (NO_3-N) contamination of groundwater. A study [17] revealed that 80% of poultry farmers avail manure and litter free of charge to other farmers while 16% applied it as fertilizer on their own fields, and the remaining 4% is disposed of at landfills. With PL being a perfect environment to produce pathogens it is a carrier for infection and diseases [18]. Costly transportation is a challenge for evacuation of PL to remote sites, causing delayed collection, and therefore increasing the biosecurity risks of broiler farms [17].

Crop production in Botswana has historically been much lower than its neighboring countries due to mainly the fact it is its huge dependent on its relatively low and unreliable rainfall. Together with the relatively poor soil quality, it has made crop farming in Botswana a high risk [19]–[22].

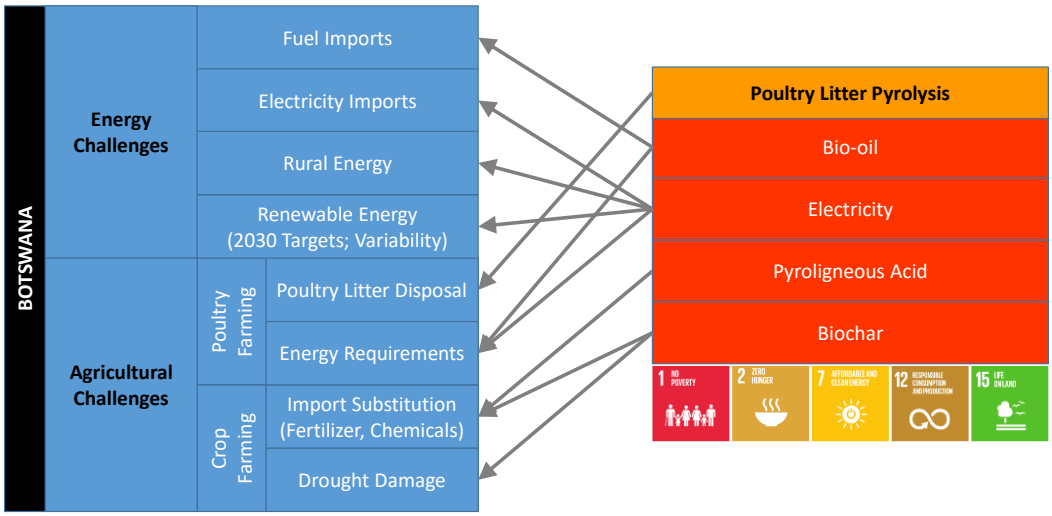

Fig. 1. Addressing energy and agricultural challenges of Botswana through poultry litter pyrolysis

The conversion of PL into high value products (biochar, pyroligneous acid, biofuel, and electricity) in a feasible manner using the pyrolysis process was investigated to address the health and environmental risks associated with disposal thereof, while simultaneously mitigating the following energy and agricultural challenges, thereby contributing to the country's actions towards the SDGs (refer to Fig. 1): (a) biochar applied as soil enhancer to improve soil nutrients, water retention, cation exchange and benevolent microbial activity, (b) pyroligneous acid used as organic fertilizer, pesticide, and herbicide, to offset the import of its chemical equivalents, (c) electricity generation from the produced gas, and (d) biofuel, which can be blended into diesel or used in heavy fuel oil (HFO) generators, boilers and burners to produce electricity, steam/hot water and heat respectively for farms and rural areas.

2. Modelling, Analysis & Validation:

A feasibility study was performed in five areas of interest (i.e.: (a) technical feasibility, (b) market feasibility, (c) organizational feasibility, (d) statutory feasibility and (e) financial), to demonstrate the feasibility of Pyro Carbon Energy's containerized pyrolysis unit (CPU), using PL as raw material. This was done through:
(a) process and financial modelling,
(b) design and construction of a commercial-scale proof-of-concept plant,
(c) experimental validation at commercial scale, as well as
(d) market, organizational and statutory studies.

The CPU is a continuous process plant (Fig. 2.) that accepts loads of PL into a feed hopper. The PL is firstly dried to remove excess moisture, whereafter it is fed into the reactor. In the reactor, the PL is subjected to elevated temperatures where volatile (VM) matter is released and separated from the residual material (biochar). The biochar is then cooled in the char cooler before it is discharged and packaged. The volatile matter (VM) is partially condensed whereafter it is scrubbed to remove any solid particulate and mist from the residual non-condensable gas stream. The non-condensable (permanent) gases, which are rich in methane and other light hydrocarbons (HC), are consumed in real time since they do not liquefy easily like liquefied petroleum gas (LPG) and therefore cannot be stored without capital-intensive equipment. The excess heat produced in the plant is used to heat up water which is used at night to regulate bird house temperatures as well as other hot water requirements on poultry farms. The non-condensable gas (and potentially a portion of the bio-oil) is utilized in an internal combustion engine to produce electricity.

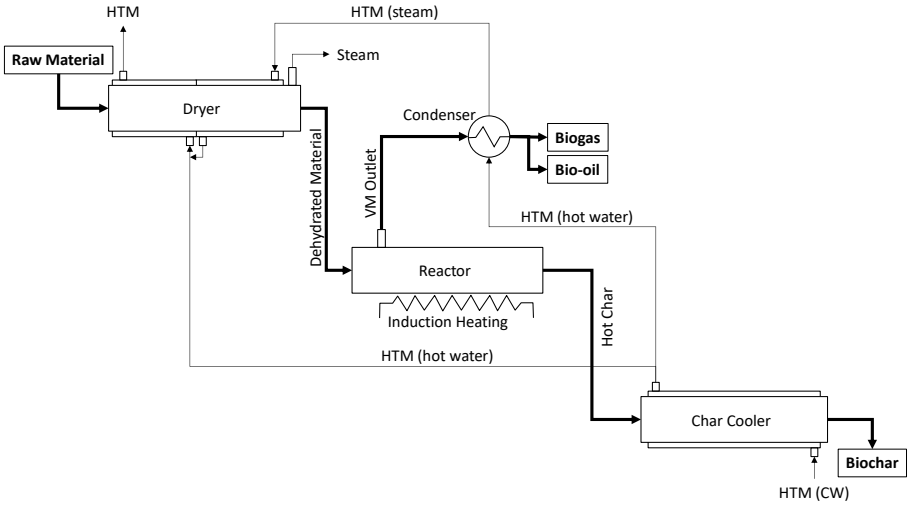

Fig. 2. Process Overview

Process Modelling:

The reactor process model is illustrated in Fig.3, showing the input stream, output streams, and the parameters that were considered. This endothermic reaction can be considered to produce two pseudo components, i.e., volatile matter (VM) and char:

$$PL \rightarrow VM + char \quad (1)$$

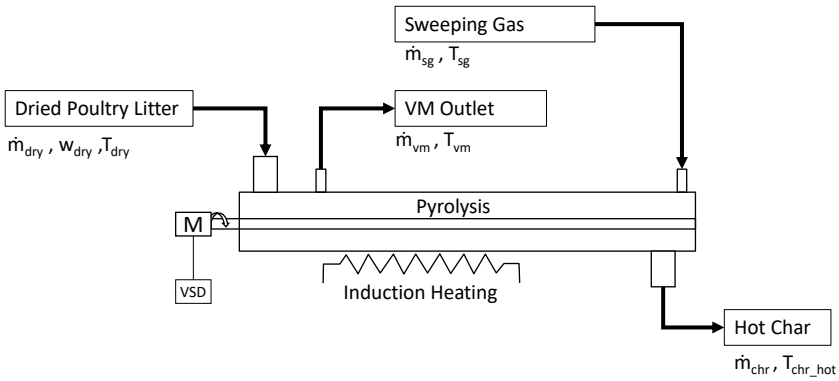

Fig. 3. The parameters used in the mathematical model of the reactor

The auger pyrolysis reactor operation very closely resembles the classical plug flow reactor (PFR) reaction, transport, and heating model as shown in Fig. 4(a). The PFR can be solved by approximating each infinitely small volume, dV, as a continuous stirred-tank reactor (CSTR) [23] as shown in Fig.4(b) and integrating the system of equations over the total length of the reactor. By representing each infinitesimal element (with thickness dz) as a small batch reactor which progresses along the PFR from position z=0 to z=L, then, with certain assumptions, experimental data can be utilized to model the integrated steady state production of the PFR.

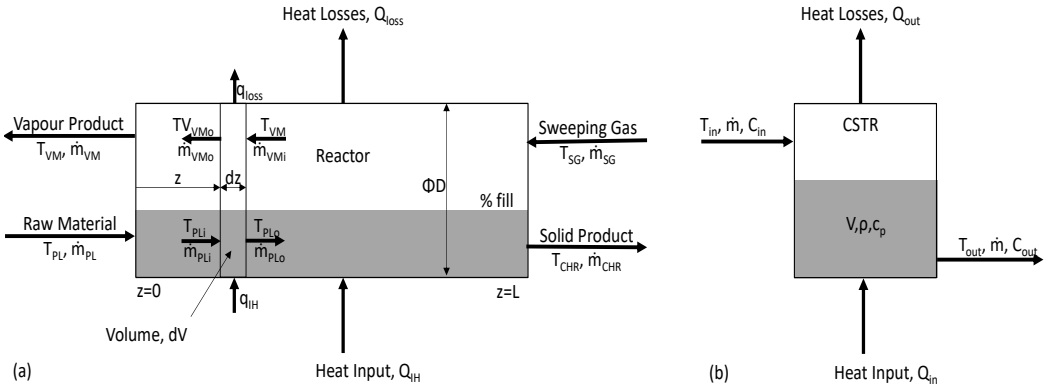

Fig. 4. (a) Pyrolysis reactor modelled as a PFR. (b) Infinitesimal volume, dV, approximated as a CSTR

The kinetics and thermodynamics of the process are described in [24], [25] and equations **Error! Reference source not found.** and (1) are the similar equations for the pyrolysis reactor which are adapted from equations 3.9 and 3.13 in [26].

$$\frac{\partial}{\partial z}\left(v\rho c_p T\right) + \frac{4K_T}{D}\left(T_{stm} - T\right) = \frac{\partial}{\partial z}\left(k_T \frac{\partial T}{\partial z}\right), \tag{2}$$

Where v is the velocity of the material in the dryer,

ρ is the average density of the material,

c_p is the average specific heat of the material,

T is the temperature of the material in the dz element,

K_T is the heat transfer coefficient from the induction heating coil to the material through the dryer's wall,

D is the auger diameter of the dryer, and

k_T heat diffusion coefficient in the solid material.

$$D_w \frac{\partial^2 w}{\partial z^2} - \frac{\partial}{\partial z}(v\, w) = 0\,, \tag{1}$$

Where v is the velocity of the material in the dryer,

w is the moisture content of the solid material, and

D_w is the mass diffusion coefficient of water in the material.

The material entering the CSTR consists of a mixture of solid material and volatile matter (VM). The mass percentage (yield) of VM can be substituted into the concentration term, C, of product formed in classical CSTR theory, starting with zero at z=0 and increasing to its final value at z=L, with the following assumptions:

Steady state conditions are considered (time derivative is equal to 0).

The volume and density in the CSTR remain constant (i.e., the fill % does not vary at any given position, z, in the reactor).

The sweeping gas is inert and only acts as a carried gas for the VM.

The sweeping gas flow rate and composition does not significantly alter the results. In practice, as volatiles are produced, they join the sweeping gas stream and therefore the sweeping gas flow rate and composition vary along the length of the PFR. The batch reactor does not take these effects into account.

The mass flow rate is considered constant.

The mass balance therefore can be written as:

$$input + generation = \text{accumulation} + \text{output} \quad (2)$$

$$\dot{m} \cdot C_{in} + r \cdot dV = \frac{d\,C_{out} \cdot \rho \cdot V}{dt} + \dot{m} \cdot C_{out} \quad (3)$$

Where: $\dot{m}$ is the mass flow rate in [kg/s] of the material through the CSTR,
dV is the volume of the CSTR in [m^3] and ρ the density of the material in [kg/m^3]
$\rho \cdot V = m_{VM}$ is the mass in [kg] of material accumulated in the reactor,
C_{in} and C_{out} are the yields in [mass%] of the VM at the inlet and outlet respectively, and
r is the rate of reaction in [$kg/(m^3 \cdot s)$] and is defined as:

$$r = -k(T) \cdot (C_{VM})^m \quad (4)$$

Where: m is the order of reaction, and

$$k(T) = k_0 \cdot e^{\frac{-E_a}{R \cdot T}} \quad (5)$$

Where: k_0 is the pre-exponential factor in [s^{-1}],
r is the order of the reaction
E_a is the activation energy in [kJ/kmol],
R is the gas constant equal to 8314 [$kJ/(kmol \cdot K)$], and
T is the temperature in [K]

For a CSTR the mass balance is given in equation (2) and for VM, equation (3) can be derived in terms of mass flow in [kg/s] and yield in [mass%].
With the assumptions of constant volume and density and rearranging:

$$\frac{dC_{out}}{dt} + \frac{m + k(T) \cdot V}{\rho \cdot V} C_{out} = \frac{m}{\rho \cdot V} C_{in} \quad (6)$$

Applying the general solution for a first order differential equation gives:

$$C_{out}(t) = e^{-\frac{m + k(T) \cdot V}{\rho \cdot V} t} \left(\int e^{\frac{m + k(T) \cdot V}{\rho \cdot V} t} \cdot \frac{m \cdot C_{in}}{\rho \cdot V} dt + C_1 \right) \quad (7)$$

Simplification of equation (7) results in the general solution for the output production of VM in mass percentage for an infinitesimal volume of the reactor:

$$C_{out}(t) = \left(\frac{m \cdot C_{in}}{m + k_0 \cdot V \cdot e^{\frac{-E_a}{R \cdot T}}} + C_1 \cdot e^{-\frac{m + k_0 \cdot V \cdot e^{\frac{-E_a}{R \cdot T}}}{\rho \cdot V} t} \right) \quad (8)$$

Where C_1, k_0 and E_a are unknown constants

Pyrolysis processes, being extremely complex to solve due to the thousands of reactions taking place, are very difficult to formulate in a CSTR process. The reaction kinetics are not as simple as it might seem because of the complexity of the reaction system. The composition depends on the nature of the

PL which is a mixture of mainly organic matter (85% according to [27]) and can vary as a function of the chicken feed (being very heterogenous), and of the litter (which can be straw, wood shavings, amongst others). It is also very difficult to determine the order of reaction, m, the rate constant, $k(T)$, the energy of activation, E_a, and the preexponential factor, k_0. Practically, the kinetics is a guess depending on too many unknown and variable factors.

On the other hand, experimental data can be obtained for pseudo-component yields of batch pyrolysis processes, which then can be used to determine the values of the unknown constants.

The heat balance (9), adapted from equation 3.13 by [24] is:

$$\frac{\partial}{\partial z}\left(\dot{m} c_p T_z + \eta q_{IH}\right) + \frac{4K_T}{D}\left(T_z - T_{shell}\right) = \frac{\partial}{\partial z}\left(k_T \frac{\partial T_z}{\partial z}\right) \quad (9)$$

Where: $\dot{m}$ is the mass flow rate of the PL through the reactor in [kg/s],

ρ is the density of the PL in [kg/m^3],
T_z is the temperature of the PL at distance z in [K]
T_{shell} is the temperature of the shell in [K],
k_T is the Fourier diffusion coefficient in [$\frac{W}{mK}$],
K_T is the transfer coefficient through the reactor shell in [$\frac{W}{m^2K}$],
D is the diameter of the reactor shell in [m],
q_{IH} is the heat input via the induction heater in [W/m], and
η is the overall efficiency of the induction heating system,

From **Error! Reference source not found.**, the heat input per unit volume, q_{IH}, can be calculated as:

$$q_{IH} = \frac{\pi^2 \cdot B_p^2 \cdot t_r^2 \cdot f^2}{6 \cdot \rho_r \cdot \delta_c \cdot L_c} \quad , \quad (10)$$

Where: B_p is the peak magnetic field in [T],

t_r is the thickness of the reactor shell in [m],
f is the frequency in [Hz],
ρ_r is the resistivity of the reactor shell material in [Ω·m],
δ_c is the density of the reactor material in [kg/m^3], and
L_c is the length of the coil in [m]

This indicates that the temperature can be controlled using the quantity of electricity delivered to the heating coil, q_{IH}, and the overall efficiency, η. Both heating rate and residence time are important parameters for PL conversion, and these depend on the mass flow and power delivered. Thus, the control scheme of the reactor is presented in Fig.5. The auger speed, which is controlled by a VSD,

determines the residence time of the char in the reactor while the feed rate is determined by the dryer's auger speed (Fig. 2.). The reactor shell temperature is controlled by the induction heater using a PID controller. The manipulated process variables, disturbances and output variables are shown in Fig.6.

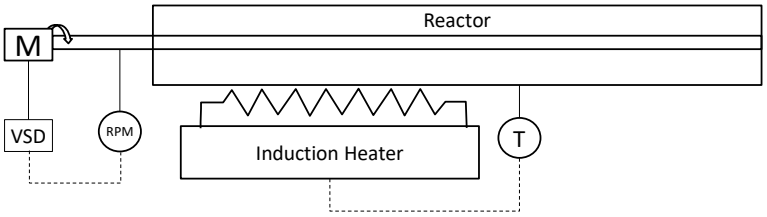

Fig. 5. Control scheme for the reactor

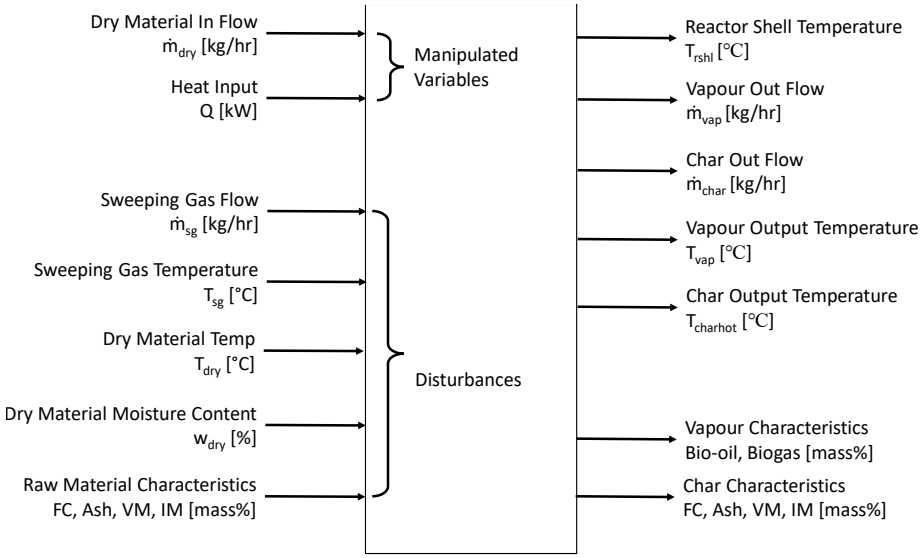

Fig. 6. Process variables and disturbances for the reactor

Financial Modelling:

A comprehensive financial model for the CPU was created using Excel®, which includes the facility to define and manipulate the process and financial parameters that drive the capital expenditure (CAPEX), operational expenditure (OPEX) and revenue streams. The financial model calculates the CAPEX required to establish the facility from the data entered relating to the estimate phase of the project and uses appropriate financial parameters (e.g., loan size, interest rate, inflation rate, etc.**Error! Reference source not found.**) to determine the interest and repayment instalments. The model calculates the revenue of all product

streams on a monthly basis for the lifetime of the facility in future values as well as present values using an appropriate discount rate. This, together with the monthly operational expenses, is used to calculate a detailed cash flow scenario (future and present values) for the lifetime of the plant. Financial indicators, including internal rate of return (IRR), return of investment (ROI) and payback period are calculated for a given set of input parameters. The proof-of-concept plant was designed 20% of typical full scale, i.e., 1 metric ton per day (TPD), to limit capital expenditure. However, for financial modelling, the full-scale scenario (i.e., 5 TPD) was considered, and specifically the scenario where two of these units are deployed to process 10 metric tons of PL per day. This financial model was used to create a series of scenarios which were used in several sensitivity analyses.

3. Results and discussions

Technical Feasibility:

The CPU was evaluated in terms of its technical feasibility at a scale that suits the commercial poultry industry, while also considering its product streams (qualitatively and quantitively), manufacturability and maintenance.

With calorific values of the bio-oil exceeding 40MJ/kg and other typical properties within acceptable ranges, this bio-oil is readily usable as a heavy fuel oil (HFO) in power generation equipment, or for blending into diesel. The oil yields by mass were typically between 47% and 60% of the raw material (depending on the source of the PL) while the char yields were typically around 20% with the balance being gas yields. Tests conducted on the biochar confirmed conclusions made from literature regarding its suitability as a soil enhancer, as well as increasing water retention capability of the soil [28] (which, in an arid country like Botswana, is a huge benefit).

The typical amounts of PL produced by broiler reared is 0.843kg which means that a large-scale poultry farm of 3,500,000 broilers per year will therefore produce an average of 2,951 tons per year (or approximately 10 TPD at a plant availability of 80%). This would require 2 x 5 TPD CPUs for a large-scale poultry farm.

Results of reactor performance at 0.25 TPD are shown in Fig.7. Steady state temperature of 500°C was obtained in the reactor shell temperature at about t=150min. However, a steady state temperature of 400 °C was only reached in the reactant after about t=225min. This was achieved with only 11% power draw of the induction heater. By extrapolation, full throughput should be reached at around 44% of the heater's capacity. In order to achieve this, further work is required to improve the induction heater/coil configuration.

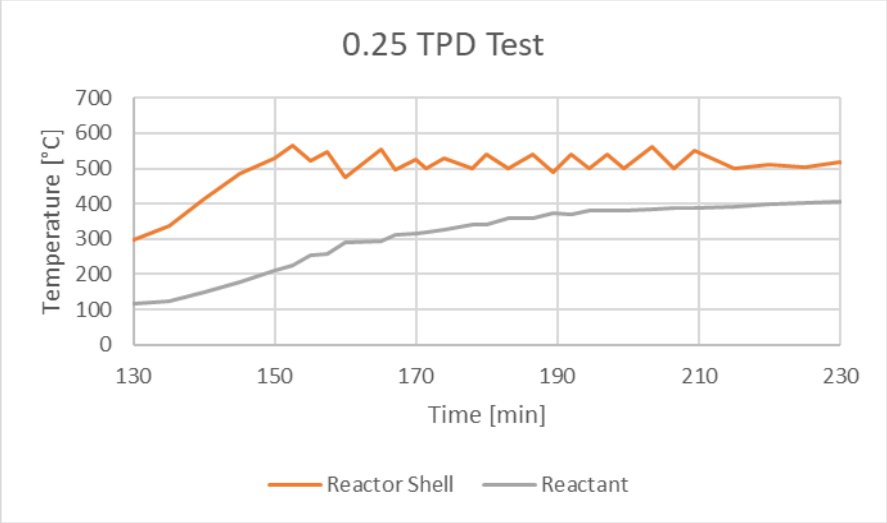

Fig. 7. Temperature measurements during 0.25 TPD performance test

Market Feasibility:

A market analysis was performed to determine whether clients were ready to accept this product, the size of the market (local and export) and to explore the marketing strategies that would work best for the promotion of the product. Distribution, availability, and sustainability of raw material supply were considered while competitiveness in the market was also evaluated.

The need to improve profitability amidst rising input costs is driving the poultry industry to (a) reduce operating expenses, and (b) find ways to convert waste streams into sources of revenue (End-of-Waste). PL pyrolysis offers such a solution by reducing the burden of waste disposal and simultaneously creating high value by-product (and therefore revenue) streams.

The largest concentration of poultry farms is around Gaborone having 11 commercial farms [8]. There are no operating pyrolysis plants in Botswana, neither supplier of pyrolysis plants. While pyrolysis plants could be imported but the available units are not at the ideal scale for the PL scenario, while this CPU was specifically sized for implementation in the typical poultry farming setup. This, together with competitive pricing and the fact that locally manufactured products are highly favored and incentivized, make these plants the preferred option.

More than 48 metric tons of PL are produced per day in Botswana [17] from commercial broiler farmers in the Gaborone area makes way for 5 of these plants in this region alone at a market share of about 50% and at least 10 CPUs throughout Botswana. In South Africa the total number of broilers reared in 2020 was 1,069.6 million [19]. At an average of 0.843kg PL per broiler's lifetime, this

amounts to 900,000 tons of PL per annum, which is enough to supply 600 of the 5TPD CPUs. If Botswana's 2.29 million birds has potential for 10 CPUs, then, by extrapolation, the potential sales in SADC could amount to 15,000 units. At a final production rate of 1 CPU per week, and a market share of 10%, this product could sustain production of CPUs for 10 years.

The prime focus will be to produce a bio-oil which can be blended with diesel to offset the more than 10,000 barrels imported per day from South Africa. Ten 5TPD CPUs will produce about 120 barrels of bio-oil per day, which, if blended into the imported diesel, gives a dilution of 1.22% (which well within the published 25% limit). The bio-oil, being from a renewable source will sell at a premium. However, following a conservative approach, a selling price of $ 0.67/liter was used (i.e., about 50% of current market price of $1.288 [28]). Even if sold as a heating oil at current prices, which far exceed $3 per gallon [29], the price assumed is still conservative by a large margin.

The biogas will not be sold but used on site in real time to generate electricity using an internal combustion engine. Although electricity generation will be for own consumption, there is potential to export some of it to consumers in proximity.

Another significant parameter in studying the feasibility of the PL pyrolysis business, is the selling price of the biochar. Typical biochar selling prices range between USD250 and USD1000 per ton and valued towards the lower end of the range in larger quantities [23].

Contrary to raw PL, biochar can be stored indefinitely without degradation and/or risk of disease spreading, which is another huge benefit offered.

Organization:

The organizational study considered human resources and management structures as well as aspects such as deployment logistics and maintenance. Although pyrolysis plants normally require highly skilled technical staff to operate the process, the technology employed in this plant was carefully chosen and the level of automation has been designed to enable low-skilled operators to start up, operate and shut down the plant. The plant is designed to optimally run for 24 hours per day and 330 days per year and therefore typically requires three shifts of operating staff, each consisting of a plant operator, a driver and two assistants. In this feasibility study, however the scenario was modelled where the plant would be operated continuously for only 6 days a week (i.e., 72% availability).

Statutory Requirements:

On the statutory feasibility front, aspects such as industrial, environmental, and energy permits and/or licenses needed consideration together with applicable rates, duties, and taxes.

In the Botswana context, permitting requirements include a manufacturing License for the fabrication of the pyrolysis plants as well as environmental permits. Industrial licenses, governed by the Industrial Development Act of 2007 [11] and the Industrial Development Regulations of 2008 [13], are required for all manufacturing enterprises. These are issued by the Industrial Licensing Authority (ILA) and the Regional Licensing Committee and are valid for an indefinite period. Two separate licenses will be required, i.e., for the manufacturing of the containerized plants and for operating the pyrolysis plant. Additionally, an Environmental Health report, Physical Planning report (confirming zoning), Environmental Impact Assessment report and a Waste Collection Commitment letter (approved by the Waste Manager) are required. Since this plant will generate electricity exceeding 100kW, a license will be required from the Botswana Energy Regulator Authority (BERA) [32]. Similarly, since the plant produces petroleum products, it may be required by BERA to obtain an appropriate license.

Financial Modelling:

Finally, a detailed financial feasibility model was created to determine return on investment (ROI), internal rate of return (IIR) and payback time based on a comprehensive set of input parameters. These financial indicators were used to evaluate financial feasibility for various deployment scenarios, which also allowed for sensitivity analyses to be performed.

The total capital required to establish a 10 TPD facility is $ 1,684,525. This is achieved by taking advantage of production line fabrication methodology. The operational and maintenance costs on a 24-hour-per-day, 6-days-a-week scenario were determined to be $ 75,433 per annum for a plant deployed in the proximity of typical poultry farms in Botswana. Using typical market related rates for products and the financial environment in the Southern Africa context yielded an Internal Rate of Return (IRR) of 39%. The following table shows the summary of the financial model parameters and results.

Pyro Carbon Energy
"unlocking resource value"

Financial Model Summary

Processing of Poultry Litter for PCE at BIUST

Summary

Material & Products	Net (average)	Installed	Price
Poultry Litter Feed Rate	9.6 TPD	10.0 TPD	$ 4.17/ton
Total Pyrolysis Gas Production	0.0 TPD	5.2 TPD	-
Total Bio-oil Production	17.6 BPD	32.6 BPD	$ 106.00/bbl
	2,792 LPD	5,176 LPD	$ 0.67/litre
Biochar Production	1.4 TPD	1.9 TPD	$ 200/ton
Briquettes Production	0.0 TPD	0.0 TPD	-
Activated Charcoal Production	0.0 TPD	0.0 TPD	$ 900/ton
Diesel Production	-	-	-
Petrol Production	-	-	-
Pyroligneous Acid Production	935 LPD		$ 0.17/litre
Power Generation	-22kWh/day	3,678kWh/day	$ 0.13/kWh

Financial Summary	
Plant Life Time	20 yrs
Start-up and Initial Capital Expenses [USD]	$ 1,684,525
Life Time Opex [USD]	$ 24,517,287
Total Start-Up Expenses	$ 919,374
Life Time Revenue [USD]	$ 70,789,931
Loan Amount	$ 919,374
Total Interest	$ 307,684
Internal Rate of Return (IRR)	39%
Net Present Value (NPV)	$ 1,135,667
Return on Investment (ROI)	28%
Payback Period	3.64 yrs
LCOE Generation	N/A
Lifetime Conversion Cost	$ 350.25/ton
Lifetime Conversion Price	$ 1,011.28/ton

Fig. 8. Financial model summary

A range of sensitivity analyses were performed using the financial model by keeping all other input parameters unchanged (i.e., as the baseline) the figures below illustrate the sensitivities of the main financial metrics (i.e., the IRR, ROI and Payback periods when each parameter is varied. It was observed that the IRR is not very sensitive to the PL acquisition cost and even at rates as high as $37.50/ton the business case remains favorable, which means that transportation costs to haul PL from remote sources can be tolerated. Since bio-oil represents the highest source of revenue, its selling price is expected to be an important factor in the financial feasibility. The sensitivity of the bio-oil yield is therefore, as expected, much higher than sensitivity to the biochar yield. However, plant availability (Fig. 9.) proved to be the parameter that influenced financial feasibility the most. As the plant availability decreases from the 72% baseline, the IRR falls and it can be seen that the case becomes unfavorable at an availability below 56%.

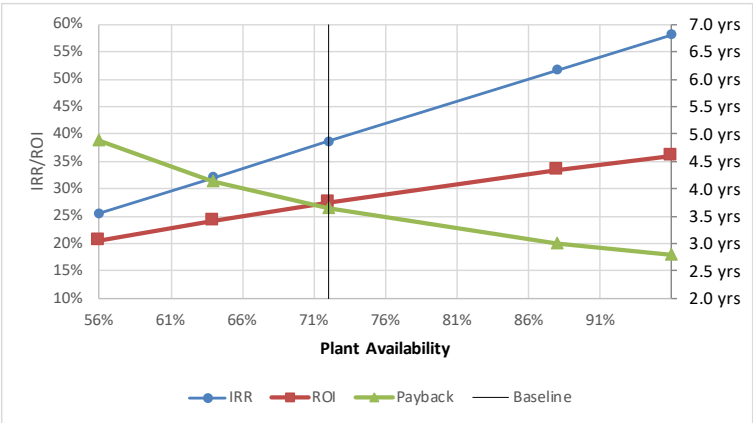

Fig. 9. Sensitivity analysis: Financial indicators vs. Plant availability

4. Conclusions

The environmental challenge of safe waste disposal which have haunted the poultry farming community can be addressed and solved using the poultry litter pyrolysis process. PL-derived biochar has been receiving increasing attention as a composting and soil enhancer. It has the potential to increase humification, enhance microbial activity, immobilize heavy metals and organic pollutants (preventing them from being absorbed by plants), reduce NH_4, increase the soil pH, retain moisture, reduce salinity stress, enhance plant growth, and improve respiration rate. Not only is it a good soil enhancer, but it also provides micro pores and a stabilized microclimate in which microorganisms can flourish. This biochar is especially suitable for Botswana's soil and climate. Further work to better quantify this value is needed together with actual plant growth trials. The move towards sustainability of organic chemical processes requires consideration of the impact of these processes on the environment.

This study has developed a mathematical model having several unknown constants. While it is very complex and difficult to determine the values for these constants analytically, these could be determined experimentally, which is scope for future work. However, technical feasibility of the containerized pyrolysis unit (CPU) concept to accomplish these objectives, has been demonstrated by successfully developing a commercial scale proof-of-concept plant through mathematical and financial modelling, multi-disciplinary design, construction, commissioning, and performance testing. In addition, the other elements of a detailed techno-economic feasibility study were performed where product suitability, the markets, organizational aspects, statutory requirements, and financial feasibility were analyzed and evaluated. It has been concluded that: The product is at the correct scale and delivers suitable products in sufficient quantities; The product will attract attention as there are no other similar local products; The demand of this product has been shown to have the potential of setting up a production line for manufacturing; A highly favourable internal rate of return (IRR), return on investment (ROI), and short payback periods, make this solution to PL waste management very attractive.

Further work is recommended in several areas, including improvement of the induction heating system, continuation of kinetics studies of poultry litter pyrolysis, addition of a distillation column to beneficiate the bio-oil, incorporating steam activation, and utilizing the non-condensable gas for power generation.

REFERENCES:

[1] UN Botswana, *2020 UN Botswana Annual Results Report*, 2021.
[2] IRENA, *Renewables Readiness Assessment*, 2021.
[3] Cebr., *World economic league table 2022*, December, (2021), 1–237, 2022.
[4] IEA, *Global Energy Review 2019*, *Glob. Energy Rev. 2019*, 2020, doi: 10.1787/90c8c125-en.
[5] *Crude oil - 2022 Data - 1983-2021 Historical - 2023 Forecast - Price - Quote - Chart*. https://tradingeconomics.com/commodity/crude-oil (accessed Mar. 25, 2022).
[6] *Surging electricity demand is putting power systems under strain around the world - News - IEA*. https://www.iea.org/news/surging-electricity-demand-is-putting-power-systems-under-strain-around-the-world (accessed Mar. 28, 2022).
[7] IEA, *Electricity Market Report*,*Electr. Mark. Rep.*, January, 2022, [Online]. Available: https://www.iea.org/reports/electricity-market-report-january-2022.
[8] *Botswana plans $2.5 bln coal-to-liquids plant to cut fuel imports | Reuters*. https://www.reuters.com/business/energy/botswana-plans-25-bln-coal-to-liquids-plant-cut-fuel-imports-2022-05-16/ (accessed Jun. 23, 2022).
[9] *Principal Imports Composition | Statistics Botswana*. https://www.statsbots.org.bw/principal-imports-composition (accessed Jun. 23, 2022).
[10] B.A. Report, *Bera annual report 2020 - 21 1*, (2020), 1–90.
[11] Sekantsi L.P., Timuno S., *Electricity Consumption in Botswana: the Role of Financial Development, Industrialisation and Urbanization*, Rev. Econ. Bus. Stud., 10, 1, (2017), 75–102, doi: 10.1515/rebs-2017-0049.
[12] Ministry of Minerals Energy and Water Resources, *National Energy Policy for Botswana*, 00, 690, 2009.
[13] Grynberg R., Motswapong M., *Development of the poultry sector in Botswana: From good intentions to legal oligopoly*, J. Dev. Agric. Econ., 8, 2, (2016), 14–26, doi: 10.5897/jdae2015.0701.
[14] Moreki J.C., *Opportunities and challenges for the Botswana poultry industry in the 21st century: A review*, 2010, Accessed: Mar. 27, 2022. [Online]. Available: https://www.researchgate.net/publication/294460886_Opportunities_and_challenges_for_the_Botswana_poultry_industry_in_the_21st_century_A_review.
[15] Moreki J.C., *Challenges in small-scale broiler production in Botswana*., Int. J. Agric. Technol., 7, 6, (2011), 1579–1587, [Online]. Available: http://search.ebscohost.com/login.aspx?direct=true&db=lah&AN=20113397927&site=ehost-live%5Cnhttp://www.cabi.org/cabdirect/showpdf.aspx?PAN=http://www.cabi.org/cabdirect/showpdf.aspx?PAN=20113397927%5Cnhttp://www.ijat-aatsea.com/pdf/v7_n6_11_November/11_IJ.
[16] *Market Study Reveals Competition Concerns in Botswana's Poultry Industry | Competition and Consumer Authority (CCA)*. https://www.competitionauthority.co.bw/market-study-reveals-competition-concerns-botswanas-poultry-industry (accessed Mar. 29, 2022).
[17] Moreki J.C., Keaikitse T., *Poultry waste management practices in selected poultry operations around Gaborone , Botswana*, 2, 7, (2013), 240–248.
[18] Hussein M.H., *Experimental Investigation of Chicken Manure Pyrolysis and Gasification*, 2016.
[19] Batlang U., Nthoiwa P.G., *Botswana Agricultural Census 2015 Analytical Papers*, Gaborone, 2015. [Online]. Available: http://www.statsbots.org.bw/sites/default/files/publications/Botswana Agricultural Census 2015 Analytical Papers.pdf.
[20] Seanama Conservation Consultancy, *Agriculture and Food Security Policy Reflecting on the Challenges of Attaining a Green Economy*," United Nations Conference on Sustainable Development. Gaborone, 2012.

[21] Hitchcock R. K., *Sandveld Agriculture in Botswana*., Botsw. Notes Rec., 18, (1986), 91–105.
[22] Kashe K., Kolawole O.D., Moroke T.S., Mogobe O., *Dryland crop production in Botswana : Constraints and opportunities for smallholder arable farmers*, in *Smallholder farmers and farming practices: Challenges and prospects*, December, New York, NY: Nova Science Publishers, 2019.
[23] Agachi P.S., *Part II: Applied Process Engineering Control*, in Process Control.
[24] Agachi P.S., Cristea M.V., Makhura E.P., *Basic Process Engineering Control*. De Gruyter.
[25] Kim S.S., Kim J., Park Y.H., Park Y.K., *Pyrolysis kinetics and decomposition characteristics of pine trees*, Bioresour. Technol., 101, 24, (2010), 9797–9802, Dec. 2010, doi: 10.1016/J.BIORTECH.2010.07.094.
[26] Kim S.S., Agblevor F.A., *Pyrolysis characteristics and kinetics of chicken litter*, Waste Manag., 27, 1, (2007), 135–140, doi: 10.1016/J.WASMAN.2006.01.012.
[27] Zhou P.P., Batidzirai B., Simbini T., Odireng M., Wright N., Tadzimirwa T., *Botswana Biomass Energy Strategy Main Report*, 2009.
[28] *Botswana gasoline prices, 26-Sep-2022 | GlobalPetrolPrices.com*. https://www.globalpetrolprices.com/Botswana/gasoline_prices/ (accessed Oct. 03, 2022).
[29] SAPA, *Annual Report 2020*, 2020. [Online]. Available: www.clicksgroup.co.za.
[30] *Heating Fuel Prices | Governor's Energy Office*. https://www.maine.gov/energy/heating-fuel-prices (accessed Oct. 03, 2022).
[31] Marshall (Sandy) P.E.A.J., *Commercial Application of Pyrolysis Technology in Agriculture*, 2013.
[32] *Botswana - Agricultural Sectors*. https://www.trade.gov/country-commercial-guides/botswana-agricultural-sectors (accessed Mar. 27, 2022).

A FEASIBILITY STUDY FOR THE PRODUCTION OF CHEMICAL FERTILIZERS IN BOTSWANA

Bokamoso K. PHUTHEGO[1*], Paul S. AGACHI[1,2]

[1]Botswana International University of Science & Technology, [2]Universitatea Babes-Bolyai, Romania

Abstract

The purpose of this study is to assess the techno economic feasibility of starting and operating an ammonium nitrate plant in Botswana. Currently Botswana imports approximately 28,000 tons and 500 tons of Ammonium nitrate and Urea respectively. This is worth a collective total of $12.5million per year. The exploration of coal bed methane (CBM) by Botala Energy in Central Botswana has yielded positive results so far, and they are confident that they will soon garner a sustainable gas off-take agreement from customers who purchase in bulk. A feasibility study instituted by the government of Botswana estimated natural gas content approaching 196Tcf (5.6 trillion cubic meters) over a 50 000 km2 area underlain by Karoo carbonaceous sediments and coals. This gas can be reformed by means of steam to produce hydrogen that will subsequently be used to produce ammonia. It is from this ammonia with which a plethora of chemical fertilizers such as Ammonium nitrate, Urea, LAN etc. can be processed. The plant can be built around Palapye, Botswana in Central district along the A14 highway road, an industrial area that currently consists of a Coal mine and 2 large scale Power generating plants. Assuming a 340-day capacity factor, the daily capacity of 85.3 tons becomes an annual capacity of 29,000 tons at a cost of $46.5million. Payback period is estimated to be 13 years.

Key words: ammonia, ammonium nitrate, chemical fertilizers, feasibility study, steam-methane reforming

1. Introduction

Botswana and the world's food demand have increased tremendously in the past 20 years. This trend has weighed heavily on Botswana's food importation rate. It is in her best interest to enhance self-sufficiency in food through crop production and food processing. A key element in crop production is the availability and usage of chemical fertilizers. Every crop has its own nutritional requirement. For example, lablab purpuras need much more nitrogen than sorghum whilst to grow corn you need a lot more phosphorus. Although soil does provide a reservoir for all these essential nutrients, it doesn't necessarily provide

* Corresponding author: bokamoso.phuthego@studentmail.biust.ac.bw

the perfect balance. It is for this reason that engineers manufacture and synthesize concentrated forms of these nutrients, to then distribute into the soil; to improve crop health and yield. These synthesized chemicals are what we call chemical fertilizers. Plants need three primary nutrients, these are: phosphorus, potassium, and nitrogen. The fertilizer industry has therefore been typically split into these three categories nitrogen-based fertilizer, potassium-based fertilizers sometimes known as potash, and phosphate-based fertilizers. Further scrutiny into the market share of these three categories shows absolute dominance by nitrogen-based fertilizers, contributing to 61% of the market value [1]. Reason being they're the most important and most lacking nutrient in soil, hence such high global demand and production.

The unemployment rate in Botswana increased from 17.63 to 19.94 between Dec 2017 and Dec 2021. Current reports by Botswana Statistics show that Botswana's population increased to 2.29 million people in Dec 2022 and average monthly earnings stood at BWP5000 (USD 611.10) in Dec 2020. The country's Labor Force Participation Rate increased to 72.2% in Dec 2021 [2]. A reason for this devastating increase in the unemployment rate could be because of the closing of the copper and Nickel BCL mine in the town of Selebi Phikwe due to the feasibility of producing copper and nickel. Approximately 6,000 people lost their jobs, and the government of Botswana is desperate to come up with a long-lasting solution to mitigate this problem. This paper will therefore assess the techno-economic feasibility of starting and operating nitrogen based chemical fertilizer (Ammonium Nitrate) plant in Botswana.

2. Research

The research method applied in this study involves using already existing data. The information is summarized and organised to enhance the overall efficiency of the research. This paper comprises of research publications and other documents attained from websites, libraries, research and industrial institutions and relevant surveys completed previously.

The following steps were taken in completing the study proposed in this paper.

a) Identifying research Sources: A comprehensive literature review was carried out. The books, journals and articles employed in this research can be found in the bibliography section. Intracen.org was used in analyzing the market of the chemical fertilizers in Botswana and Southern Africa, under the recommendation of officers from the ministry of investment, trade, and industry. Commercial information sources with exclusive information to demographic segmentation, market research, economic and industrial development and similar subjects were

also used. Companies such as Tlou energy and Kalahari energy provided information of natural gas quantification in the country.
b) Combine and Compare: Once the data was gathered, it was composed and compared to consolidate and avoid duplication. The sources used were published in reputable journals and/or other authenticated platforms. Assurance can be made to the accuracy and credibility of employed documentation.
c) Data Analysis and Compilation: The chosen information was consolidated with scientific principles and engineering software such as aspen. It was then applied to the situation in Botswana, putting into consideration factors such as climate, plant location and government policies.

Market Analysis

Common nitrogen based chemical fertilizers are ammonia, ammonium nitrate, urea and CAN. 41% of global production comes from the East Asian; with China contributing to 33%, India at 8% and the USA and Russia at 7% each. Currently, every year Botswana imports on average 23 000 tons and 634 tons of Ammonium nitrate and Urea respectively [2]. On average these products are worth a collective total of $12.5million (BWP125million) per year. Furthermore, the Southern African Development Community (SADC) imports on average $430billion (BWP4.3trillion) worth of these products (ammonium nitrate and urea) every year. Zambia, South Africa, Namibia, and Zimbabwe, who Botswana shares borders with import collectively $340billion (BWP3.4trillion). Adding Botswana's imports to this group makes up 80% of the region's nitrogenous chemical fertilizer market.

Process Outline

The process of producing ammonium nitrate starts off with a natural gas feedstock. Whatever NG chosen and wherever its place of origin, it will still contain some organic sulfur compounds. The sulfur needs to be removed, otherwise it will damage equipment and catalysts downstream. And this is done in the desulfurization unit. Steam is injected into the desulfurized natural gas before entering the reformer section. Here the catalytic reforming of the hydrocarbon and steam mixture to produce the ammonia synthesis gas or syngas is done.

The aim is to convert hydrocarbon into hydrogen. Carbon monoxide is formed as a byproduct in this process, it needs to be removed, but it's difficult to remove the CO as it is, so it's first converted into CO2, in the shift converters. The CO2 can then be absorbed in the CO2 absorption columns. There's a final purification stage to convert any remaining hydrocarbon into hydrogen. The hydrogen then enters the ammonia synthesis loop where it reacts with nitrogen to

form ammonia. The chemical reaction that produces ammonium nitrate is between nitric acid and ammonia. There are several industrial processes for manufacturing ammonium nitrate that involve various combinations of neutralization, evaporation and drying and finishing methods.

Economic Studies

This chapter uses charts to provide a rough estimate of costs of process equipment. It is important to note in using this method that, the prices stated are not exact or fixed because of equipment's unique design. Charts for different variations could be made but this would make the process complex and because designs may change as the process is developed, it is convenient to use average representatives of equipment. All costs were factored to a 2010 basis i.e Chemical Engineering Plant Capacity Index (CEPCI) number of 320. The CEPCI was introduced in 1963 and has since been important for chemical process industry professionals in regulating plant costs from one period to another. It consists of a compound index put together from a set of 4 sub-indexes: Buildings, equipment, Engineering & Supervision and Construction labour.

$$cost\ size\ 2 = cost\ size\ 1 \left(\frac{size\ 2}{size\ 1}\right)^{size\ exponent} \quad (1)$$

Several authors estimate the installation cost to be a fraction of the purchased equipment in a method that generally incorporates shipping costs, mounting, freight and piping connections.

$$Installed\ cost = purchase\ price \times installation\ factor \quad (2)$$

Guthrie 1975 and Ulrich 1984 have listed similar numbers that incorporate these minor costs. This is called the module factor.

$$cost\ of\ the\ installed\ module = purchase \times module\ factor \quad (3)$$

The cost associated with hydrogen production by steam reforming is extremely sensitive to the cost of natural gas. Gray and Tomlinson have advanced an equation to show this correlation, as thus [13].

$$\text{Hydrogen Cost (\$/MMBtu)} = 1.27*\text{NG price (\$/MMBtu)} + 0.985 \quad (4)$$

Applying this equation with a natural gas cost of 10.00 USD/MMBtu gives a

cost of 3.17 USD/kg in adjusted 2007 dollars, which is higher than the cost given by the Gray and Tomlinson value of 2.48 USD/kg.

Project Budget

The assumption made in determining the number of personnel required for plant operation is that the labourer is directly related to the main process units and the plant capacity. Ammonia plants are assumed to operate all year at 3 shifts per day at every hour. This means in a year; 1095 operating shifts are required. The standard number of personnel per shift to run the plant to cater for Botswana's consumption of ammonium nitrate and urea is a 1038 including plant managers, artisans, and manual labourers.

Table 1

Core Team in the developing and operating of the plant

Position	**Qualification & Experience**	**Salary/Allowance (BWP)**
Fertilizer Expert (Team leader)	Ph.D./M.Sc. with minimum 10 years' experience or equivalent	60,534.01
Civil Engineer	M.Sc. Civil Engineering with 5 minimum years' experience or equivalent	43,238.58
Legal Expert	LLM with minimum5 years' experience or equivalent	43,238.58
Financial Expert	Master's in finance with minimum 5 years' experience or equivalent	43,238.58
Chemical Engineer	Master's in chemical engineering with minimum 5 years' experience or equivalent	43,238.58
Total		**233,488.33**

Table 2

Operators of the plant

Position	**Qualification & Experience**	**Quantity**	**Salary/Allowance (BWP)**
Plant Manager	M.Sc./Degree. Engineering with minimum 5 years' experience or equivalent	3	77,829.44
Technical Staff	M.Sc./Degree/Diploma. Relevant Field with 2 minimum years' experience or equivalent	10	145,281.63
Administration Staff	M.Sc./Degree/Diploma. Relevant Field with 2 minimum years' experience or equivalent	20	166,036.15
Labourer	N/A	1000	1,037,725.92
Total		**1,033**	**1,426,873.14**

Project Costs-Assets

Costing of the equipment was done theoretically and practically. A company in China by the name Chengdu TCWY New Energy Technology Co., Ltd was contacted for a quotation of the equipment required. This company is internationally reputable in manufacturing and delivering of plant engineering equipment. Furthermore, a common engineering software called Capcost was used.

Table 3

List of the main Fixed Assets required to establish the plant

ITEM	QUANTITY	SUPPLIER	UNIT COST(USD)	TOTAL(USD)
Reformer	2	Chengdu TCWY New Energy Technology Co., Ltd	325,000	650,000
Hydrogenator	1	Chengdu TCWY New Energy Technology Co., Ltd	300,000	300,000
Desulfurization Tank	2	Chengdu TCWY New Energy Technology Co., Ltd	250,000	500,000
Middling Temp Shift Reactor	1	Chengdu TCWY New Energy Technology Co., Ltd	219,000	219,000
Heat Exchanger	1	Chengdu TCWY New Energy Technology Co., Ltd	272,000	272,000
Reforming Gas Boiler	1	Chengdu TCWY New Energy Technology Co., Ltd	78,000	78,000
BFW Preheater	1	Chengdu TCWY New Energy Technology Co., Ltd	275,000	275,000
Stripper Column	1	Chengdu TCWY New Energy Technology Co., Ltd	170,000	170,000
PSA Unit	1	Chengdu TCWY New Energy Technology Co., Ltd	380,000	380,000
Crystallizer	1	Chengdu TCWY New Energy Technology Co., Ltd	79, 000	79, 000
Buildings		Construction Company	572,288	572,288
Installation Fee		Chengdu TCWY New Energy Technology Co., Ltd		99,998
Subtotal				**3,595,286**

This software incorporates the theoretical plant's requirements (such as volumetric flowrates, conditions i.e., Temperature and Pressure and material of construction) to calculate an estimated cost. The figures found from both methods of research coincide closely. All the assets bought during construction are fixed assets and are assumed to be functional for 15 to 20 years and will therefore only need to be replace or updated after then. A lot of the initial investment is used for acquiring and installing them.

Project Costs-Working Capital

Working or operating capital costs are calculated and estimated based on the production rate of the plant. These include expenses such as water, electricity, and human resource.

Table 4

List of the main working capital items required to establish the plant. Total amount required is: $ 7,199,657.35 (in figures) Seven million, one hundred and ninety-nine thousand, six hundred and fifty-seven dollars and thirty-five cents (in words)

Item of working capital	**Number of Months**	**Total working capital required (USD)**
Feedstock, Solvents and Catalysts;		
Raw Natural Gas (1)	12 months	1,113,096.88
Nickel Oxide (3)	12 months	35,050.00
Chromium (4)	12 months	25,170.70
Aluminium (2)	12 months	13,576.86
Iron Magnetite (3)	12 months	42,000.79
methyldiethanolamine (MDEA) (3)	12 months	14,000.02
Equipment		
Reformer Module	24 months	81,000.78
Switch	12 months	6,000.11
Hydrogen Analyser	24 months	2, 000.85
Oxygen Analyser	24 months	1,660.04
Offline Chromatography	24 months	30,000.68
Others		
Salaries and Wages	12 months	1,660,361.47
Water	12 months	187,545.18
Fuel	12 months	194,573.61
Marketing	12 months	86, 477.16
Stationery	12 months	12,197.58
Sub total		**3,604,371.35**

3. Discussions

A feasibility study instituted by the government of Botswana in association with some private companies has confirmed the content of over 5 trillion cubic meters of coal bed methane in Central district Botswana. This gas can be processed to produce syn gas that can be further refined to produce hydrogen gas. Botswana also has a large coal reserve which can be gasified to also produce syn gas and ultimately hydrogen. Once hydrogen gas is attained, it can be reacted with nitrogen gas to produced ammonia and subsequently produce ammonium nitrate. The consumption of ammonium nitrate in the last decade both regionally and globally has proven that a sufficient market exists for this product. In costing the plant, a Chemical Engineering Plant Capacity Index (CEPCI) number of 320 was used in comparison to similar plants previously manufactured.

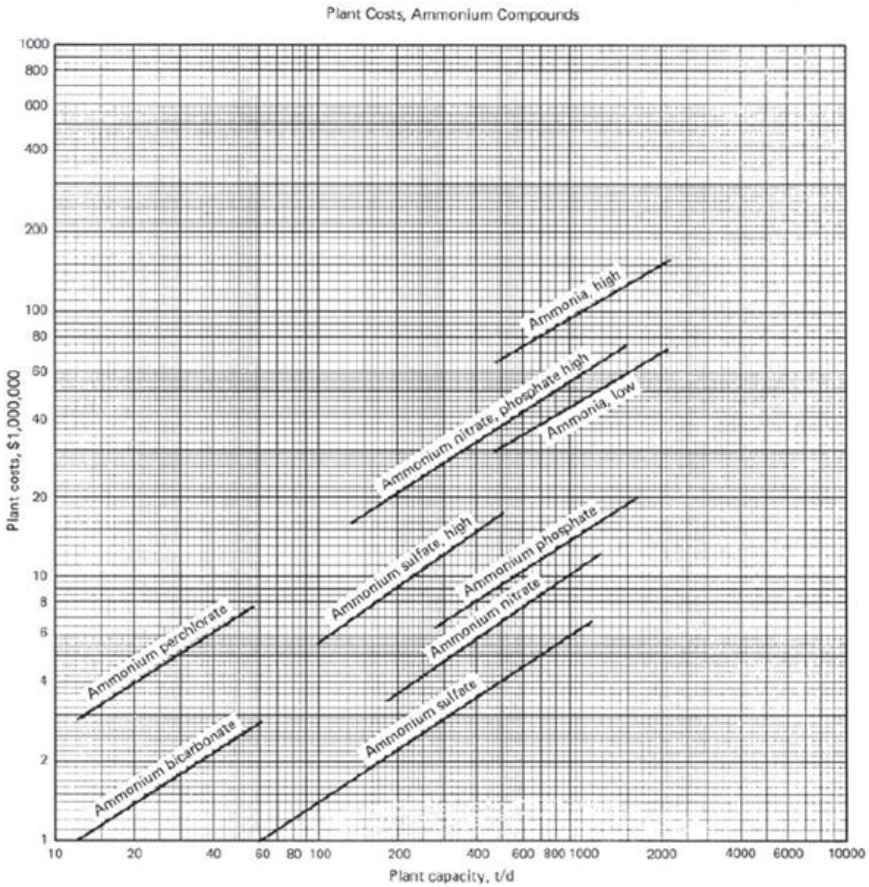

Fig 1. Above shows the estimated equipment cost of some ammonium related plants [13].

4. Conclusions

This is a desktop study and needs more oriented research on the catalytic activity, purity, calorific values, and magnitude of the specific CBM deposit. Nonetheless, the study shows that the establishment of an ammonium nitrate plant in Botswana is very feasible. The cost of starting and operating such a plant will be USD 9million. The plant would be built near Palapye, Botswana in Central district along the A14 highway road, an industrial area that currently consists of a Coal mine and Power generating plants. Assuming a 340-day capacity factor, an annual production rate of 29,000 tons at a cost of USD 38.5million. Payback period would be 12-13 years.

REFERENCES

[1] Sefhako S., *Kalahari Energy awaits customers*, The Daily News Botswana, (2014), A4.
[2] ITC I., (n.d.), *Trade statistics for international business development*, Retrieved August 20, 2020, from https://www.trademap.org/Country_SelProductCountry_TS.aspx?nvpm=1|072||||310230|||6|1|1|1|2|1|2|1||1
[3] Hignett T.P., *Developments in Plant and Soil Sciences*, Fertilizer manual, Dordrecht, Alabama: Springer, 15, (2011).
[4] Frankenburger W. G., *Catalysis* 3, 171, (1955), 1954 – 1960.
[5] Bohnet M., *Ullman's encyclopedia of industrial chemistry*, Weinheim, Dannstadt-Schauernheim, Germany, Wiley-VCH, (2003).
[6] Brill R., *et al.*, Ber. Bunsenges. Phys. Chem. 73, (1969), 999.
[7] Huberich T., Krabetz R., Slack A.V. (ed.), *Ammonia, part III*, Marcel Dekker, New York – Basel, (1977).
[8] Mittasch A., *Geschichte der Ammonia synthese*, Verlag Chemie, Weinheim, (1951).
[9] Mittasch A., Adv. Catal., 2, (1950), 82.
[10] Bosch C., Z. *Elektrochem. Angew. Phys. Chem*., 24, (1918), 361.
[11] Aika K., Yamaguchi J., Ozaki A., *Chem. Lett*., (1973), 161.
[12] Logan S.R., Kemball C., *Trans. Faraday Soc*., 56, (1960), 144.
[13] Appl M., *Ammonia: principles and industrial practice*, Weinheim, (1999).

POTENTIAL SOURCE IDENTIFICATION OF SO_2 AND COMPARISON BETWEEN MODELLING RESULTS WITH IN-SITU MONITORING DATA: STUDY CASE, ROAD NETWORKS OF KIGALI-RWANDA

Elisephane IRANKUNDA[1*], Zoltán TÖRÖK[1], Alexandru MEREUTA [1], Alexandru OZUNU[1], Jimmy GASORE[2], Egide KALISA[2], Beatha AKIMPAYE[3], Theobald HABINEZA[4], Olivier SHYAKA[4], Gaston MUNYAMPUNDU[4]

[1] Faculty of Environmental Science and Engineering, University of Babeş-Bolyai, 30 Fantanele Street, RO-400294, Cluj-Napoca, Romania
[2] College of Science and Technology, University of Rwanda, KK737 Street, PO BOX 4285, Kigali Rwanda
[3] Division of Environmental Compliance and Enforcement, The Rwanda Environment Management Authority, KG 7 Street, Kigali Rwanda, PO BOX 7436 Kigali Rwanda
[4] Department of Technical Expert, Rwanda Space Agency, KG 7 Street, PO BOX 6205, Kigali Rwanda

Abstract

The exposure to sulphur dioxide (SO_2) emissions from the transportation sector exert a high level of attention within the scientific community and public view due to the rise in short and long-term human health effects. The Real-time affordable multi-pollutant (RAMP) monitors were installed in Kigali city, the capital of Rwanda, to fill the gap in air quality datasets. Since RAMP installation, this is the first research aiming to report the level of SO_2 in Rwanda by comparing In-situ monitored data with modelled results. We targeted SO_2 emissions from 27 road networks of Kigali to address the impacts of traffic emissions on air quality over 2021. The American Meteorological Society and Environmental Protection Agency regulatory models (AERMOD and ISCST3) were used for simulation. Statistical indexes include fractional bias (FB), the fraction of the prediction within the factor of two of the observations (FAC2), normalized mean square error (NMSE), geometric mean bias (MG), and geometric variance (VG) used to assess models' reliability. In-situ monitoring shows the annual mean of 59.8 µg/m^3, 62.0 µg/m^3, and 34.8 µg/m^3 at Gikondo-Mburabuturo, Kimihurura, and Gacuriro air quality stations, respectively. Modelling shows a mean of 106 µg/m^3 (daily) and 53.4 µg/m^3 (annually) with AERMOD and 135 µg/m^3 (daily) and 58.8 µg/m^3 (annually) with ISCST3. The spatial dispersion maps of SO_2 were presented and discussed. The FB, NMSE, MG and VG showed good agreement, while FAC2 showed moderate agreement with the AERMOD and ISCST3 dispersion models. Traffic and urban residential emissions were identified as potential sources of SO_2. The study highlights the effectiveness of using models as support for ground-based observations. Findings will help track the effectiveness of Rwanda's recently executed pollution-control policy and suggest evidence based on recommendations to use numerous long-term monitoring stations and further dispersion models for future research to improve the quality of the environment and public health.

Keywords: SO_2, traffic emission, In-situ Monitoring, AERMOD, ISCST3, and potential pollutant sources

[*] Corresponding author: Email address: elisephane@gmail.com

1 Introduction

Emissions from the transportation sector remain a substantial source of urban air pollutants and exert a high level of attention within the scientific community and public view due to the rise in short and long-term human health effects. In addition, air pollutants contribute massively to the existing environmental impact; these include acid rain [1], global warming [2], climate change and weather variabilities [3].

Air pollutants from traffic emissions are directly based on the fossil fuel combustion from petrol, fuel oil, and natural gas in the internal combustion engine of vehicles. The emission of Sulphur dioxide (SO_2) from vehicle circulations globally decreased over the past decade due to the implementation of emission rate control methodology and fuel sulfur content standards within in-use vehicles. Still, its emissions remain a significant concern due to its contribution to forming the sulfate aerosol and sulfur acid as further pollutants in the lower part of the atmosphere [4], [5].

The quality of vehicles in-use influence the level of traffic-related emissions. The United Nations Environmental Program (UNEP) assessed that around 70% of second-hand vehicles (used vehicles) are imported from developing countries, of which a percentage of 40% are imported from African countries [6]. The assessments of the number of vehicles in Rwanda during 2018 indicated that the overall number of vehicles in-use reached about 185140, corresponding to 14 vehicles per 1000 inhabitants [7], [8]. However, the need to increase the number of vehicles in Rwanda is remarkable but subjected to the importation of second-hand vehicles. In 2016, around 8000 vehicles were imported into the country. In 2017, the number of imported vehicles rose to 7055 from 7000, dominated by second-hand vehicles. Also, in 2018, the country imported 10576 motorbikes, 2351 jeeps, 1886 sedan cars, and 838 tracks. The Leading daily of Rwanda (The New Times) mentioned the affordable prices of second-hand vehicles, which may have been manufactured about ten years ago or above, as the leading cause of such importation [9].

In Rwanda, similarly to other Sub-Saharan African countries, the lack of long-term air quality monitoring activities is still problematic in improving environmental management and protection [10]. The Lower-cost and Real-time affordable multi-pollutant (RAMP) air quality monitors were installed in Kigali city, Rwanda, to fill the gap in the air quality datasets. We did not find any published article indicating the concentration level of SO_2 using long-term monitoring data or modelling approaches in Rwanda. Therefore, this research aims: (1) to report the SO_2 concentration level in Kigali city over 2021 using RAMP air quality monitors and compare the In-situ monitored data with the modelled results. The American Meteorological Society and Environmental Protection Agency (AMS/EPA) regulatory models (AERMOD and ISCST3 air dispersion models) were used in the simulation. (2) to evaluate the models' reliabilities in simulation using statistical indexes. (3) to identify additional potential pollutant sources of SO_2 in Kigali, focusing on atmospheric circulation and In-situ monitoring datasets through bivariate pollutant contour polar diagrams.

2 Material and methods

2.1 Study Area Description

Kigali, the capital city of Rwanda, is located in the country's centre at (X: 173103.23 m E, Y: 9784840.19 m S) Universal Transverse Mercator (UTM) coordinate system. Kigali has an area of 730 km^2, a population of about 1.2 million, and a density of 1.5 inhabitants per km^2 [11]. Currently, Kigali city represents rapid development in commercial buildings (modern markets), road networks, household apartments, and hotels with modelled conference halls [11]. Therefore, a total of 27 selective trafficked and jammed roads within Kigali city (Figure 1) were considered the study case of this research.

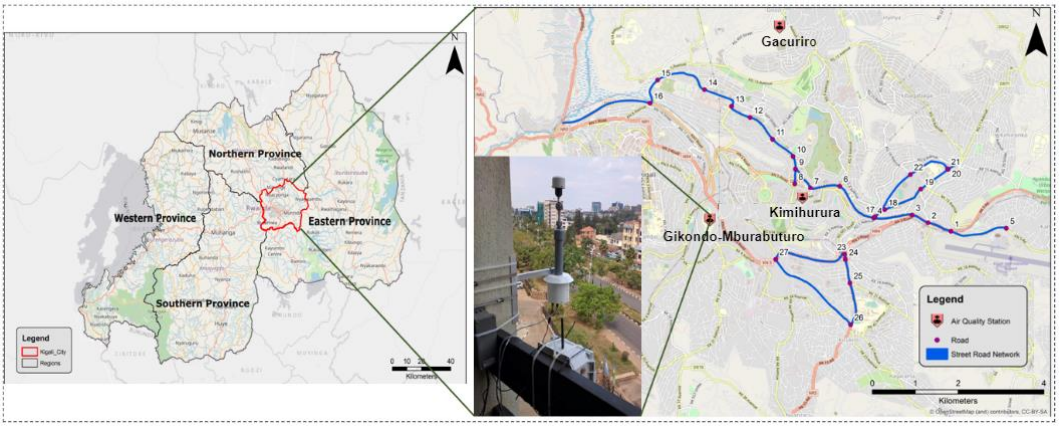

Fig. 1. The 27 Road Networks and Air Quality stations Considered for In-situ Monitoring with RAMPs in Kigali City, Capital of Rwanda

2.2 Monitoring and Instrument Calibration

The simultaneous measurements of SO_2 were done at three air quality stations, namely, Gikondo-Mburabuturo, Kimihurura, and Gacuriro. Measurements were done using Real-time Affordable Multi Pollutant (RAMPs) air quality monitors (Figure 1) for one year (2021). The RAMPs were developed by Sensit-Technologies, Valparaiso, in the USA. RAMPs use the passive alpha sense branded as electrochemical gas sensors to screen concentrations of pollutants within the air. The raw signals of these sensors are sensed four times every minute, then treated and averaged to provide hourly datasets using the RAMPs generalized calibration model (gRAMPs) [12] established in Pennsylvania, USA (Pittsburgh). We identified various scientific publications that used and described the calibration of these RAMPs in full detail [13].

2.3 Model Setup and Urban Traffic Emission Rates

The AMS/EPA regulatory models (ISCST3 and AERMOD) were used to predict the ground-level concentration [14] of SO_2. The ISCST3 and AERMOD use the implication theory of the plume rise and dispersion under the planetary boundary layer

(PBL) influences, focusing on the location's topography characteristics and time zones [14]. The algorithm Tier-1 approach of the European Monitoring Evaluation Programme/European Environmental Agency (EMEP/EEA) that covers the exhaust emissions of air pollutants and heavy metal content from road vehicle movement was used to get SO_2 traffic emission rates [15]. The Rwanda Meteorological Agency (Meteo Rwanda) Gitega station located at (X: 172630.13 m E, Y: 9783560.62 m S) UTM coordinates provided the data for the year 2021 and the available algorithm for estimating the upper meteorological data was used rather than the default options [16], [17] in the AERMOD model.

2.4 Model Performance Evaluation

The performance evaluation between AERMOD and ISCST3 was accomplished using statistical indexes, including the fractional bias (FB), the fraction of the prediction within the factor of two of the observations (FAC2), normalized mean square error (NMSE), geometric mean bias (MG), and geometric variance (VG). The MG and FB indexes quantify the systematic bias of the model as an indicator of the model's over-prediction and under-prediction interrelated to the In-situ field-monitored values. The VG and NMSE show the random scatter measures and systematic bias, while FAC2 is the robust ratio measure which implies the fraction of data in the range of 0.5-2.0. A perfect air pollutant dispersion model would have the FAC2, MG, and VG equal to 1.0, the FB, and the NMSE equal to 0.0 [18]. The negative and positive values of FB imply the over and under-prediction of the model, respectively [18]. In this study, the related equations of FB, MG, VG, FAC2, and NMSE were detailed and applied by Chang and Hanna [19], so we used the same calculation approach.

3 Results and Discussion

3.1 Monitoring and Modelling Results

Results presented in Figure 2 show the SO_2 temporal variation of simultaneous measurements at Gikondo-Mburabuturo, Kimihurura, and Gacuriro air quality stations. Monitoring results over 2021 indicated that the mean concentration level of SO_2 is 59.8 $\mu g/m^3$, 62.0 $\mu g/m^3$, and 34.8 $\mu g/m^3$ at Gikondo-Mburabuturo, Kimihurura, and Gacuriro air quality stations, respectively.

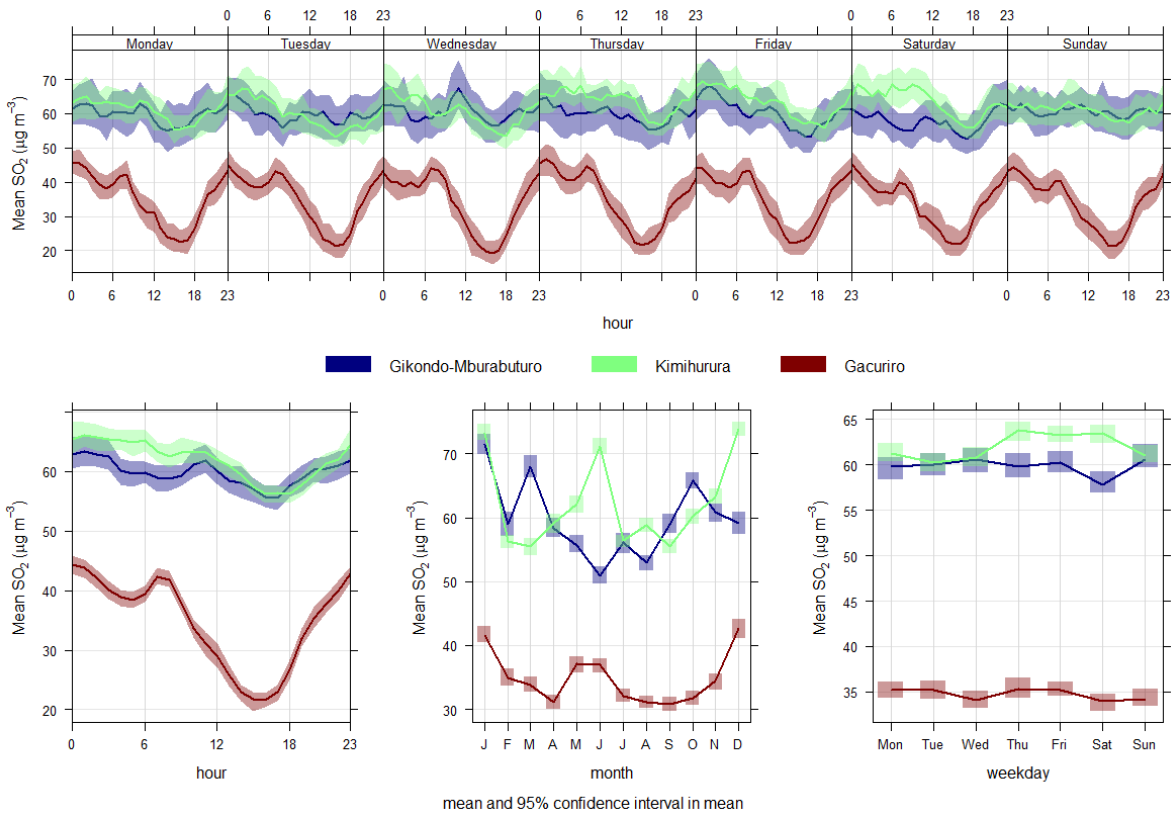

Fig. 2: Temporal Variation of SO_2 at The Considered Air Quality Stations

Via the temporal variation graph of weekdays, it was identified that Saturday represents the low emissions, while Thursday and Friday represent high emissions of SO_2 compared to other days; this explains the contribution of vehicle emissions during working days compared to weekend days, believed that the majority of people stay at home for a weekend break. The hourly temporal variation indicated that noon hours (12:00-17:00) represent low emission of SO_2 while in the morning (6:00-9:00) and evening hours (19:00-00:00) represent high emission of SO_2; this explains the vehicle emission related to jammed and traffic movement based on people circulation heading and leaving to their jobs but with a break corresponding to few emissions within noon hours, and this can also be explained by the variability of the planetary boundary layer between morning, noon, and evening hours to influence the measurement of SO_2.

The daily and annual spatial dispersion maps of the SO_2 ground-level concentration were represented in Figures 3 through 6 for the entire modelling domain (Kigali city). The reported maps are evidence of each other based on the identified point of highest ground-level concentration (X: 179975.65 m, Y: 9784329.79 m UTM coordinate). At this point, it was determined that the variability of SO_2 concentration was 106 µg/m^3 (daily mean) and 53.4 µg/m^3 (annual mean) with the AERMOD and 135 µg/m^3 (daily mean) and 58.8 µg/m^3 (annual mean) with the ISCST3 dispersion model.

These modelled values suggest the influence of the SO_2 emission rate from the nearby considered roads and other specific traffic-related characteristics; these include (1) roads 5, 4, 3, 2, and 5 (Figure 1). The above respective roads represent the back-and-forth movement of passenger cars (PC) to the Kigali international airport, which is approximately 0.58 km from the identified point and to the nearby Kanombe residential areas. (2) The point falls on the REMERA road roundabout. This roundabout connects the road from the Eastern province of Rwanda to MAGERWA (Magasins Generaux du Rwanda s.a). MAGERWA is a public company that deals with Rwanda's most exported and imported products. (3) The roundabout connects roads 17, 27,6, and 5 (Figure 1) with the KIMIRONKO market (the first famous market in Kigali city), REMERA national stadium, and REMERA Arena. (4) The roundabout connects the nation road (NR4) from Rwanda's Northern and Eastern provinces to Kigali city (NR4 road incorporates buses (coaches), consumer and semi-trucks, vans, and other vehicle types from neighbouring countries Tanzania and Uganda). (5) In approximately 162 m through road 4 (Figure 1) away from the roundabout, there is a bus station (REMERA bus station) which is generally a destination for all passengers heading to Kigali from Rwanda's Northern and Eastern provinces.

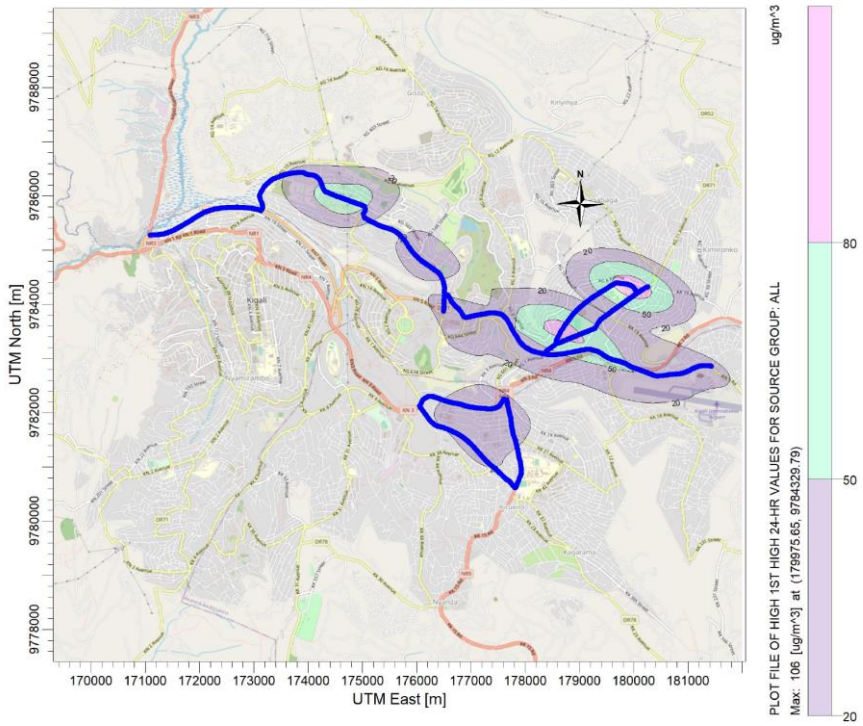

Fig. 3: Modelled Spatial Maps of Daily Ground-Level Concentration of SO_2 with The AERMOD Dispersion Model Over 2021

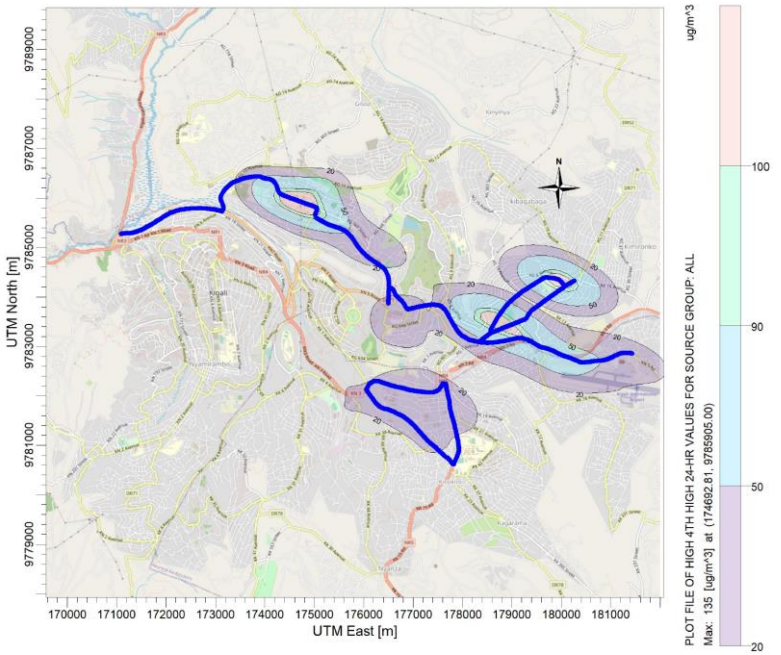

Fig. 4. Modelled Spatial Maps of Daily Ground-Level Concentration of SO_2 with The ISCST3 Dispersion Model Over 2021

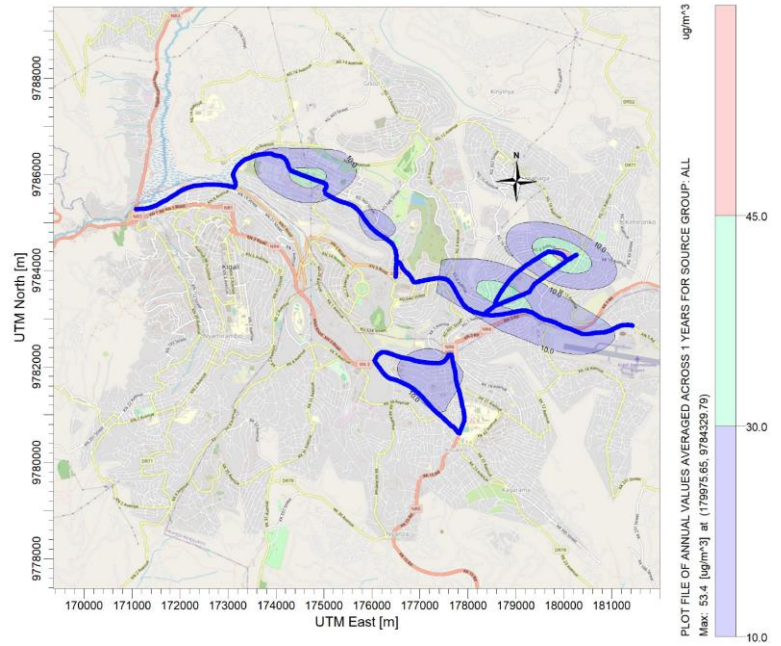

Fig.5. Modelled Spatial Maps of Annually Ground-Level Concentration of SO_2 with The AERMOD Dispersion Model Over 2021

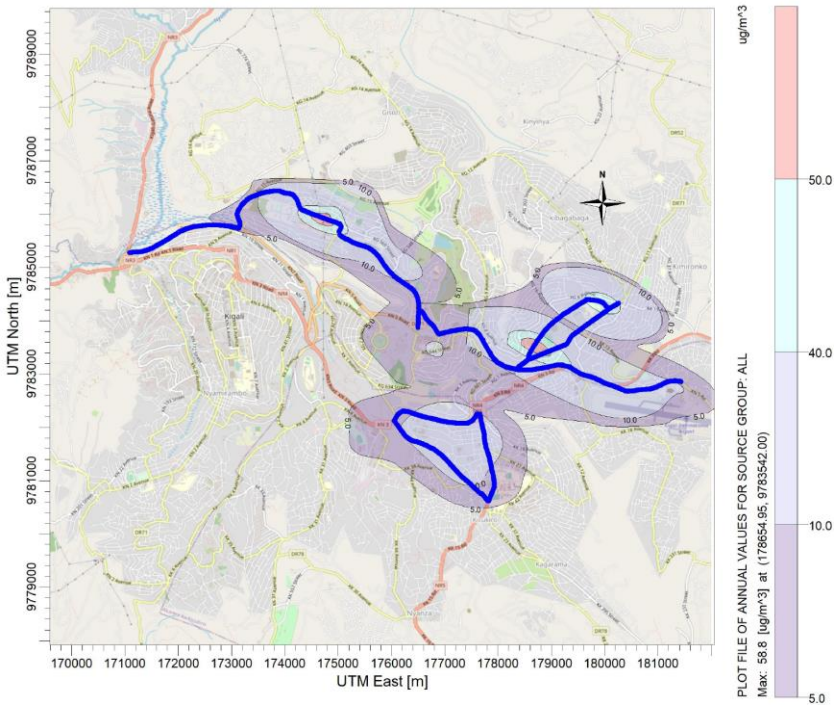

Fig. 6. Modelled Spatial Maps of Annually Ground-Level Concentration of SO_2 with The ISCST3 Dispersion Model Over 2021

3.2 Performance Evaluations

Statistical indexes, including FB, NMSE, MG, VG, and FAC2, reported in Table 1, were discussed for evaluating the reliability of AERMOD and ISCST3 models using monitored data and modelled results at each air quality station. With the AERMOD, the FB showed a model under-prediction at Gikondo-Mburabuturo and Kimihurura stations but with an over-prediction of -0.4 at the Gacuriro air quality station. The NMSE were 0.0 at Gikondo-Mburabuturo and Kimihurura stations and slightly closer to 0.0 at the Gacuriro air quality station (0.2). The VG were 1.0 at Gikondo-Mburabuturo and Kimihurura stations and slightly closer to 1.0 at the Gacuriro air quality station (1.2). The MG and FAC2 were slightly close to 1.0 at all air quality stations, except the FAC2 (1.5) at the Gacuriro air quality station.

On the other hand, with the ISCST3, the FB showed a model under-prediction at Gikondo-Mburabuturo and Kimihurura stations but with an over-prediction of -0.5 at the Gacuriro air quality station. The NMSE were 0.0 at Gikondo-Mburabuturo and Kimihurura stations and slightly closer to 0.0 at the Gacuriro air quality station (0.3). The VG were 1.0 at Gikondo-Mburabuturo and Kimihurura stations and slightly closer to 1.0 at the Gacuriro air quality station (1.3). The MG and FAC2 were 1.0 at the Gikondo-Mburabuturo air quality station and slightly close to 1.0 at other air quality stations, except the FAC2 (1.7) at the Gacuriro air quality station.

Table 1

Model Performance Evaluation at Each Air Quality Station

	Model performance									
	AERMOD					ISCST3				
Air Quality Station	**FB**	**NMSE**	**MG**	**VG**	**FAC2**	**FB**	**NMSE**	**MG**	**VG**	**FAC2**
Gikondo-Mburabuturo	0.1	0.0	1.1	1.0	0.9	0.0	0.0	1.0	1.0	1.0
Kimihurura	0.1	0.0	1.2	1.0	0.9	0.1	0.0	1.1	1.0	0.9
Gacuriro	-0.4	0.2	0.7	1.2	1.5	-0.5	0.3	0.6	1.3	1.7

The identified uncertainties may have resulted from random atmospheric turbulence, which may cause the field monitored and meteorological input datasets to fluctuate or from the embedded algorithm required to run the models [20]. Therefore, it is critical to understand and estimate errors in air pollutant dispersion results if possible. Thus, this study mainly focuses on the model performance evaluation and does not go into the analysis of model errors.

3.3 Potential Source Identification

Bivariate polar plots explain the changes in pollutants concentration jointly with wind direction and wind speed in the three-dimension coordinate [21]. Figure 7 shows the bivariate polar plots for SO_2 monitored at Gikondo-Mburabuturo, Kimihurura, and Gacuriro air quality stations and were computed using the hourly profile of the monitored SO_2 concentrations and hourly datasets of meteorological parameters for 2021 (wind speed and wind direction) to allocate other potential pollutant sources apart from the 27 road networks.

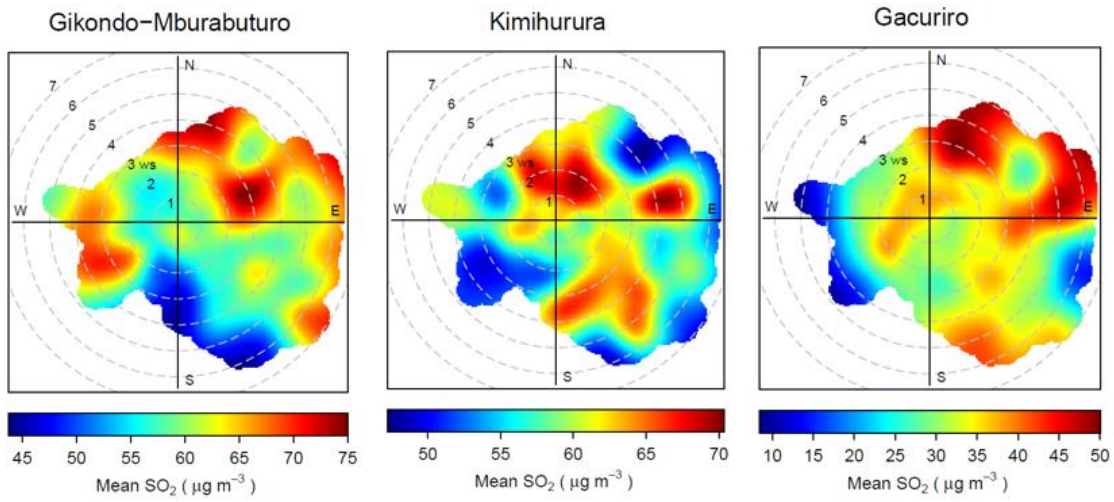

Fig. 7. Bivariate Polar Plots of SO_2 at All Considered Air Quality stations

Results in Figure 7 indicate that at the Gikondo-Mburabuturo air quality station, the highest concentration level between 65-75 µg/m^3 was identified when air masses were close to wind speed from 1.0 m/s to 6.5 m/s in northern and northeastern directions and when air masses were close to wind speed from 6 m/s to 7 m/s in the southeastern direction, and at low wind speed ranging between 2-4 m/s in western direction; this implies further potential sources of SO_2 from the western direction at low wind speed (this may include emission from Gikondo residential areas, student hostels of University of Rwanda, and further vehicle emissions from other local street networks). Further potential sources identified in the northern, northeastern and southeastern directions imply the contribution of the 27-street road network (Figure 1). At Kimihurura air quality station, the identified potential sources were evidence implying the contribution of the considered 27 road networks (Figure 1). While at the Gacuriro air quality station, the northern and northeastern identified potential sources ranging between 40-50 µg/m^3 moving at wind speed ranging between 3-6 m/s were attributed to the Gacuriro residential contributions, and the southern sources explain the contribution of the considered road networks.

4 Conclusions

This air quality modelling research reports the SO_2 concentration level in Kigali, the capital city of Rwanda. We compared In-situ monitored data and modelled results over 2021 using the lower-cost and real-time affordable multi-pollutant (RAMP) air quality and the American Meteorological Society and Environmental Protection Agency regulatory models (AERMOD and ISCST3). We also reported further potential sources of SO_2 within our modelling domain. Statistical indexes include fractional bias (FB), the fraction of the prediction within the factor of two of the observations (FAC2), normalized mean square error (NMSE), geometric mean bias (MG), and geometric variance (VG) used to assess models' reliability. The study concludes that:

- In-situ monitoring shows the annual mean of 59.8 µg/m^3, 62.0 µg/m^3, and 34.8 µg/m^3 at Gikondo-Mburabuturo, Kimihurura, and Gacuriro air quality stations, respectively.
- Modelling shows a mean of 106 µg/m^3 (daily) and 53.4 µg/m^3 (annually) with AERMOD and 135 µg/m^3 (daily) and 58.8 µg/m^3 (annually) with ISCST3.
- The FB, NMSE, MG and VG showed good agreement, while FAC2 showed moderate agreement with the AERMOD and ISCST3 dispersion models.
- Traffic and urban residential emissions were identified as potential sources and attributed to the increase of SO_2 in 2021 in Kigali city.

ACKNOWLEDGEMENTS

The authors gratefully acknowledge: (1) The Foundation National Centre APELL for Disaster Management (CN APELL-RO) for providing the financial support referenced ROC/Busa/RFB/58. (2) The Romania Ministry of Education for providing the financial support referenced DGRIAE-0713/III/139/CMJ/26.08.2021. (3) The Rwanda

Environment Management Authority provided air quality data sets, and Meteo Rwanda provided meteorological data sets.

REFERENCES

[1] R. Terán, K. A. Garcia Bustos, F. P. Sanchez Vera, G. J. Colina Andrade, and D. A. Pacheco Tanaka, 'Acid precipitation followed by microalgae (Chlorella vulgaris) cultivation as a new approach for poultry slaughterhouse wastewater treatment', *Bioresour. Technol.*, vol. 335, p. 125284, Sep. 2021, doi: 10.1016/j.biortech.2021.125284.

[2] R. M. Kaplan and A. N. Vidyashankar, 'An inconvenient truth: Global worming and anthelmintic resistance', *Vet. Parasitol.*, vol. 186, no. 1, pp. 70–78, May 2012, doi: 10.1016/j.vetpar.2011.11.048.

[3] Peters *et al.*, 'The challenge to keep global warming below 2 °C', *Nat. Clim. Change*, vol. 3, no. 1, Art. no. 1, Jan. 2013, doi: 10.1038/nclimate1783.

[4] D. L. Hall *et al.*, 'Using near-road observations of CO, NOy, and CO2 to investigate emissions from vehicles: Evidence for an impact of ambient temperature and specific humidity', *Atmos. Environ.*, vol. 232, p. 117558, Jul. 2020, doi: 10.1016/j.atmosenv.2020.117558.

[5] T. Miyakawa, N. Takegawa, and Y. Kondo, 'Removal of sulfur dioxide and formation of sulfate aerosol in Tokyo', *J. Geophys. Res. Atmospheres*, vol. 112, no. D13, p. 2006JD007896, Jul. 2007, doi: 10.1029/2006JD007896.

[6] UNEP, 'Used Vehicles and the Environment: A Global Overview of Used Light Duty Vehicles - Flow, Scale and Regulation', 2020, [Online]. Available: https://stg-wedocs.unep.org/handle/20.500.11822/34175

[7] G. K. Ayetor, I. Mbonigaba, J. Ampofo, and A. Sunnu, 'Investigating the state of road vehicle emissions in Africa: A case study of Ghana and Rwanda', *Transp. Res. Interdiscip. Perspect.*, vol. 11, p. 100409, Sep. 2021, doi: 10.1016/j.trip.2021.100409.

[8] RRA, 'Cumulative number of registered vehicles by category. Kigali: Rwanda Revenue Authority.', 2020. https://www.rra.gov.rw/ (accessed Sep. 01, 2022).

[9] C. Mwai and sam Ngendahimana, 'Rwanda records slight rebound in vehicle imports', *The New Times | Rwanda*, Aug. 19, 2019. https://www.newtimes.co.rw/news/rwanda-records-slight-rebound-vehicle-imports (accessed Mar. 11, 2022).

[10] E. Kalisa *et al.*, 'Characterization and Risk Assessment of Atmospheric PM $_{2.5}$ and PM $_{10}$ Particulate-Bound PAHs and NPAHs in Rwanda, Central-East Africa', *Environ. Sci. Technol.*, vol. 52, no. 21, pp. 12179–12187, Nov. 2018, doi: 10.1021/acs.est.8b03219.

[11] V. Manirakiza, L. Mugabe, A. Nsabimana, and M. Nzayirambaho, 'City Profile: Kigali, Rwanda', *Environ. Urban. ASIA*, vol. 10, no. 2, pp. 290–307, Sep. 2019, doi: 10.1177/0975425319867485.

[12] C. Malings *et al.*, 'Development of a general calibration model and long-term performance evaluation of low-cost sensors for air pollutant gas monitoring',

Atmospheric Meas. Tech., vol. 12, no. 2, pp. 903–920, Feb. 2019, doi: 10.5194/amt-12-903-2019.

[13] R. Subramanian, Egide Kalisa, Jimmy Gasore, Paulina Jaramillo, Carl Malings, and Nathan J Williams, 'Air pollution in Kigali, Rwanda: spatial and temporal variability, source contributions, and the impact of car-free Sundays | Clean Air Journal', 2020. https://www.cleanairjournal.org.za/article/view/8023 (accessed Mar. 04, 2022).

[14] A. J. Cimorelli *et al.*, 'AERMOD: A dispersion model for industrial source applications. Part I: General model formulation and boundary layer characterization', *J. Appl. Meteorol.*, vol. 44, no. 5, pp. 682–693, 2005.

[15] EEA, *EMEP/EEA air pollutant emission inventory guidebook 2019: technical guidance to prepare national emission inventories.* LU: Publications Office, 2019. Accessed: Mar. 19, 2022. [Online]. Available: https://data.europa.eu/doi/10.2800/293657

[16] M. Kalhor and M. Bajoghli, 'Comparison of AERMOD, ADMS and ISC3 for incomplete upper air meteorological data (case study: Steel plant)', *Atmospheric Pollut. Res.*, vol. 8, no. 6, pp. 1203–1208, Nov. 2017, doi: 10.1016/j.apr.2017.06.001.

[17] K. Seangkiatiyuth, V. Surapipith, K. Tantrakarnapa, and A. W. Lothongkum, 'Application of the AERMOD modeling system for environmental impact assessment of NO2 emissions from a cement complex', *J. Environ. Sci.*, vol. 23, no. 6, pp. 931–940, Jun. 2011, doi: 10.1016/S1001-0742(10)60499-8.

[18] M. D. Gibson, S. Kundu, and M. Satish, 'Dispersion model evaluation of PM2.5, NOx and SO2 from point and major line sources in Nova Scotia, Canada using AERMOD Gaussian plume air dispersion model', *Atmospheric Pollut. Res.*, vol. 4, no. 2, pp. 157–167, Apr. 2013, doi: 10.5094/APR.2013.016.

[19] J. C. Chang and S. R. Hanna, 'Air quality model performance evaluation', *Meteorol. Atmospheric Phys.*, vol. 87, no. 1–3, Sep. 2004, doi: 10.1007/s00703-003-0070-7.

[20] C. A. Barton, C. J. Zarzecki, and M. H. Russell, 'A Site-Specific Screening Comparison of Modeled and Monitored Air Dispersion and Deposition for Perfluorooctanoate', *J. Air Waste Manag. Assoc.*, vol. 60, no. 4, pp. 402–411, Apr. 2010, doi: 10.3155/1047-3289.60.4.402.

[21] Carslaw and S. D. Beevers, 'Characterizing and understanding emission sources using bivariate polar plots and k-means clustering', *Environ. Model. Softw.*, vol. 40, pp. 325–329, Feb. 2013, doi: 10.1016/j.envsoft.2012.09.005.